

Seasonal and interannual variability of pan-Arctic surface mixed layer properties from 1979 to 2012 from hydrographic data, and the dominance of stratification for multiyear mixed layer depth shoaling

Cecilia Peralta-Ferriz*, Rebecca A. Woodgate

Polar Science Center, Applied Phys. Lab., University of Washington, 1013 NE 40th Street, Seattle, WA 98105, USA



ARTICLE INFO

Article history:

Received 16 August 2014

Received in revised form 4 December 2014

Accepted 7 December 2014

Available online 3 February 2015

ABSTRACT

Using 21,406 hydrographic profiles from 1979 to 2012, we present the first observational, pan-Arctic assessment of Mixed Layer (ML) properties, including quantification of seasonal and interannual variability, and identification of multiyear ML depth shoaling.

Arctic Mixed Layer Depths (MLDs) vary strongly seasonally, being deeper (~25 to >50 m) in winter than summer (~5–30 m). Eastern Arctic MLDs (regional mean ~20 m in summer, ~70 to 100+ m in winter) are deeper than western Arctic MLDs (~8 m in summer, 30 m in winter). Patchiness, likely related to small-scale sea ice cover variability, is large – standard deviations ~40% of the regional mean.

By binning data into 6 regions (i.e., Chukchi Sea, Southern Beaufort Sea, Canada Basin, Makarov Basin, Eurasian Basin and Barents Sea), we quantify regional seasonal climatologies and interannual variability of ML depth, temperature and salinity. In most regions, ML changes are consistent with seasonal ice melt (~1–3 m) with a ~1.5 times greater sea ice change required in the western Arctic than in the eastern Arctic. In the Southern Beaufort Sea and the Canada Basin, however, other freshwater sources contribute to observed seasonality.

MLDs are significantly correlated with wind only during ice-free times, and even then the relationship only explains 1–20% of the MLD variance. The same wind is 2–3 times more effective at deepening the ML in the eastern Arctic than in the (more stratified) western Arctic. Changes in underlying stratification ($\Delta\rho$) explain ~60% of the MLD variance, with MLDs proportional to $\Delta\rho^{-0.45}$. Weak eastern Arctic stratification permits a wind–MLD coupling comparable to an Ekman model, while the stronger western Arctic stratifications reduce the wind's effectiveness by a factor of 6.

Remarkably, record-length (up to 30-year) trends indicate almost ubiquitous ML shoaling, order 0.5–1 m/yr, both in winter and summer over all the high Arctic (Canada, Makarov and Eurasian basins) and in winter in the peripheral seas (Chukchi, Southern Beaufort and Barents seas), coincident with ML freshening and increased stratification, while wind speed trends are either not significant or decreasing. The freshwater change related to this shoaling is small – order 100 km³/yr. In contrast, the Southern Beaufort Sea shows ML deepening, coincident with decreasing stratification, possibly related to river water being driven away from the coast. Changes in T-S space suggest decreased convection in the Eurasian Basin in the 2000s.

Although in these results it is the absence of sea ice that allows wind-driven ML deepening, the dominance of stratification over wind in determining MLD suggests that even small changes in the Arctic freshwater budget may control MLD variability, with implications for mixing nutrients and heat up into the surface layer and photic zone.

© 2014 Elsevier Ltd. All rights reserved.

Introduction

The depth and properties of the surface Mixed Layer (ML) of the Arctic Ocean are important for many Arctic physical, chemical and

biological processes, e.g., for transfer of heat between ocean, sea ice and atmosphere [e.g., Jackson et al., 2011; Sirevaag et al., 2011; Steele et al., 2011]; and melting/freezing of sea ice (and hence sea ice distribution) [e.g., Morison and Smith, 1981; Shimada et al., 2006; Polyakov et al., 2013]. The ML properties and changes in those properties also influence upper ocean stratification and the supply of nutrients to the photic zone for Arctic ecosystems,

* Corresponding author. Tel.: +1 206 543 6615 (office).

E-mail addresses: ferriz@apl.washington.edu (C. Peralta-Ferriz), woodgate@apl.washington.edu (R.A. Woodgate).

with impacts on the evolution and characteristics of phytoplankton blooms [e.g., Smith and Niebauer, 1993; McLaughlin et al., 2004; McLaughlin and Carmack, 2010; Popova et al., 2010].

The annual cycle of sea ice melt and sea ice formation (and resultant brine rejection) is expected to drive a significant annual cycle in Mixed Layer Depth (MLD), and this has long been locally observed and indeed modeled [e.g., Morison and Smith, 1981; Lemke and Manley, 1984; Polyakov et al., 2013]. There has been much less recognition of the potential for MLD to be affected by wind-driven surface forcing in the Arctic, e.g., by mechanical mixing by storms either directly on the ocean [e.g., Steele and Morison, 1993; Yang et al., 2001], or via sea ice effects such as ice-keel stirring [e.g., Lemke and Manley, 1984] [for a review, see Rainville and Woodgate, 2009; Rainville et al., 2011]. As summer Arctic sea ice extent and thickness have dramatically decreased in recent years [e.g., Stroeve et al., 2008; Kwok and Rothrock, 2009], there is a greater opportunity for Arctic storms to directly stir the ocean, due to increased open water, increased available fetch, and the lesser ability of thin ice to damp surface waves. In competition with these effects, however, is the tendency for increased ice-melt to produce thinner MLDs due to the formation of a strong salinity (and thus density) stratification near the surface, and indeed, the underlying stratification (i.e., the stratification just below the ML) needs also to be taken into account when considering processes affecting MLDs.

Several studies (see discussion below) have quantified MLD at specific locations, and more recently, Ice Tethered Profiler (ITP) data [e.g., Toole et al., 2010; Jackson et al., 2012; Timmermans et al., 2012] have allowed a somewhat less regional (i.e., basin-wide) consideration of Arctic MLD. However, due to the sampling methods (e.g., from ice bergs, ice camps, or from ITPs moored to thick ice), these measurements are still most often highly localized, and frequently have an intrinsic bias towards ice-covered regions.

To the best of our knowledge, there is, to date, no detailed pan-Arctic assessment of observed Arctic MLDs. Moreover, there have been, so far, only point-wise comparisons of interannual changes in MLD within the Arctic [Jackson et al., 2012], and indeed, these comparisons are complicated by different methodologies used to determine MLD and differing spatial sampling. To address these deficiencies, in this paper we compile hydrographic profiles from the entire Arctic Ocean (ice-free and ice-covered regions) from 1979 to 2012 (Fig. 1) and, by using one consistent method of determining MLD, consider the seasonal and interannual evolution of the Arctic ML.

Prior studies of Arctic MLD

The importance of investigating and characterizing the Arctic Ocean's Mixed Layer Depth (MLD) has long been recognized [e.g., Treshnikov and Baranov, 1973] and estimates of Arctic MLDs have been documented since the early 1960s (see Table 1). Yet, for over four decades, there has been no consensus of how best to define the MLD in the Arctic Ocean. For a detailed discussion of MLD estimation methods, see e.g., de Boyer Montégut et al. (2004), Holte and Talley (2009), Kara et al. (2000), Large et al. (1994) and Thomson and Fine (2003), although most of these studies focus on lower latitude observations and draw on the temperature (or temperature-dominated density) variation in the upper ocean, rather than considering the salinity-dominated density typical of the Arctic Ocean.

Within the Arctic, MLD is typically defined by one of the following methods:

- (a) the minimum depth at which a large increase in density occurs [e.g., Morison and Smith, 1981]; or the depth of the maximum density gradient between the surface and a certain depth [e.g., at 70 m deep, Timmermans et al., 2012];

- (b) the depth at which, compared to the surface value, density has increased by 20% of the difference between the surface value and the density at 100 m deep, with the surface density value being defined as the shallowest density measured [Shaw et al., 2009] or the density at 10 m depth [Sirevaag et al., 2011].
- (c) the maximum depth at which the density is within a certain threshold of the shallowest measured density (e.g., 0.01 kg/m³ [Jackson et al., 2010; Toole et al., 2010; Gimbert et al., 2012; Timmermans et al., 2012]; 0.03 kg/m³ [Toole et al., 2010; Jackson et al., 2012]; 0.1 kg/m³ [Toole et al., 2010]; 0.125 kg/m³ [Polyakov et al., 2013]; 0.2 kg/m³ [Steele et al., 2011]; and 0.25 kg/m³ [Timmermans et al., 2012]); and
- (d) the depth of the maximum buoyancy frequency, N [e.g., Jackson et al., 2012].

In addition, as per Rudels et al. (1996) and more recently Korhonen et al. (2013), the depth of the winter mixed layer may be inferred from the depth of the temperature minimum left in summer as a remnant of winter convection (defined by these authors as the Polar mixed layer).

With the exception of (d), all of these methods are to some extent arbitrary, requiring a threshold value either in a property or in the percentage of change of a property. While most of these methods give similar results, differences in methodology often confound a quantitative inter-comparison of different studies.

Table 1 summarizes different methods that have been used to estimate Arctic MLDs, including quantification of MLD when provided. Early studies [e.g., Coachman and Barnes, 1961; Morison and Smith, 1981] suggest Arctic MLDs of ~50 m, but it is important to remember that these measurements are taken from the ice-island T-3, a floating iceberg with a draft of ~30 m which might influence mixing in the region around the berg. Treshnikov and Baranov (1973) find MLDs of 25–50 m from many regions of the Arctic, and also report (but do not quantify) MLD seasonality. From ice camps in the Beaufort Sea, Lemke and Manley (1984) find MLDs varying seasonally from 20 to 60 m, very similar to values obtained from the northeast of Svalbard [Steele and Morison, 1993], though in the latter case, storms also cause upwelling along the slope, enhancing vertical mixing leading to ice melt, thus restratifying the upper ocean and shoaling the MLD. From the Eurasian Basin Oden expedition in 1991, Anderson et al. (1994) report significant spatial variability in MLDs (from 10 m to 40 m) in summer, while from the same cruise, Rudels et al. (1996) show summer profiles with similar MLDs (~35 m), but infer much deeper winter MLDs (~64–120 m). More recent work [Korhonen et al., 2013] similarly infer winter MLDs (equivalent to the thickness of the Polar mixed layer, see Rudels et al. (1996)) of between 36 and 70 m across the Arctic from 1991 to 2011.

Generally, both older and recent estimates of MLD consistently suggest that Arctic MLDs are deeper in winter than in summer but published observations are generally sparse in space, and winter MLD estimates are still very rare. Recent year-round hydrographic data from Ice-Tethered Profilers (ITP) partly address this and have contributed to our understanding of the seasonal evolution of MLDs. Beaufort Sea measurements indicate an annual cycle with MLDs ~16 m in summer and ~24 m in winter [Toole et al., 2010], although the drift of these buoys aliases temporal and spatial variability. Also note that these ITP studies are from thick ice regions and prior to 2007 are not pan-Arctic, but have been mainly focused in the Canada Basin [e.g., Toole et al., 2010; Jackson et al., 2012; Timmermans et al., 2012], although since 2007 ITPs are being deployed in other basins of the Arctic [Toole et al., 2011; Polyakov et al., 2013].

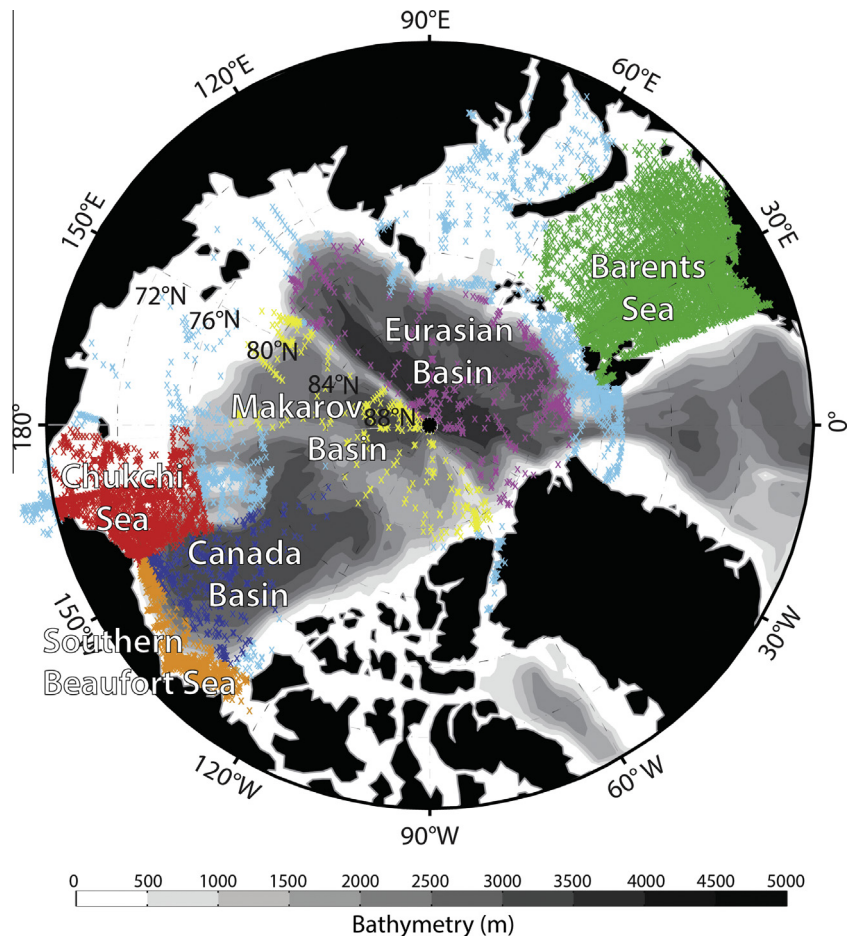


Fig. 1. Arctic Ocean map showing the locations of all the 21,406 CTD/XCTD casts used in this study, color-coded by region – Chukchi Sea (red), Southern Beaufort Sea (orange), Canada Basin (dark blue), Makarov Basin (yellow), Eurasian Basin (magenta), and Barents Sea (green). Bathymetry is from GSHHG (Global Self-consistent, Hierarchical, High-resolution Geography Database, <http://www.ngdc.noaa.gov/mgg/shorelines/gshhs.html>). Cyan dots indicate observations not used in the regional averages of Section ‘Defining Arctic regions for a regional monthly MLD climatology’ onwards. (For interpretation of the references to color in this figure legend, the reader is referred to the web version of this article.)

Goals of current work

In this current work, we aim to close the gaps in past analysis, by using a consistent definition of MLD over the *entire* Arctic basin to analyze hydrographic casts from ships and from ice camps taken in the last 3 decades.

The primary goal of this work is to describe seasonal and interannual variability in observed Arctic MLDs, and provide quantitative, pan-Arctic climatologies that may be used for various Arctic studies, including, for example, ecosystem studies and model verification. We also seek to understand the physical drivers of MLD change. As Arctic sea ice extent and thickness have dramatically decreased in recent years, an immediate question is how these sea ice changes have impacted Arctic MLDs. Are we moving to an Arctic where increased open water allows for summer wind-driven increases in MLD? Or are the thermodynamic processes of brine rejection and melt water formation dominant? We will attempt to address these questions from the observational dataset.

Section ‘Pan-Arctic hydrographic observations from 1979 to 2012’ of this paper describes the datasets used in this study. Section ‘Determination of Arctic Mixed Layer Depth (MLD)’ considers the methodology used in this paper to estimate MLD, including comparisons with prior work. Section ‘Observed temporal and spatial variability of Arctic Mixed Layer Depths (MLDs)’ quantifies temporal and spatial variability in MLD, including monthly clima-

tologies for six Arctic regions. Physical drivers of MLD change (sea ice thermodynamics, wind-driven mixing, and the effects of stratification) are investigated in Section ‘Physical drivers of seasonal Mixed Layer Depth (MLD) change’. Section ‘Interannual and decadal variability in Arctic Mixed Layer properties’ considers interannual variability and long-term trends. Summary and conclusions are given in Section ‘Summary and conclusions’.

Pan-Arctic hydrographic observations from 1979 to 2012

Hydrographic data – inventory, quality control, and accuracy

For this study, we use historic Arctic hydrographic data from the National Oceanographic Data Center’s World Ocean Database (NODC-WOD) (<http://www.nodc.noaa.gov/>), supplemented with data from the individual Arctic expeditions listed in Table 2. Temperature and salinity (T-S) profiles are from CTD (Conductivity-Temperature-Depth) or XCTD (eXpendable-Conductivity-Temperature-Depth) casts. In our analysis, we chose to exclude the observations from ITP data because we wish to be able to quantify MLDs that may be shallower than the minimum MLD the ITPs can identify (order 10 m [Toole et al., 2010]). Throughout the paper, unless otherwise stated, we cite salinity on the Practical Salinity Scale [Lewis, 1980] and indicate this by using the dimensionless

Table 1

Summary of methodology and estimates from prior observational Arctic Mixed Layer Depth (MLD) studies.

Publication	Region of observation	MLD definition	Winter MLD	Summer MLD	Comments
Coachman and Barnes (1961) Data from 1902 to 1960	North Pole	Loosely defined by T and S gradient	~50 m all 3 regions, undefined seasonality		Taken from iceberg T-3, which had a draft of 40–50 m
Treshnikov and Baranov (1973) Data from 1937 to 1955	Fram Strait Canada Basin Chukchi, Spitsbergen, Severnaya Zemlya, Central Arctic Basin, North of Greenland	Loosely defined as vertical density distribution: cites Blinov (1963)'s criterion (not referenced here)	~25 m 10–25 m 25–50 m 25–50 m		Various stations. No seasonality specified, but they record that seasonal variability exists
Morison and Smith (1981) Data from 1970 to 1973	Eastern Beaufort	Depth of largest density (σ) gradient	56 m	41 m	Taken from iceberg T3, which had a draft of ~30 m
Lemke and Manley (1984) Data from 1975 to 1976	Beaufort Sea	$\Delta S = 0.1 \text{ psu}$	60 m	20 m (min)	AIDJEX ice camp observations and 1D model
Steele and Morison (1993) Data from October 1988	NE of Svalbard	Fit of profile to idealized salinity structure	30–40 m (October)		SALARGOS buoy – central to shelf
Anderson et al. (1994) Data from 1991	Eurasian Basin	$\Delta S = 0.1 \text{ psu}$	–	South 10 m; Central 25 m; near Morris Jessup Plateau 40 m	Oden91 cruise
Rudels et al. (1996) Data 1980, 1987, 1991	Nansen and Amundsen basins	Relative to salinity ~34.3 psu (winter)	50 m, individual casts often reach 60–124 m	25–35 m	Oden91 and previous cruises
Yang et al. (2004) Data from 1992 to 1998	Beaufort Sea	Inferred from homogeneity of T and S between 2 sensors at 8 and 45 m	45 m	8 m	IOE Buoys (only 2 depths were measured)
Shaw et al. (2009) Data from 1997 to 1998	Canada Basin	Depth where σ increases by 20% of the density difference between 100 m and the surface value	40 m	20 m	SHEBA ice camp
Toole et al. (2010) Data from 2004 to 2009	Canada Basin	$\Delta\sigma = 0.01 \text{ and } 0.1 \text{ kg/m}^3$	24 m	16 m	ITP buoys deployed on thick ice
Sirevaag et al. (2011) Data from 2008	Eurasian Basin	Depth at which σ increases by 20% of the density difference between 100 m and the avg. upper 10 m	67–74 m	20–35 m	ITP buoys and ice camp
Jackson et al. (2012) Data from 2005 to 2010	Canada Basin	$\Delta\sigma = 0.01 \text{ and } 0.03 \text{ kg/m}^3$	30 m	10 m	ITP buoys
Mizobata and Shimada (2012) Data from 2007 to 2010	Chukchi Borderland	Sea surface temperature (SST) technique			Used microwave radiometer AMSR-E in open-water only, validated with 3 casts from Mirai2008 ITP buoys (winter only)
Timmermans et al. (2012) Data winter 2009/2010	Canada Basin	$\Delta\sigma = 0.01 \text{ and } 0.25 \text{ kg/m}^3$ and maximum gradient criterion	10–30–40 m	–	ITP buoys (winter only)
Polyakov et al. (2013) Data from 2009 to 2010	Eurasian Basin	$\Delta\sigma = 0.125 \text{ kg/m}^3$	~60 m (March)	~20 m (September)	Two ITP buoys
Korhonen et al. (2013) Data from 1991 to 2011	Nansen, Amundsen, Makarov and Canada basins	Depth of temperature minimum; if unclear, depth of rapid Salinity change	~70 m (Nansen); ~57 m (Amundsen and Makarov); ~45 m and ~35 m (North and South Canada Basin)		Infers winter MLD from remnant of winter convection in summer data

designator “psu”. Also, in keeping with the vintage of the data, we use the UNESCO 1980 standards for properties of sea-water to convert temperature, conductivity and pressure to density [EOS-80, Fofonoff, 1985].

The accuracy of temperature, salinity, and pressure data has improved significantly over three decades of data used in this study. The accuracies of modern (i.e., 1990s to present) Arctic data are ~0.002 °C, 0.002 psu and 1–2 dbar [e.g., Anderson et al., 1994; Swift et al., 1997; McLaughlin et al., 2004; Woodgate et al., 2007], although individual sets of recent data may have lower accuracy

(e.g., some data cited in McLaughlin et al. (2004) as 0.02 °C, 0.02 psu). Older references are cited as less accurate (e.g., Coachman and Aagaard (1974), their Fig. 7, ~0.1 °C, 0.1–0.15 ppt; Coachman and Barnes (1962), their Fig. 6, ~0.1 °C, ~0.1 ppt). As will be seen below, our identification of MLD relies only on an accuracy of ~0.1 kg/m³, equivalent to >0.1 psu at the freezing point, easily resolved by all but the oldest data. In practice, we find that even the oldest data accuracy is sufficient for our purpose.

To match the start of remotely-sensed sea ice observations, we consider only casts with both temperature and salinity (T - S) in the

Table 2

Datasets used to supplement NODC-WOD data collection (see Section 'Hydrographic data – inventory, quality control, and accuracy'). Numbers in parenthesis indicate number of cruises.

Program/cruise	Region	Expedition dates
AIWEX 1985	Beaufort Sea	March–May, 1985
ARKTIS IV-3, 1987	Eurasian Basin	July–August, 1987
CEAREX 1989	Northern Fram Strait	March–April, 1989
SHEBA 1997–1998	Canada Basin	October 1997–September 1998
JOIS 1997	Beaufort Sea	September–October, 1997
Oden 2001	Eurasian Basin	July–August, 2001
SCICEX 2001 xctds	Central Arctic	June, 2001
SBI2002: Healy (2) & Polar Star (1)	Chukchi and Beaufort Seas	May–August, 2002
CBL 2002	Chukchi Borderland	August–September, 2002
SBI2003: Healy (1) & Palmer (1)	Chukchi and Beaufort Seas	July–October, 2003
SBI Heto winter 2003	Chukchi and Beaufort Seas	April, 2003
SCICEX 2003	Central Arctic, North Pole, Eurasian and Makarov basins	October, 2003
SBI2004: Healy (3)	Chukchi and Beaufort Seas	May–September, 2004
SBI winter 2004	Chukchi and Beaufort Seas	April, 2004
Oden 2005	Pan-Arctic	August–September, 2005
NPEO 2009–2012	North Pole and Beaufort Sea	April, 2009–2012
SWITCHYARD	Lincoln Sea	May, 2004–2005, 2007–2011
MIRAI 2008	Chukchi and Beaufort Seas	August–September, 2008
Smirnitsky 2008	Siberian Shelves	August–September, 2008
BGEP 2009–2011	Beaufort Sea	August and September 2009–2011
MIRAI 2010	Chukchi and Beaufort Seas	September–October, 2010

time period 1st January 1979 to 31st December 2012 inclusive, and that are north of 66.5°N (but excluding the Greenland and Norwegian seas and the Canadian Archipelago). This yields a total of 34,165 profiles. Next, obviously erroneous TS profiles are rejected (e.g., those with salinity values greater than 35 psu; those with density decreasing with depth), as are very noisy profiles. We then reject profiles with insufficient vertical resolution to estimate MLD, i.e., since we anticipate MLDs may be less than 10 m, we discard profiles with sampling vertical resolution equal to or greater than 5 m (depth resolution in the collected casts is generally 1–2 m), and profiles where the first measurement is 10 m or deeper. We note that several of the data used in this study are collected from ice-breakers, which often have drafts of more than 5 m (e.g., the USCGS Polar Star and the German Polarstern both have drafts ~10 m). It is an open question as to what extent these deep ship's drafts may mix the upper water column sampled in the hydrographic casts, likely dependent on the ship and CTD/XCTD deployment method [Jackson et al., pers. comm.]. Thus, since a complete assessment of this is beyond the scope of our current work (and indeed it is unclear if sufficient data currently exist to address this question), in this work we will treat the archived casts to be a true representation of the upper water column, while noting that ship-draft issues may cause us to overestimate shallow MLDs.

Supporting datasets: sea ice concentration and surface wind speed

For sea ice concentration data, we use daily-averaged sea ice concentration values from the National Snow and Ice Data Center (NSIDC, <http://nsidc.org/data/nsidc-0051>), estimated from Passive Microwave satellite data. This NSIDC sea ice concentration product has a spatial resolution of 25 km × 25 km and quoted accuracies of ±5% during winter and between ±15% and ±30% during the summer [Cavalieri et al., 1996; Comiso and Kwok, 1996].

Since *in situ* measurements of wind speed are sparse in the Arctic, as an estimate of local wind speed we compute speed from daily averages of surface winds (u and v at 10 m) obtained from NCEP/NCAR Reanalysis 1 data [Kalnay et al., 1996] provided by the NOAA/OAR/ESRL PSD, Boulder, Colorado, USA, <http://www.esrl.noaa.gov/psd/data/reanalysis/reanalysis.shtml>, with a spatial resolution of 2.5° latitude × 2.5° longitude. A comparison [Schweiger, pers. comm.] of these NCEP data with daily wind speeds from

the SHEBA (Surface Heat Budget of the Arctic Ocean, www.eol.ucar.edu/projects/sheba) experiment and observations at the NPEO (North Pole Environmental Observatory, <http://psc.apl.washington.edu/northpole/>) suggests that NCEP daily wind speeds are well correlated with observations ($r \sim 0.8$), but that NCEP magnitudes are ~20% lower than observed wind speeds. This bias should be kept in mind in the relationships derived below in Section 'Relationship of MLD to wind forcing and sea ice cover'.

In addition to NCEP data, for comparison we use daily averages from three other 10 m wind products, viz.

- (a) hourly data from the Modern-Era Retrospective Analysis for Research and Applications (MERRA) with spatial resolution ½° latitude and 2/3° longitude (<http://disc.sci.gsfc.nasa.gov>);
- (b) 6-hourly ERA Interim data from the European Centre for Medium-Range Weather Forecast (ECMWF) with spatial resolution of 0.7° (<http://www.ecmwf.int/en/forecasts/datasets>); and
- (c) 6-hourly JRA data from the Japanese 55-year Reanalysis [JRA55, Japan Meteorological Agency, 2013] with spatial resolution of 0.56° (CISL Research Data Archive, <http://rda.ucar.edu/datasets.ds628.0/>).

Determination of Arctic Mixed Layer Depth (MLD)

As introduced in Section 'Prior studies of Arctic MLD', there are many methods used in the literature to estimate MLD from hydrographic data (Table 1). After several tests, we choose for this paper to estimate MLD by using a threshold criterion of $\Delta\sigma = 0.1 \text{ kg/m}^3$, where $\Delta\sigma = \sigma(z) - \sigma(z_{min})$; $\sigma(z)$ is the potential density at a given depth, z ; and z_{min} is the shallowest measured depth. Thus, the MLD used in this paper is the maximum depth at which the potential density is within 0.1 kg/m^3 of our best estimate of the surface density, i.e., the density of the shallowest measurement. (Recall that we reject profiles that start at 10 m or deeper, as discussed above.)

We choose this method since, by inspection of large numbers of profiles in all the regions of the Arctic, we find that this method and threshold yield – with a very few exceptions – results that agree well with a typical user's heuristic assessment of MLD, which identifies (primarily) the shallowest significant step in water prop-

erties. Although the heuristic assessment often corresponds to the maximum density gradient (or buoyancy frequency, N) as illustrated by Jackson et al. (2012) (their Figs. 2–4), use of an N -based criterion frequently overestimates the MLD, since the base of the ML is the shallowest significant change in density, which is not necessarily the largest change in density in the profile.

To see how sensitive results are to the choice of threshold and to allow for useful inter-comparison with prior Arctic work using other thresholds (Section 'Prior studies of Arctic MLD' and Table 1), we compare our 0.1 kg/m^3 threshold method with three other methods that have been used in the Arctic Ocean, viz. (a) a smaller threshold criterion of $\Delta\sigma = 0.03 \text{ kg/m}^3$ [Toole et al., 2010; Jackson et al., 2012]; (b) larger threshold criterion of $\Delta\sigma = 0.3 \text{ kg/m}^3$ (e.g., $\Delta\sigma = 0.2 \text{ kg/m}^3$ for the full Arctic Ocean [Steele et al., 2011] and $\Delta\sigma = 0.25 \text{ kg/m}^3$ for the Canada Basin [Timmermans et al., 2012]); and (c) as per Shaw et al. (2009), taking MLD as the maximum depth where, compared to the shallowest density measured, the potential density is within 20% of the density difference between the surface (or shallowest sample measured) and 100 m (or the deepest measurement available if maximum sampling depth was less than 100 m). See Fig. 2 for examples.

In all three tests (not shown), ~60% of the results are within 3 m of results from our MLD method, though we find the smaller (greater) threshold criterion method tends to underestimate (overestimate) the MLD compared to the heuristic assessment discussed above.

Thus, we use 0.1 kg/m^3 in this work because it provides a better comparison with the heuristic method in all the pan-Arctic profiles. Note our threshold falls in the middle of all ranges of density thresholds used in the Arctic Ocean. Note also that the temporal evolution of MLD is generally consistent from method to method (not shown). Therefore, selecting any of the other threshold density values previously reported would likely provide qualitatively similar results to the analysis presented here.

(In 40 of the 519 profiles from the Eurasian Basin, we find that the upper ocean stratification is so weak that the threshold criteria of $\Delta\sigma = 0.1 \text{ kg/m}^3$ yields MLD estimates more than 20 m deeper than those from a heuristic assessment of the profile. Thus, for these 40 profiles (all in winter), we use instead a threshold criteria of $\Delta\sigma = 0.03 \text{ kg/m}^3$, which gives closer agreement with the heuristic assessment. This change has a small but noticeable effect on the Eurasian basin-averaged winter MLD (see Table 3), reducing it from 80 m, with standard deviation (std) of 33.7 m, to 73 m (std 26.5 m).)

Once MLDs are estimated, we apply one further selection criteria. If the estimated MLD falls within 2 m of the shallowest sampled density or within the first three samples of the profile, that cast is eliminated. This is to avoid profiles that started too deep to capture the surface mixed layer properly. This criterion removes ~5000 casts, leaving us with a final set of 21,406 CTD and XCTD profiles, which then fulfill all our selection criteria, viz.:

- lie between 1st January 1979 and 31st December 2012; lie north of 66.5°N , but not in the Greenland or Norwegian Seas or the Canadian Archipelago;
- satisfy basic quality control criteria (e.g., density increasing with depth, salinity values less than 35 psu, and reasonable signal to noise-ratio);
- have vertical resolution $\leq 5 \text{ m}$;
- have shallowest depth $< 10 \text{ m}$;
- have estimated MLD $> 2 \text{ m}$ deeper than the shallowest measurement; and
- have at least 3 data points shallower than the estimated MLD.

The coverage of these 21,406 casts is shown in Fig. 1.

Observed temporal and spatial variability of Arctic Mixed Layer Depths (MLDs)

Monthly seasonality of Arctic Mixed Layer Depths (MLDs)

Using this set of 21,406 CTD and XCTD casts (Fig. 1), we compute the MLD for each profile as discussed above, i.e., using the density threshold criterion of $\Delta\sigma = 0.1 \text{ kg/m}^3$ apart from 40 profiles in the Eurasian Basin.

Fig. 3 shows MLD collated by month of measurement (regardless of measurement year). This collation clearly shows significant seasonal changes in MLD, with MLDs being generally deeper (~25 to >50 m) in winter (i.e., November through May) than in summer (~5 to 30 m) (i.e., June through September), although coverage is very poor in winter months of November to March.

To assess the representativeness of our results, we must first consider how well our data capture the evolution of the seasonal cycle. There are two processes that act to increase MLD – brine rejection from sea ice formation, and wind-driven stirring either through ice or over open water – and two processes that act to decrease MLD – addition of stratification (e.g., local ice melt providing a fresh surface layer, advection of less dense waters such as river waters, or warming) and restratification processes [e.g., eddy-driven stratification of horizontal density differences, Boccaletti et al., 2007; Timmermans et al., 2012]. The seasonality of these processes is different. If MLD change were dominated by sea ice growth/melt, one would expect the maximum MLD at the time when brine-rejection is complete, i.e., the time of maximum ice thickness [e.g., April–May, Rothrock et al., 1999; Perovich et al., 2008]. The thinnest MLDs would then occur at the onset of melt (likely under existing ice), with MLD increasing with increasing melt. In contrast, the seasonality of wind-driven stirring depends on both the seasonality of the wind (which in the Arctic is weak, only a 10% seasonal change, with winds being weakest in May–July, e.g., Lindsay (1998) and Martin et al. (2014)) and the seasonality of the wind-water coupling, which is mediated by the ice cover. Prior observational results from the Chukchi Sea [Rainville and Woodgate, 2009] suggest maximum wind-driven deepening of the MLD at ice-free times (late summer). One may also hypothesize wind-driven stresses transferred through the ice would be maximum when sea ice is the most mobile [i.e., August–October, Rampal et al., 2009], which is also the time of the minimum sea ice extent. However, recent modeling work [Martin et al., 2014] suggests that a greater sea ice concentration (~80%) may be more efficient at transferring wind-stress to the ocean, and finds instead the maximum transfer of momentum to the ocean in the early winter (September–January).

Prior observations from Jackson et al. (2012) (from one ITP in the Canada Basin) suggest a minimum MLD in August, with deepening from September through the end of February, in agreement (at least in winter) with the theoretical ice-growth/ice-melt scenario. Similarly, Toole et al. (2010) report that Canada Basin MLDs are shallowest in July and August, and deepen through September to November to a winter maximum that increases only slightly for the rest of the year. Possibly this reduced increase in late winter reflects that the ITPs are under thick ice with only modest ice growth.

Our data have good coverage in April and to some extent May (Fig. 3), and thus likely do a reasonable job of estimating the MLD at the end of the winter, the expected maximum if related to sea ice growth. Similarly, the summer coverage of our data is good in the low-ice months of August and September, and thus likely provides a reasonable estimate of summer MLDs, even though this is probably not the minimum of the MLD, which likely occurs earlier in the year. Coverage in the transition months is

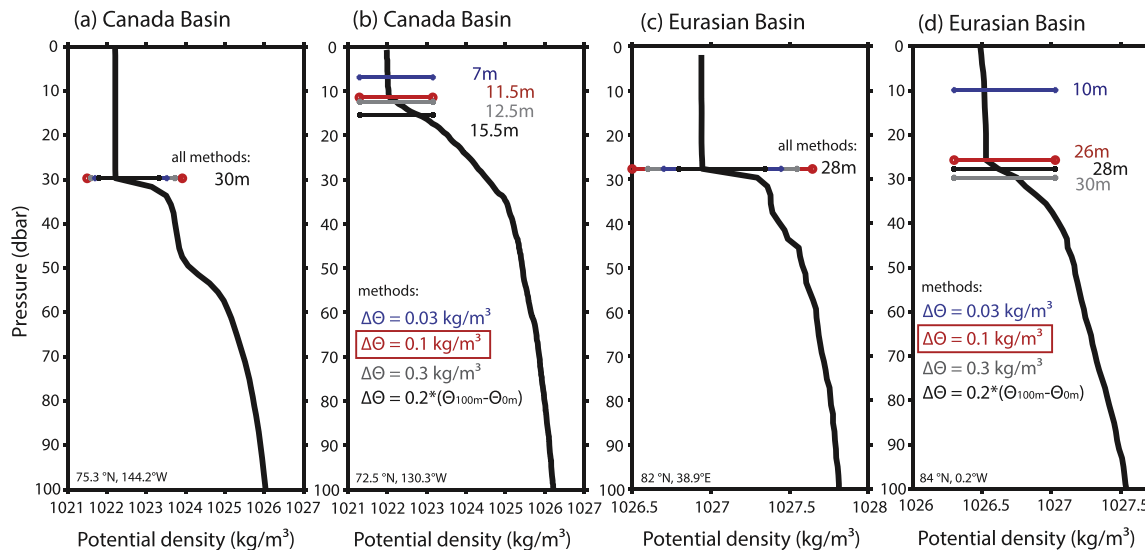


Fig. 2. Four selected potential density profiles from the Canada Basin (a and b) and the Eurasian Basin (c and d) illustrating estimates of mixed layer depth using some of the different methods explained in Section 'Prior studies of Arctic MLD' and discussed in Section 'Determination of Arctic Mixed Layer Depth (MLD)'. For a sharp change in the gradient of potential density (a and c), all methods agree in their estimate of MLD, however, for less extreme changes in potential density gradient (b and d), estimates differ substantially, and our chosen threshold ($\Delta\sigma = 0.1 \text{ kg/m}^3$, shown in red) best matches a heuristic measure of MLD. In the cases presented here, our best estimate would also match the maximum in buoyancy frequency, however this is not always the case (see e.g., Jackson et al. (2012), their Figs. 2–4). (For interpretation of the references to color in this figure legend, the reader is referred to the web version of this article.)

Table 3

Statistics of monthly averaged winter (November–May) and summer (June–September) Mixed Layer Depths (MLDs) as estimated for the 6 regions of this study (see Section 'Defining Arctic regions for a regional monthly MLD climatology') for all observations in that region (first row for each region, indicated by italics); for ice-free observations (ice concentration, ic, <15%), and for ice-covered observations (ic $\geq 15\%$), showing mean (in bold), median, standard deviation (SD), 95% Confidence Interval (CI, designated by the \pm symbol, calculated assuming all measurements are independent), and month of the maximum/minimum MLD (second and third row for each region).

Region	Winter maximum		Summer minimum	
	MLD (mean, median, SD, \pm CI) in m	Month of max MLD	MLD (mean, median, SD, \pm CI) in m	Month of min MLD
Chukchi Sea	34.6 , 32.6, 13.9, ± 3.3	March	12.3 , 10.8, 7.0, ± 0.8	July–August
Ice free	–	–	10.4 , 9.0, 3.9, ± 2.4	June
Ice-covered	34.6 , 32.6, 13.9, ± 3.3	March	11.3 , 10.8, 5.4, ± 1.2	July–August
Southern Beaufort Sea	29.0 , 28.7, 12.1, ± 1.6	March	8.5 , 7.4, 5.1, ± 1.4	July–September
Ice free	–	–	8.8 , 7.9, 5.7, ± 1.8	July
Ice-covered	29.0 , 28.7, 12.1, ± 1.6	March	8.0 , 6.9, 4.0, ± 1.8	July–September
Canada Basin	33.1 , 34.5, 8.1, ± 1.8	April	8.9 , 7.9, 3.6, ± 1.2	July–August
Ice free	–	–	8.7 , 8.9, 3.8, ± 1.4	August
Ice-covered	33.1 , 34.5, 8.1, ± 1.8	April	8.7 , 7.9, 3.6, ± 1.2	July
Makarov Basin	52.0 , 50.0, 14.0, ± 2.9	May	16.0 , 15.8, 2.4, ± 1.4	September–October
Ice free	–	–	11.8 , 12.8, 4.7, ± 1.8	September
Ice-covered	52.0 , 49.9, 14.0, ± 2.9	May	16.0 , 15.8, 2.4, ± 1.4	October
Eurasian Basin	72.5 , 77.5, 26.5, ± 4.6	April	22.3 , 19.0, 13.5, ± 2.9	July–September
*all casts $\Delta\sigma = 0.1 \text{ kg/m}^3$	*80.3 , 82.0, 33.7, ± 5.9	*April		
Ice free	–	–	11.9 , 12.9, 4.3, ± 2.0	September
Ice-covered	72.5 , 77.5, 26.5, ± 4.6	April	22.4 , 19.8, 12.8, ± 2.9	July–August
Barents Sea	168 , 165, 77.5, ± 3.3	February	17.7 , 15.0, 12.2, ± 1.0	July
Ice free	170 , 168, 76.7, ± 3.3	February	18.0 , 15.0, 12.3, ± 1.0	July
Ice-covered	111 , 105, 72.4, ± 6.4	March	10.3 , 8.0, 5.9, ± 1.0	July

As discussed in Section 'Determination of Arctic Mixed Layer Depth (MLD)', 40 casts in the Eurasian Basin winter average use $\Delta\sigma$ of 0.03 kg/m^3 for MLD identification, and for comparison, indicated by *, are the statistics using the usual $\Delta\sigma$ of 0.1 kg/m^3 .

generally rather sparse however. Moreover, there is a strong seasonal spatial bias – different regions of the Arctic are sampled in different seasons. For example, in the high Arctic, winter measurements are typically found in the (thick ice) region north of the Canadian Archipelago and Greenland, while in summer measurements are generally taken in the other regions of the Arctic.

Throughout the paper, motivated by the seasonal change in ice cover, we will consider November to May as winter, and June to September as summer.

Spatial variability of Arctic Mixed Layer Depths (MLDs)

Fig. 3 suggests that, in any month, MLD varies significantly across the Arctic. For example, summer MLDs are deep (>40 m) in the southeastern Barents Sea and the center of the Arctic (~30–50 m), with some shoaling of MLDs towards the southern Canada Basin (MLD < 20 m). Given changing spatial sampling from year to year, this figure may alias interannual change into spatial change, and thus, to avoid this, we first consider MLD patterns

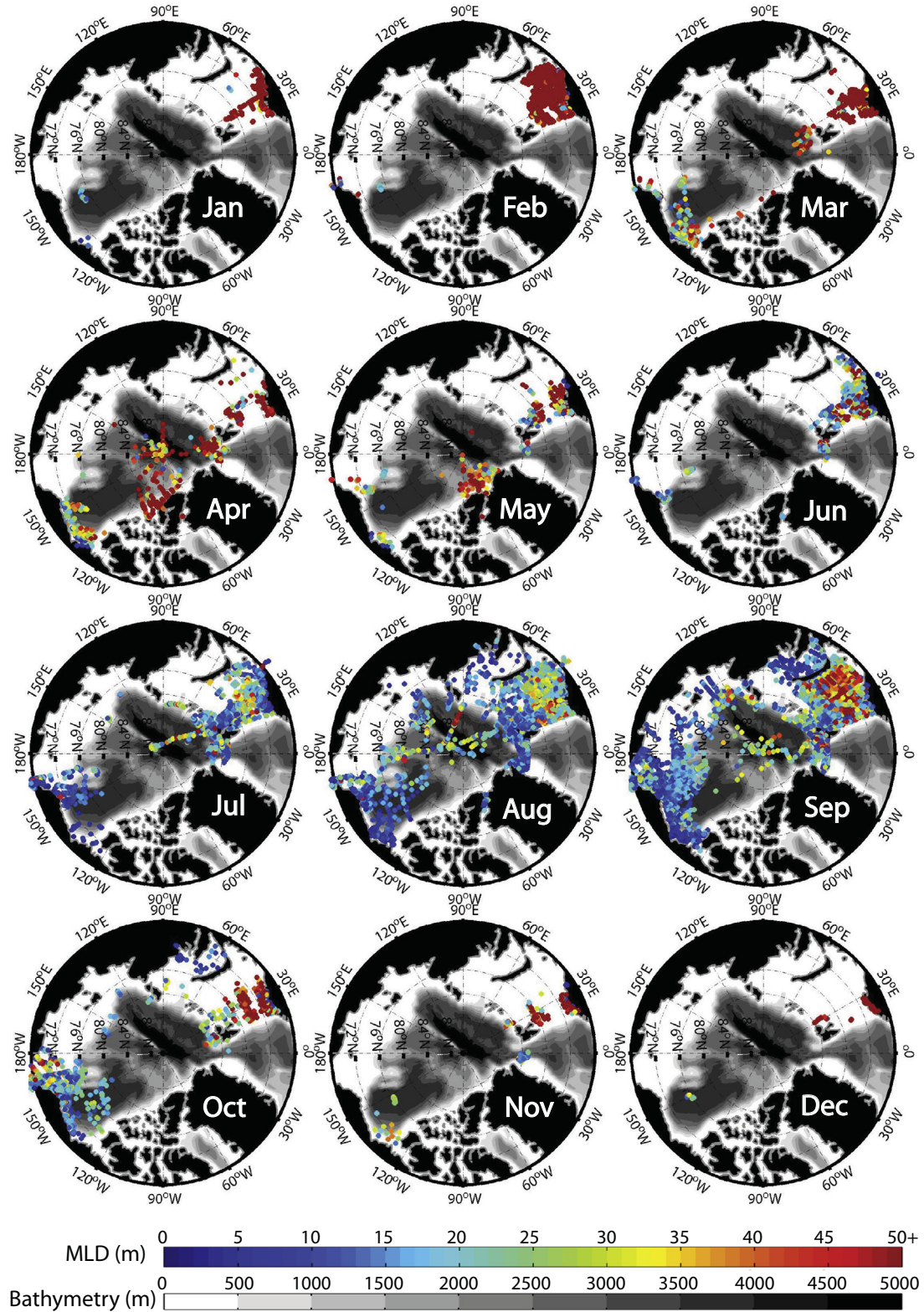


Fig. 3. Mixed Layer Depths (MLDs) estimated from all profiles from 1979 to 2012, collated by month. Bathymetry from GSHHG.

from individual years (Figs. 4 and 5). Within the year, to avoid aliasing the seasonal cycle, we similarly consider only distinct parts of the year, viz. late winter (taken as April and May) and late summer (taken as August and September), choosing two months in each case to give reasonable spatial coverage.

For late winter, the years with the most extensive spatial coverage in the high Arctic are 1993, 2002, 2004, 2005, 2007, 2008, 2010 and 2011, some of which are shown in Fig. 4. In the central Arctic, these winters generally show MLDs are deeper in the Eurasian Basin ($\sim 60\text{--}80$ m) than in the Makarov and Canada basins ($\sim 40\text{--}$

60 m). Earlier winters (e.g., 1992 and 1994, not shown) suggest the further shoaling of the MLD towards the Southern Beaufort Sea and the Beaufort coast (from ~40 m to ~10 m). In the central Arctic, 2005 somewhat contradicts this pattern, however, with deeper MLDs north of Greenland. The salinities of the ML show a clearer pattern, with the Eurasian Basin always being saltier than the Makarov Basin or the regions to the west, consistent with known surface distribution of salinity [e.g., Coachman and Barnes, 1962; Jones et al., 2008]. Similar basin-wide variability is found in a recent analysis [Korhonen et al., 2013] of winter ML properties inferred from a smaller set of ice-breaker data from 1991 to 2011. Their data similarly shows winter MLD shoaling and freshening from ~70 m and ~33.9 psu in the Nansen Basin to ~36 m and ~28.6 psu in the Southern Canada Basin.

For late summer, similar pan-Arctic shoaling from the Eurasian Arctic to the Canadian Arctic is observed (Fig. 5), e.g., in 1993 and 2005, data show deeper MLDs in the Eurasian Basin (~30–40 m), and MLD shoaling towards the Canada Basin (~20 m) and further towards the Southern Beaufort Sea (~10–15 m). The late summer ML salinities show similar basin scale differences as in late winter, with the ML in the Eurasian and Makarov basins and the Barents Sea being saltier (~35 psu) than the ML in the Canada Basin (~28–30 psu) and in the Southern Beaufort Sea (~15–20 psu).

In both winter and summer, there is also substantial spatial variability within the Barents Sea. While data coverage is typically sparse in winter, summer data suggest MLDs of ~30 m near the central Barents Sea, shoaling to 20 m and 10 m towards the coast and towards the Arctic Basin. There is also strong interannual variability, and this will be discussed further in Section 'Interannual and decadal variability in Arctic Mixed Layer properties'.

In addition to the basin-wide trends, another notable feature of these collations is the variability of MLD on comparatively short spatial scales (i.e., scales much smaller than the Arctic basins). For example, consider the two summer pan-Arctic crossings – one in 1994 and one in 2005 (Fig. 5). Part of the 1994 AOS section in the western Arctic from 80.7°N to the Pole (~1000 km), taken over 15 days (August 9th–23rd, 2004) has MLDs ranging from 8 to 33.6 m (mean 21.5 m, standard deviation (std) 7.6 m, 42 measurements). Similarly, the comparable part of the Oden 2005 section from ~79.5°N to the Pole (~1150 km total), taken over 18 days (August 27th–September 13th, 2005) has MLDs ranging from 8 to 39.6 m (mean 19.5 m, std 7.5 m, 24 measurements). In both cases, the station spacing varies greatly across the section, i.e., from ~0.02 km (repeat stations) to 164 km in the 1994 AOS section, and from ~0.28 km (repeat stations) to 179 km in the Oden 2005 section. However, inspection of the MLDs along these sections shows little coherence between stations, suggesting MLD may vary on spatial scales of much less than 10s of kms, although this result relies on considering the sections as synoptic, which is obviously not the case.

Although the number of available casts is small, in winter the MLD variability appears to be even larger. For example, in 2005, the profiles along the NPEO expedition from 86°N to the North Pole along 90°E (~450 km) in the Eurasian Basin (Fig. 4), taken over 1 day (April 27th–28th), show MLDs ranging from 43 to 79 m (mean 63 m, std 15 m, 4 measurements). The comparable part of the NPEO expedition in 2008, taken over 9 days (April 10th–19th) has MLDs ranging from 61 to 75 m (mean 71 m, std 6 m, 5 measurements). In 2011, the same section of the NPEO expedition, taken over 2 days (April 17th–19th), has MLDs ranging from 37 to 71 m (mean 57 m, std 13 m, 5 measurements).

These examples illustrate the patchy (or possibly rapidly changing) nature of MLD in the Arctic. In terms of spatial scales, since atmospheric forcings of MLD (heating, cooling, wind stress) are large scale (e.g., ~1000s km), the short spatial scales likely arise from structure in the ocean (e.g., in ocean fronts or stratification,

meso and submesoscale features), or in the sea ice cover, which can vary on length scales of meters and up. For example, leads in the ice may give rise to regions of enhanced ice formation (and thus brine rejection) or increased absorbed solar radiation (and thus melt); and changes in surface roughness (ice concentration, as well as ridges and keels) may locally change the wind-driven stirring imparted to the ocean on the scales of floes (10s–1000s of m).

In our dataset, we have little scope for assessing temporal MLD change on time scales shorter than e.g., a month. The time scales of atmospheric forcings (e.g., wind events, changes in cloudiness affecting heating and cooling) are likely both the storm time scales of days and seasonal scale of months. While storm-driven MLD deepening has been seen to occur over several hours [e.g., in the ice-free Beaufort, Rainville et al., 2011], thermodynamic driven MLD change (via brine rejection or melt) likely acts on somewhat longer time scales (days to weeks), closely related to ice melt/growth rates [e.g., Perovich et al., 2003, 2008]. Similarly, the ocean processes driving restratification act on time scales of days [e.g., Mahadevan et al., 2010; Timmermans et al., 2012; Martini et al., 2014]. Thus, we should expect significant MLD change on order days and on small space scales, in addition to a longer seasonal timescale change. However, for the analysis of this paper which, as we will see below, will be by necessity on longer time and space scales, this short time and space scale variability will appear only as a contribution to uncertainty in the longer term or area means.

Defining Arctic regions for a regional monthly MLD climatology

In light of the sparse coverage in time for any location in the Arctic, and the limited coverage in space for any particular time, it is hard to make meaningful progress from these data without performing some spatial and temporal averaging. The basin-scale variability found above suggests different dominating processes in different areas of the Arctic, which we hypothesize relates to differences in ocean stratification, freshwater inputs and ice-cover. Thus, in what follows, we show the characteristics and temporal evolution of mixed layer depth binned into six different regions, chosen to reflect different physical regimes in the Arctic and defined as follows (see also Fig. 1):

- (i) *The Chukchi Sea*, 68–76°N and 155–180°W, area $\sim 5.4 \times 10^5 \text{ km}^2$ (containing 2967 profiles); very shallow (~0–50 m) with extensive coasts; strongly influenced by the comparatively fresh Pacific inflow, including the warm, fresh Alaskan Coastal Waters; ice-covered seasonally.
- (ii) *The Southern Beaufort Sea*, 68–72°N and 120–155°W, area $\sim 1.8 \times 10^5 \text{ km}^2$ (containing 1485 profiles); comparatively shallow (~0–700 m), coastal; influenced by the comparatively fresh Pacific inflow and the fresh water input of the Mackenzie River; ice-covered seasonally;
- (iii) *The Canada Basin*, 72–84°N and 130–155°W, area $\sim 9.5 \times 10^5 \text{ km}^2$ (containing 671 profiles); deep (>1000 m); dominated by the Beaufort Gyre, with some influence from the Pacific inflow and the Mackenzie River; still with perennial ice, but experiencing recent sea ice loss.
- (iv) *The Makarov Basin*, 83.5–90°N between 50–180°W, and 78–90°N between 141–180°E, area $\sim 8.2 \times 10^5 \text{ km}^2$ (containing 343 profiles); deep (>2000 m); upper layers marking a transition zone from Pacific to Atlantic influence, somewhat influenced by Russian river outflow; with perennial and seasonal sea ice, but with reduced in area and thickness in recent years;
- (v) *The Eurasian Basin*, 82–90°N between 30–140°E, and 78–82°N between 110–140°E, area $\sim 1.4 \times 10^6 \text{ km}^2$ (containing 519 profiles); deep (>3500 m); generally not influenced by

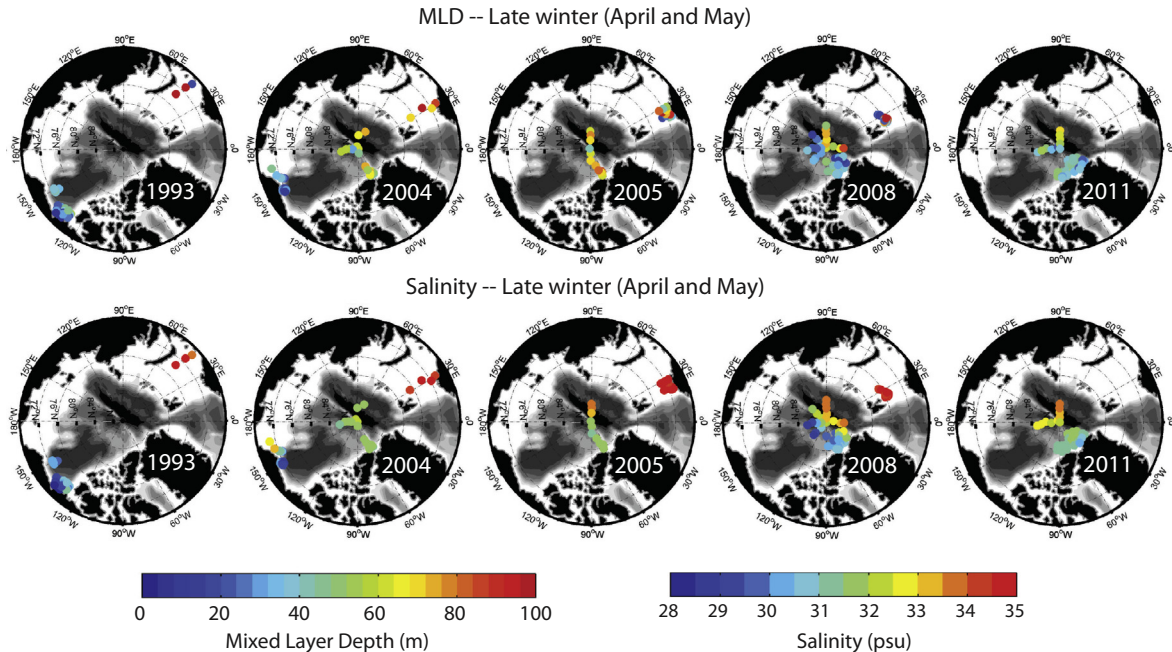


Fig. 4. For each of five years (1993, 2004, 2005, 2008 and 2011), Mixed Layer Depth (MLD) (top) and salinity averaged over the ML (bottom) for late winter (April and May) profiles. Bathymetry from GSHHG.

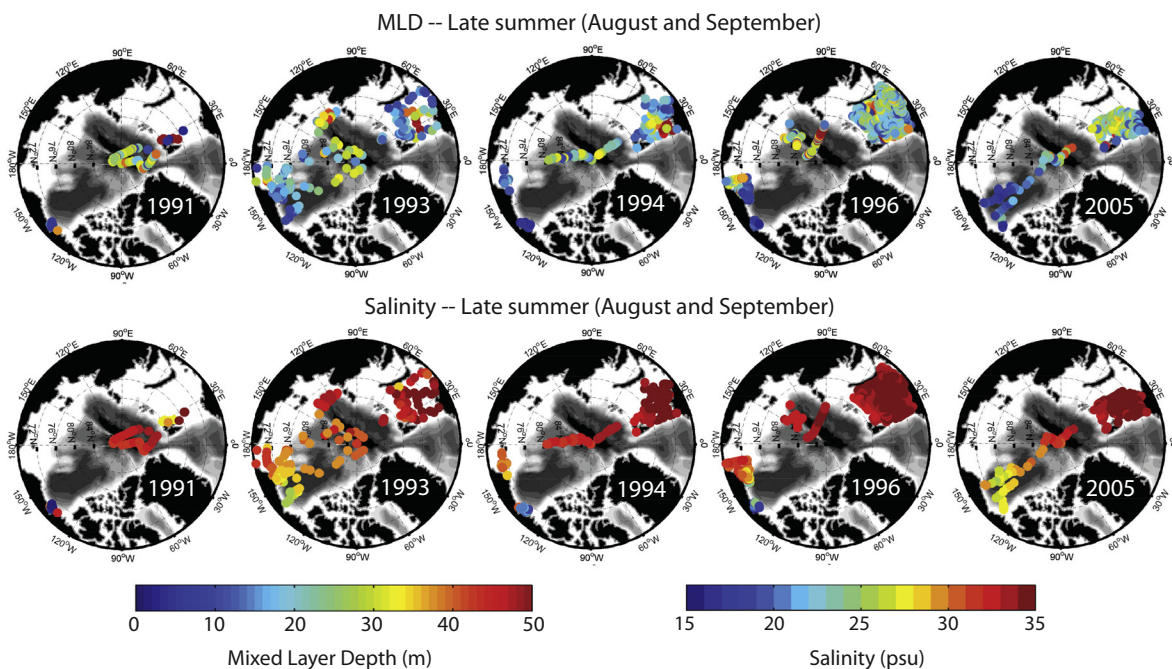


Fig. 5. For each of five years (1991, 1993, 1994, 1996, and 2005), Mixed Layer Depth (MLD) (top) and salinity averaged over the ML (bottom) for late summer (August and September) profiles. Bathymetry from GSHHG.

the fresh Pacific waters, but can experience freshwater input from Russian rivers; with perennial and seasonal sea ice, but with reductions in sea ice area and thickness in recent years.

- (vi) *The Barents Sea, 75–80°N between 15–60°E, and 67–75°N between 15–55°E, area $\sim 1.4 \times 10^6 \text{ km}^2$ (containing 10,642 profiles); moderately deep (~ 0 –400 m); strongly influenced by the warm, salty Atlantic inflow and fresher coastal Norwegian waters; with perennial and seasonal sea ice, but with reduction in sea ice area and thickness in recent years.*

Since upper ocean density stratification likely influences MLD evolution, this separation is chosen to reflect regions with different upper ocean water mass structures [e.g., McLaughlin et al., 1996]. Although in all regions the upper ocean is more stratified during summer than in winter due to the presence of fresher water near the surface (be it ice melt, river water or Pacific water), there are distinct differences between the regions (see also Fig. A1 in the Appendix A). Of all the regions, the Southern Beaufort Sea shows the lowest potential density values (and thus strongest stratification) during the summer, likely due to the direct influence of the

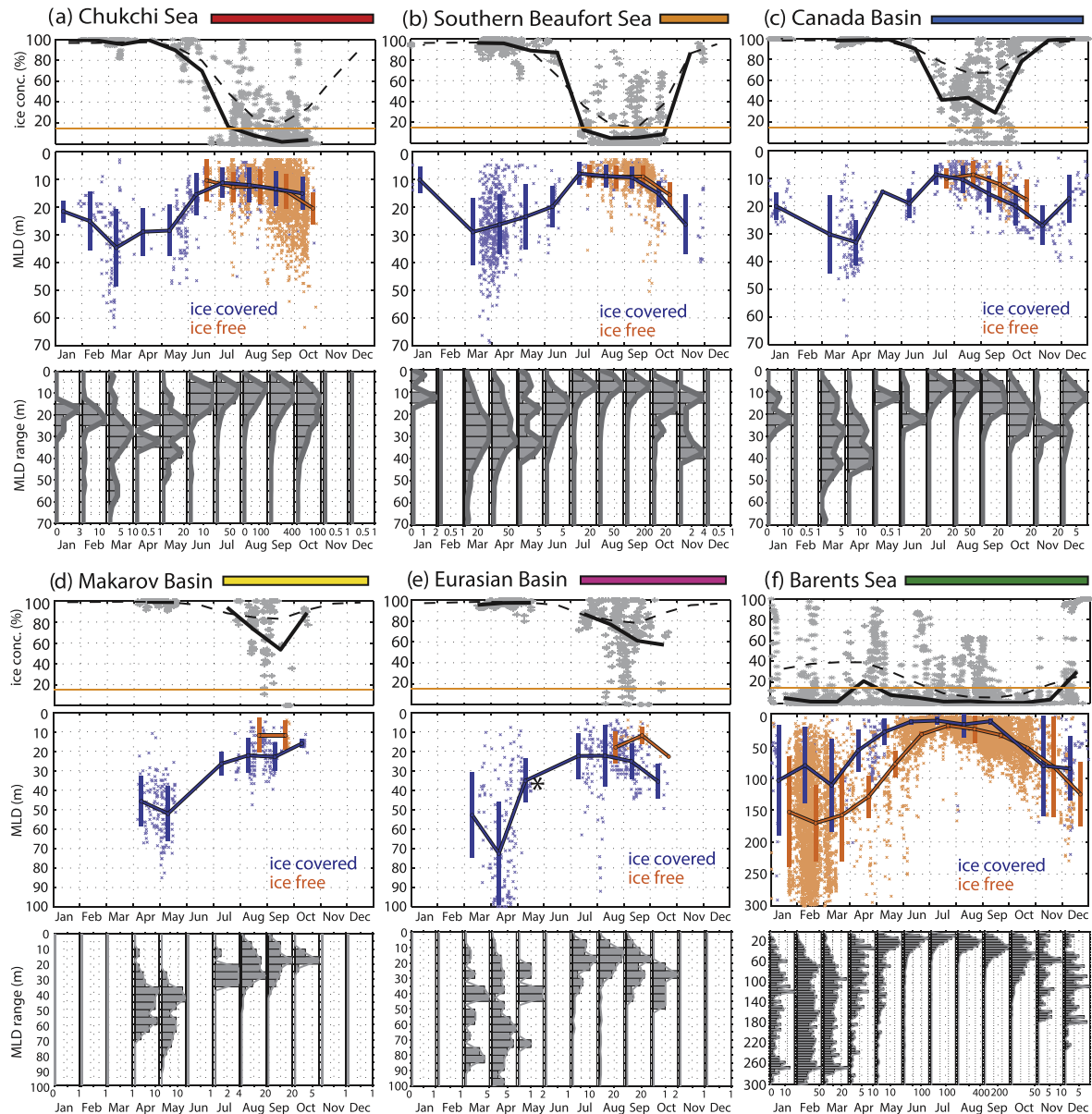


Fig. 6. For each of the 6 regions of Section ‘Defining Arctic regions for a regional monthly MLD climatology’, monthly variation of Mixed Layer Depth (MLD) and sea ice concentration combining all data from 1979 to 2012. For each region (color-coded as per Fig. 1), upper panel shows ice concentration at the observation location (gray dots), monthly average of those concentrations (black solid line), monthly average of ice concentrations averaged over the entire region (thin black dashed line), and the 15% ice concentration threshold (thin orange line), used to differentiate ice-free versus ice-covered observations. Bottom panel shows histogram of all MLDs within that region binned in 5 m intervals (note different horizontal scales, indicating different numbers of measurements). Middle panel shows MLDs from ice-covered (blue dots) and ice-free (orange dots) observations, with their monthly means joined by solid lines and the standard deviation for each mean marked with vertical bars. Note different vertical scales on the MLD plots. Asterisk in (e) marks significant spatial bias in the Eurasian Basin data in May, where all observations are confined to the Greenland side of the Basin (see Section ‘Decadal change in temperature–salinity (T – S) space’). (For interpretation of the references to color in this figure legend, the reader is referred to the web version of this article.)

fresh Mackenzie River runoff [see e.g., Macdonald et al., 1999]; the second strongest stratification is generally found in the Canada Basin, which is the largest freshwater reservoir in the Arctic Ocean due to strong surface Ekman convergence [Proshutinsky et al., 2002; Jackson et al., 2011]. Strong stratification is also found in the Chukchi Sea, which is dominated by the relatively fresh Pacific Waters entering through the Bering Strait, including the Alaskan Coastal Water, a source of freshwater stratification within the Chukchi [Woodgate and Aagaard, 2005; Woodgate et al., 2012]. Higher surface density values (and hence weaker stratification) are generally observed in the Makarov Basin, Eurasian Basin and in the Barents Sea, where the upper ocean is more directly influenced by Atlantic Waters than the other sectors studied here [Rudels et al., 2004].

Monthly climatology of MLD properties (depth, temperature and salinity) in 6 regions of the Arctic

By binning the 1979–2012 data by month and region and ice-cover, we compute a monthly climatology of MLD (Fig. 6 and Table 3) and ML-averaged temperature and salinity (Figs. 7 and 8) for each region for ice-free and ice-covered times (defining ice-free as times when ice concentration, ic , is less than 15%).

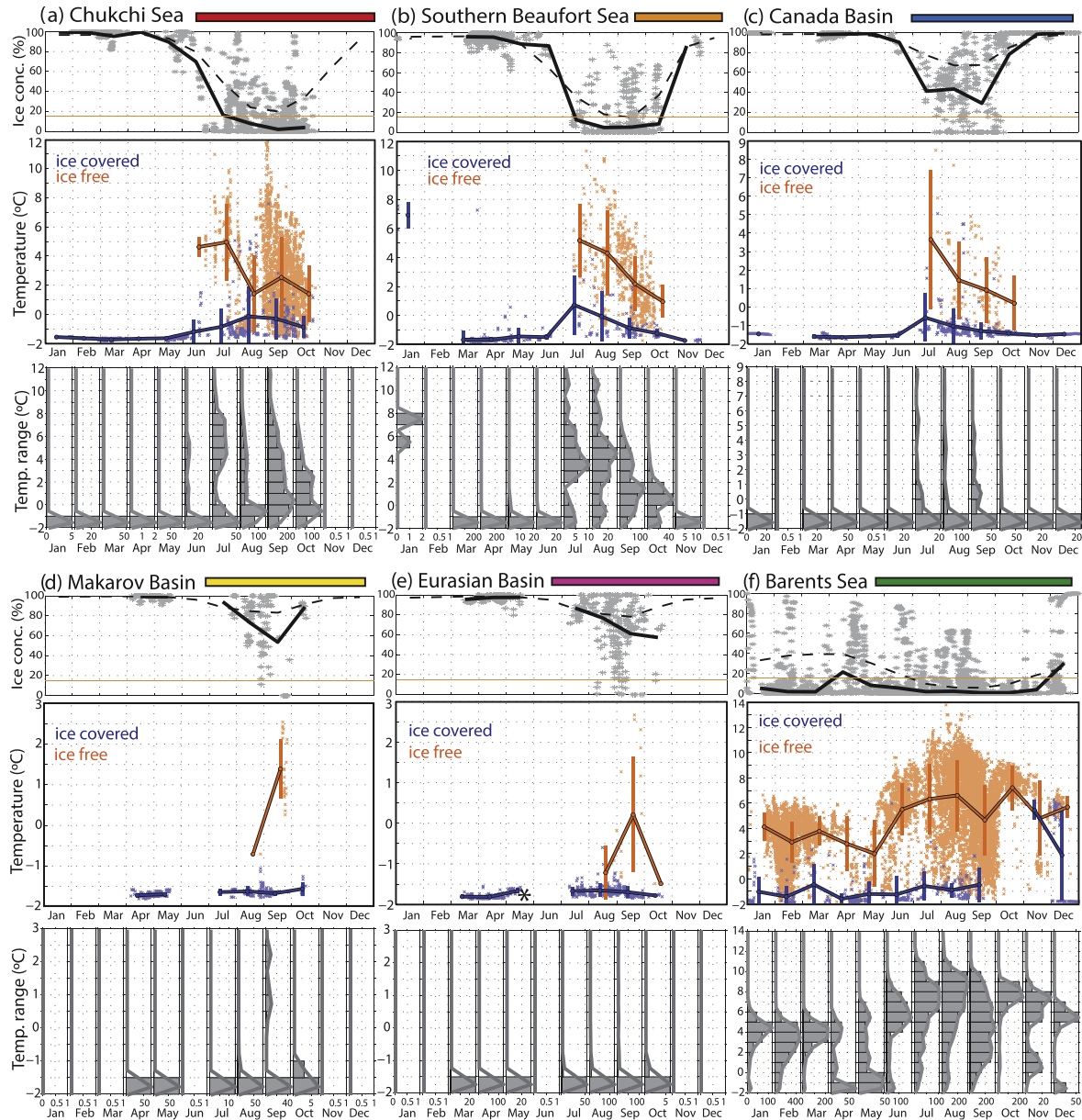


Fig. 7. As per Fig. 6 but for mixed layer averaged temperature ($^{\circ}\text{C}$) instead of MLD.

The number of casts varies by region and month, as illustrated by the frequency of occurrence histograms in each panel (Figs. 6–8). Regions with many observations suggest that summer MLDs have a narrow, quasi-normal distribution which, despite some skewness to deeper MLDs, often show a clear mode (e.g., Fig. 6, Chukchi Sea, August–September; Barents Sea, July–September). In contrast, in late winter, data-rich regions (e.g., Southern Beaufort Sea, Canada Basin, Barents Sea, March–May), have MLD distributions that are much broader and irregular, suggestive of extensive small-scale inhomogeneity, as discussed in Section ‘Spatial variability of Arctic Mixed Layer Depths (MLDs)’.

In all regions, however, there is a clear seasonal cycle from deeper (and more varied) MLDs in the winter months, to shallower and more homogeneous MLDs in the summer. MLD temperature distributions (Fig. 7) reflect the sea ice cover, with ML temperatures being around freezing when ice cover is high, and showing various irregular and broad temperature distributions in summer/ice-free times, presumably due to solar input and/or advec-

tion. ML salinity distributions (Fig. 8), similarly, are irregular and broad in summer, relating likely to various freshwater sources, such as ice melt and advected freshwater.

To quantify statistics for our data collection, it is necessary to ascertain to what extent our data points are independent. To establish this, we seek decorrelation scales in space and time (the latter frequently called the integral time scale), usually defined as the scale over which the correlation falls to $1/e$. Since our data are irregular in space and time, we seek through our data for pairs of points separated by the same time and distance intervals, binning these time and space intervals (e.g., 1 day resolution, and 30 km resolution) to give meaningful numbers of pairs. To avoid pan-Arctic spatial trends, we consider points in each region separately. To avoid aliasing seasonality or interannual trends, we consider each month in each year separately. We then look for significant ($>1/\text{eth}$) correlations within the pairs of points for each combination of space/time differences. These constraints yield 39 regional months with plausible, if thin, data coverage. Within these, we find

rare occurrences of significance at the 1 day and 30 km scale (while using bins of these sizes, suggesting decorrelation scales may be smaller than this), but these higher correlations are not present in the same region in different months or years, and for the majority of our data, we do not find significant correlations. We consider this overall lack of correlation as a fair indication that our data points are dominantly independent, and we treat them as such in the statistical analyses in the rest of the paper. (Note also that we are unable to quantify the decorrelation scales themselves, as our data are, it appears from this analysis, too sparse.)

To provide a climatology (Table 3), we compute the mean and standard errors of the ML properties for each region and month, estimating standard errors by assuming measurements are independent and normally distributed. Details of these errors are given in Table 3, but in general winter and summer means have standard errors of ~ 3 m and ~ 2 m, respectively. Recall that, as discussed in Section 'Hydrographic data – inventory, quality control, and accuracy', these summer MLD estimates may be artificially deep due to stirring effects from the measurement platform. This is not reflected in our uncertainty estimate.

Overall, mean winter MLDs (regardless of ice-cover) shoal from deep values in the Barents Sea (~ 168 m) and Eurasian Basin (~ 73 m, see Section 'Determination of Arctic Mixed Layer Depth (MLD)' for discussion of this average) towards much shallower values in the western Arctic (Canada Basin ~ 33 m, Southern Beaufort Sea ~ 29 m) and the Chukchi Sea (~ 35 m). Summer MLDs, everywhere shallower than winter MLDs, show a smaller but spatially similar east to west decrease (Eurasian Basin ~ 22 m, Makarov Basin ~ 16 m, Canada Basin and Southern Beaufort Sea ~ 9 m), with the Chukchi (~ 12 m) being regionally perhaps slightly deeper. The Barents Sea, although giving by far the deepest winter MLDs (~ 168 m), has summer MLDs that are in general a little shallower (~ 18 m) than the adjacent Eurasian Basin (~ 22 m).

This east to west shoaling is most likely a consequence of the underlying stratification, which is stronger in the western Arctic, corresponding to lower surface salinities (Figs. 4 and 5, and comparison of separate panels in Fig. 8). Stronger underlying stratification (which provides a barrier to MLD deepening) could also explain the summer MLD shoaling between the Eurasian Basin and the Barents Sea, since at that time the Barents Sea is more strongly stratified by freshwater sources, such as ice melt [e.g., Harris et al., 1998] and the Norwegian Coastal Current [e.g., Schauer et al., 2002] (for seasonality, see Skagseth et al. (2011)). In Section 'Controlling effects of stratification and influence of sea ice cover', we will attempt to quantify such underlying stratification effects.

Our Canada Basin maximum winter MLD ($\sim 33 \pm 2$ m) is comparable to MLDs estimates from a few individual ITPs [e.g., winter MLD maximum ~ 35 m, Jackson et al., 2012; Timmermans et al., 2012], although given the spatial variability discussed in Section 'Spatial variability of Arctic Mixed Layer Depths (MLDs)', this may just be a fortuitous agreement of individual measurements with a regional mean. A more meaningful comparison is with Toole et al. (2010)'s estimates. Their winter MLD values (~ 24 m, standard deviation ~ 8 m), based on 5 years of ITP data, are slightly shallower than ours ($\sim 33 \pm 2$ m, standard deviation ~ 8 m), possibly since the ITPs are deployed on thick ice, which will have less sea ice growth during winter (and thus less brine-driven convection) than open water. Similarly, Eurasian Basin ITP data Polyakov et al. (2013) yield a winter MLD estimate of ~ 50 m, shallower than ours ($\sim 73 \pm 2$ m). In contrast, our Canada Basin summer MLD ($\sim 9 \pm 1$ m) is significantly shallower than Toole et al. (2010)'s estimate (~ 16 m), likely since the ITPs cannot resolve MLDs shallower than 10 m, biasing their estimate deep as they discuss. In contrast, average summer MLD from Eurasian Basin ITP data [~ 20 m, Polyakov et al., 2013] agrees well with our estimate

($\sim 22 \pm 2$ m), possibly since the deeper MLDs of the Eurasian Basin are deep enough to be properly measured by the ITPs.

In all regions, the seasonal change in MLD (given in Table 3) is greater than any ice-covered versus ice-free differences within a particular season, although Fig. 6 suggests that summer MLDs are a little shallower in ice-free regions than in ice-covered regions in the Eurasian and Makarov basins, and perhaps also in the Canada Basin. Only the Barents Sea has significant numbers of ice-free measurements in the winter, and these show that MLDs in winter are ~ 50 m deeper than in ice-covered regions. This might be due to regional difference of water mass characteristics in the Barents Sea, viz. the shallower values under ice reflecting the fresher Arctic-dominated waters of the Barents Sea as opposed to the saltier Atlantic-dominated waters.

In all regions, minimum MLDs are found coincident with the largest reduction in sea ice extent in early summer (June/July; August in the Makarov Basin). This is presumably driven by melt-water stratification at the surface, since the shoaling is usually accompanied by a drop in salinity (Fig. 8) and frequently modest warming (Fig. 7) and it is early in the year for riverine sources of freshwater to be available to the central basin (river outflow generally starts in May and peaks in June [e.g., Macdonald et al., 1995; Overeem and Syvitski, 2010], and advection times to the central Arctic are order months or even years [Ekwurzel et al., 2001; Bauch et al., 2009, 2014]). From this summer minimum, MLDs then deepen through the ice-free times, and generally continue to deepen as sea ice starts to reform. MLD is deepest during times of maximum sea ice cover, typically around March. (Note that apparent April/May deepening of MLDs in the Eurasian Basin may be an artifact of changes in spatial sampling, see Fig. 6 caption.) Interestingly, there is some evidence of MLD shoaling from the winter maximum in \sim March, prior to significant decline of sea ice concentration. The histograms (e.g., for the Chukchi and the Barents Sea) suggest this is due to a loss of the deeper MLDs, rather than an increase in very shallow MLDs. Given this, and the fact that this shoaling is not generally associated with significant freshening or warming, we hypothesize this may be due to restratification processes [e.g., Mahadevan et al., 2010], rather than input of freshwater near the surface. Further investigation of this, however, is beyond the scope of this paper.

Physical drivers of seasonal Mixed Layer Depth (MLD) change

To what extent can this dataset elucidate the physical drivers of MLD properties in the Arctic? The physical drivers of MLD evolution have been studied extensively at the lower latitudes using observations [e.g., Lukas and Lindstrom, 1991; Lentz, 1992; Kara et al., 2003], and various models [e.g., Pollard et al., 1973; Price et al., 1986; Large et al., 1994; Sallée et al., 2013]. For the Arctic, a 1-dimension Price–Weller–Pinkel [PWP, Price et al., 1986] vertical mixing model has been utilized by Toole et al. (2010) to understand change in Arctic MLD properties, but the model showed limited success under ice in the Beaufort region, likely due to inadequate parameterization of sea ice processes, restratification and advection. Since a more detailed modeling effort is beyond the scope of this current paper, rather than repeat prior work we consider instead simplistic basin or even Arctic-wide budget and scaling arguments to estimate the influence of various physical drivers on Arctic MLDs, with a view to guiding subsequent investigations.

We focus on two main drivers of Arctic MLD change, viz. the influence of sea ice thermodynamics (i.e., brine rejection from ice growth, freshwater forcing from ice melt), and the influence of wind-driven mixing. To quantify the relative importance of these forcings, we start by considering each separately, and then consider their combined effect.

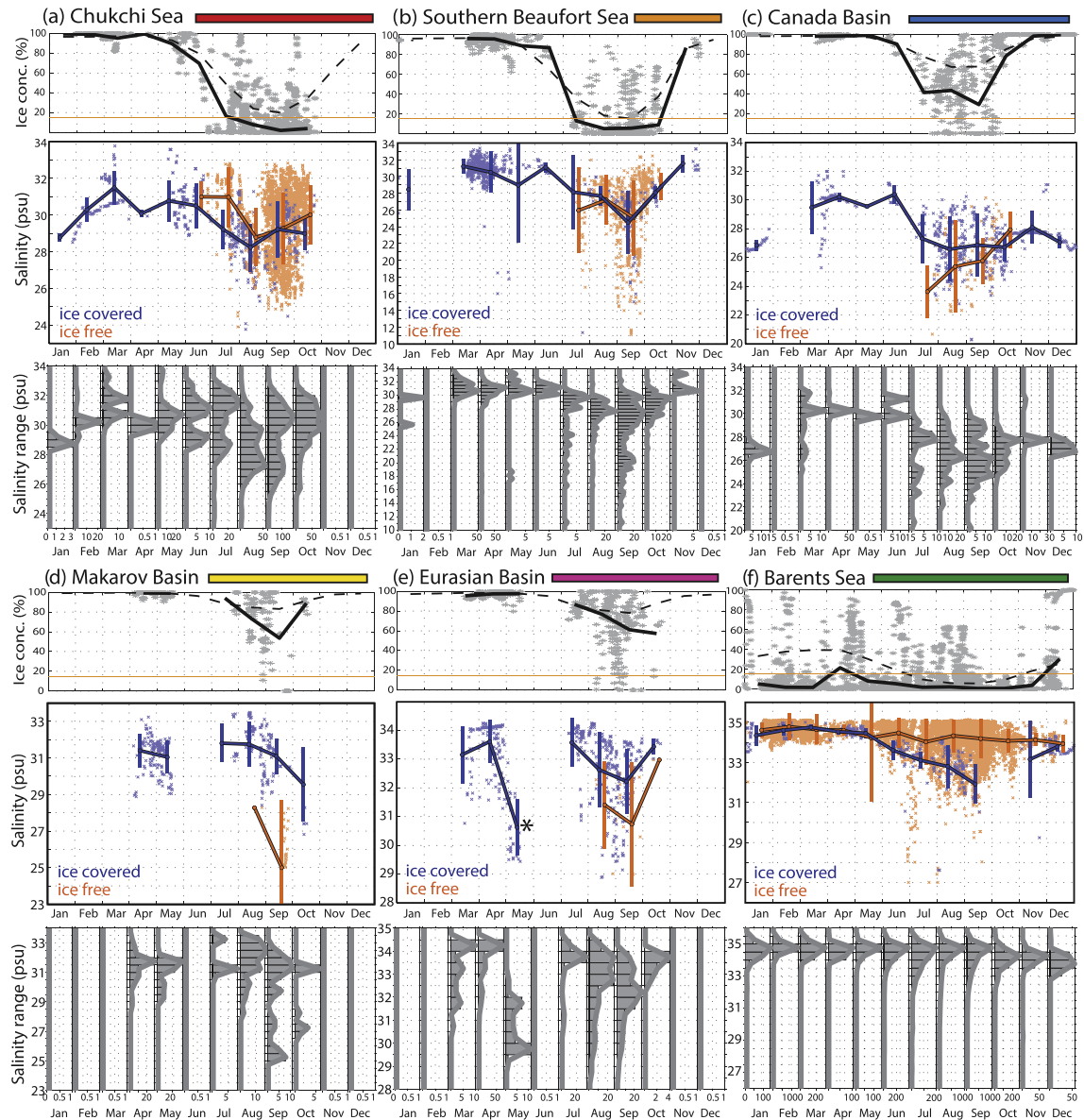


Fig. 8. As per Fig. 6, but for mixed layer averaged Salinity (psu) instead of MLD.

Quantifying influence of sea ice growth/melt

We consider first to what extent sea ice thermodynamics, via either brine rejection from ice growth or surface layer formation from ice melt, may explain the MLD changes in our dataset.

Consider initially the summer to winter transition, starting with a summer profile of a shallow, fresh ML below which density increases (Fig. 9a). Brine rejection from sea ice formation deepens the MLD by density-driven convection, reaching (we assume) the depth at which the increased ML density matches that of the underlying profile (Fig. 9a and b). Assuming density (and thus also salinity, since at these temperatures density is dominated by salinity) increases uniformly with depth below the summer ML (Fig. 9a), and conserving mass and salinity above the winter MLD, we can estimate the thickness of ice growth, t_{growth} , as:

$$t_{growth} = \frac{\rho_w}{2\rho_i} \frac{(S_w - S_s)}{(S_w - S_i)} (H_w + H_s) \quad (1)$$

where H_s and H_w are the summer and winter MLDs; S_s and S_w are the summer and winter ML salinities; S_i is the salinity of sea ice,

and ρ_i and ρ_w are the densities of ice and sea water (see Appendix 'Estimate of sea ice growth, t_{growth} , associated with observed seasonal MLD change' for derivation).

For the winter to summer transition (Fig. 9, from b to c), from a deep homogeneous ML ice melt will form a thin layer at the surface. In the absence of mixing, this layer would be as thin as the melted ice, but in reality it is deepened by mixing processes yielding (in the simplest case) a 2-step structure (Fig. 9c) with the thickness of ice melted, t_{melt} , given by:

$$t_{melt} = \frac{\rho_w}{\rho_i} \frac{(S_w - S_{so})}{(S_w - S_i)} (H_s) \quad (2)$$

where S_{so} is the salinity of the summer ML in this 2-step profile (see Appendix 'Estimate of sea ice melt, t_{melt} , associated with observed seasonal MLD change' for derivation).

Although we do observe this 2-step profile in our data, often the salinity profile under the summer ML is stratified (as per Fig. 9a). This could form, for example, from diffusion or mixing of the summer surface ML with waters below, which would increase the ML salinity from S_{so} to S_s , yielding again Eq. 1.

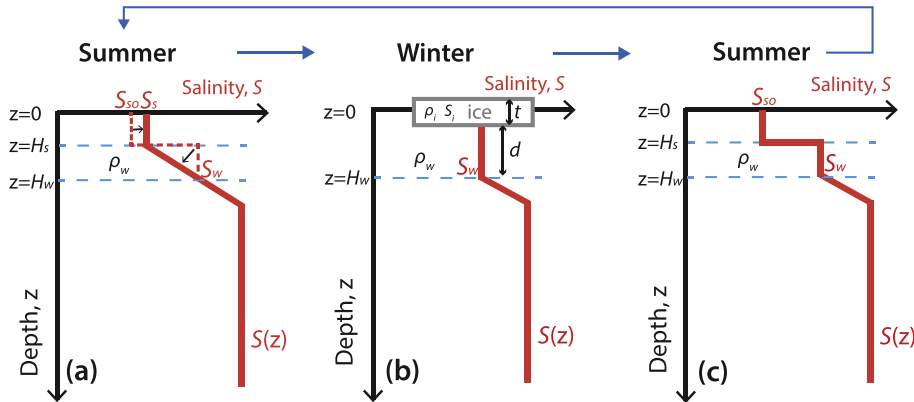


Fig. 9. Idealized change in salinity profiles between seasons, as discussed in Section 'Quantifying influence of sea ice growth/melt'. Brine rejection driven convection (from a to b) homogenizes the summer ML with waters below to give a deeper, saltier ML. Ice melt in summer yields a thin summer ML (c) with a step change to the winter ML salinities below. Mixing processes erode these sharp gradients to give a smoother summer halocline likely saltier (S_s) than the original ice melt layer (S_{so}) (a).

These two estimates (differing due to the different assumptions of stratification below the summer ML) give us bounds on the sea ice thickness change necessary to deepen or shoal the seasonal MLD. Taking ML properties from our summer and winter climatologies (Table 3), we calculate t_{growth} and t_{melt} for each region (Table 4), taking ρ_i as 920 kg/m^3 , ρ_w as 1025 kg/m^3 , and S_i as 6 psu. These calculations show that, to drive the observed MLD change, an ~1.5 times greater sea ice change is required in the western Arctic than in the eastern Arctic, a result that is consistent with spatial variation of seasonal sea ice melt, which is more extensive in the western Arctic [e.g., Kwok and Cunningham, 2002; Perovich et al., 2008]. While our estimates assuming linear stratification below the ML (t_{growth}) are generally unrealistically high, our lower bound (t_{melt} , corresponding to the 2-step profile) is typically 1–2 m, in reasonable agreement with observational estimates of seasonal sea ice change, e.g., pan-Arctic average of ~1.5 m from submarine data [Rothrock et al., 1999]; ~1.4 m in the Bering Strait (taken as a proxy for the Chukchi Sea) from mooring data [Travers, 2012]; and from ~0.5 m (North Pole) to 0.5–2 m (Beaufort Sea) from Ice Mass Balance (IMB) buoys [Perovich et al., 2008]. (Note that seasonal change estimated from IMB data may be lower than the basin average as IMB buoys are deployed on thick ice, which has less ice melt/growth than thin ice [e.g., Untersteiner, 1964].)

Our calculation does not confirm that MLDs are solely set by ice melt/freeze processes. In fact, the evidence that summer MLD are deeper than the thickness of ice melted indicates that some other processes must mix freshwater into the water column. To ascertain if winter MLDs are set by convection alone would require tracking

an individual water column from summer to winter, which is beyond the scope of our data.

However, we can investigate to what extent basin-wide averages reflect such mixing. For this, we use (for each region) average winter and summer salinity profiles, $S_w(z)$ and $S_s(z)$, for months of maximum and minimum MLD to estimate the seasonal salinity change with depth, and integrate over the whole profile to obtain an equivalent thickness of ice, $t_{profile}$, viz.:

$$t_{profile} = \int_{bottom}^{surface} \frac{\rho_{ww}(z)}{\rho_i} \frac{(S_w(z) - S_s(z))}{(S_s(z) - S_i)} dz \quad (3)$$

where $\rho_{ww}(z)$ is the profile of water density in winter (see Appendix 'Full water column winter-to-summer freshening, estimated as equivalent of sea ice melt, $t_{profile}$ ' for derivation of $t_{profile}$ and salinity profiles for each region, and Table 4 for results).

In essence, $t_{profile}$ is a measure of the full water column freshening between winter and summer. Although we compute this as equivalent sea ice melt, the freshening could also be from other Arctic freshwater sources, e.g., net precipitation, rivers, or Pacific inflow [Serreze et al., 2006]. If sea ice melt is the dominant source, however, this $t_{profile}$ is a third way of calculating the impact of sea ice melt on the water column. Details of the calculation also allow us to assess the depths at which the water column has freshened.

In the Chukchi Sea, the Eurasian Basin and the Barents Sea, this profile calculation yields an estimate of equivalent ice melt (0.9 m Barents; 2.0 m Eurasian Basin; 1.6 m Chukchi) within the range of the prior estimates (t_{growth} and t_{melt}), and within the range of expected seasonal sea ice melt (Table 4). In the Eurasian Basin and the Barents Sea, almost all (>95%) of this freshwater (FW)

Table 4

For each of the 6 regions, the monthly average winter maximum and summer minimum MLD, and winter and summer ML salinity for the month given in Table 3. Highlighted by the black border are the 3 estimates (with 95% confidence intervals) of ice thickness change commensurate with MLD change as discussed in Section 'Quantifying influence of sea ice growth/melt', viz. t_{growth} , the summer to winter transition of MLD properties; t_{melt} , the winter to summer transition of MLD properties; and $t_{profile}$, the estimate based on differences between full-depth summer and winter profiles (see Appendix A, and Fig. A1). Penultimate column gives the depth above which 50% of the $t_{profile}$ freshening is found. Final column shows the percentage of $t_{profile}$ found above the winter MLD. See Section 'Quantifying influence of sea ice growth/melt' and Appendices, especially Fig. A1.

Region	Winter maximum MLD (m)	Summer minimum MLD (m)	Winter ML salinity (psu)	Summer ML salinity (psu)	Ice change (t_{growth}) (m)	Ice change (t_{melt}) (m)	Ice change ($t_{profile}$) (m)	Depth (m) of 50% of $t_{profile}$	% of $t_{profile}$ above winter MLD
Chukchi Sea	34.6 ± 3.3	12.3 ± 0.8	31.5 ± 0.24	28.7 ± 0.15	2.9 ± 0.4	1.5 ± 0.2	1.6 ± 0.3	15	75
Southern Beaufort	29.0 ± 1.6	8.5 ± 1.4	31.2 ± 0.12	25.0 ± 0.39	5.1 ± 0.4	2.3 ± 0.2	6.1 ± 0.2	6.5	85
Canada Basin	33.1 ± 1.8	8.9 ± 1.2	30.2 ± 0.07	26.9 ± 0.64	3.2 ± 0.6	1.4 ± 0.3	5.4 ± 0.8	17.2	70
Makarov Basin	52.0 ± 2.9	16.0 ± 1.4	31.4 ± 0.20	28.9 ± 0.88	3.7 ± 1.4	1.8 ± 0.6	-2.8 ± 0.4^a	^a	^a
Eurasian Basin	72.5 ± 4.5	22.3 ± 2.9	33.6 ± 0.13	32.0 ± 0.23	3.1 ± 0.5	1.4 ± 0.2	2.0 ± 0.3	15.3	99
Barents Sea	111 ± 6.4	17.7 ± 1.0	34.6 ± 0.06	34.2 ± 0.04	1.7 ± 0.3	0.3 ± 0.1	0.9 ± 0.03	17.6	100

^a As discussed in Section 'Quantifying influence of sea ice growth/melt', the apparently negative ice growth in the Makarov Basin (Fig. A1d) likely results from spatial bias in the sampling from summer (near Russia) to winter (near Greenland), and thus should be disregarded.

change is found to be shallower than the winter MLD (Table 3), suggesting surface/near surface processes dominate. In contrast, in the Chukchi and Southern Beaufort Seas, and the Canada Basin, only ~75% of the FW change is above the winter MLD, suggesting that non-surface sources of freshwater, e.g., advection of Pacific Waters at depth, are important.

In the Southern Beaufort Sea, $t_{profile}$ is ~6.1 m, unrealistically high for sea ice melt alone (Table 4). This is equivalent to ~800 km³ of freshwater, and is likely made up of contributions from other possible freshwater inputs to this region, e.g., the Mackenzie outflow [~340 km³, Aagaard and Carmack, 1989], the Alaskan Coastal Current (ACC) from the Chukchi Sea [~400 km³, Woodgate and Aagaard, 2005], and indeed a portion of the Pacific inflow [~2100 km³ without the ACC, Woodgate and Aagaard, 2005]. Our Southern Beaufort Sea profile calculation shows 50% of the freshwater change is found in the upper 7 m suggestive of a particularly fresh source, such as the ACC or the Mackenzie River. To separate these sources requires further information. For example, Macdonald et al. (1999) use delta O¹⁸ values to attribute the observed equivalent of net 1 m of seasonal freshening of the ML in near coastal stations in the eastern Beaufort to ~3 m of riverine freshening opposed by net sea ice formation (equivalent to ~1 to 2 m of freshwater). Their calculation is more closely related to our initial calculations (t_{growth} , t_{melt}) since they consider only change above the MLD. Their much lower net value (~1 m, compared to our 2–5 m) may reflect the different regions used for the computation, or interannual change.

Similarly, our full profile salinity change for the Canada Basin (~5 m, $t_{profile}$ in Table 4) is indicative of significant other freshwater sources than just sea ice melt. This region includes the freshwater dome of the Beaufort Gyre, the FW storage of which is known to respond also seasonally and interannually to wind-forcing [e.g., Proshutinsky et al., 2009; Giles et al., 2012]. (Our basin-average seasonal change is somewhat larger than the point calculations of Proshutinsky et al. (2009) (<3 m), possibly due to differences in location and/or calculation method.) In our calculation, only ~70% of the FW change was above the winter MLD and summer/winter salinity differences exceeded ~3 psu down to ~0.25 psu at ~100 m in the water column, suggestive of the influence of different states of spin-up of the gyre.

We reject the profile calculations from the Makarov Basin as an aliasing of spatial difference into temporal change, since winter casts are from northeast Greenland and summer casts are in the central Arctic. Indeed, the salinity profiles (see Fig. A1 in the Appendices) suggest a strong freshening of the mid water column (summer to winter mean salinity decrease of 1.5 psu at ~50 m deep, and ~1 psu at ~100 m deep) that is unlikely to occur on a seasonal timescale.

In essence, our calculation is a check of salinity budgets, showing that, in most regions, the seasonal salinity cycle of the ML can reasonably be explained by seasonal melt and freeze of sea ice. That said, in both the Canada Basin and the Southern Beaufort Sea, ML changes are too large to be reasonably explained by local sea ice processes and inputs of advective freshwater to the ML are required. Note that seasonally ice melt contributes ~9000 km³ of freshwater to the Arctic Ocean (conservatively estimated from seasonal ice extent change, ~6 × 10⁶ km² (NSIDC data) and ice thickness, ~1.5 m). This is comparable to estimates of seasonal change in the entire Arctic Ocean freshwater content [~10,000 km³, Serreze et al., 2006], and much greater than the variability in any of the freshwater inputs to the Arctic – indeed the total annual mean freshwater input to the Arctic [~8500 km³, Serreze et al., 2006] is of the same magnitude as seasonal sea ice melt, and moreover issues of transit time from the Arctic rim into the Arctic interior need also to be considered [see e.g., Macdonald et al., 1995; Ekwurzel et al., 2001; Bauch et al., 2009, 2014]. Simply

put, it appears that overall Arctic Ocean freshwater seasonality is primarily driven by Arctic sea ice processes, rather than seasonality in the inputs of freshwater to the Arctic.

Relationship of MLD to wind forcing and sea ice cover

We consider next the role of wind forcing and sea ice cover on MLD, asking most simply if greater wind speeds result in deeper MLDs, and if ice noticeably mediates this linkage. We seek a relationship between MLD and wind speed, since in the simplest form, the Ekman depth, D_E , is proportional to wind speed, W [e.g., Pond and Pickard, 1983]:

$$D_E = \frac{\pi \rho_a C_d}{\sqrt{2} \rho_w \Omega \alpha} \frac{1}{\sqrt{\sin(\theta)}} W \sim 4.3W \quad (\text{in S.I. units}) \quad (4)$$

where ρ_a is density of air (1.3 kg/m³); ρ_w is density of water (1025 kg/m³); C_d is the drag coefficient (taken as 1.4×10^{-3}); Ω is the rotation of the earth (radians/s), θ is latitude (taken as 80°N) and α is a constant (0.0127) in the observed empirical relationship between wind speed, W , and surface water velocity, V_o , viz. $V_o \sim \alpha W / \sqrt{\sin(\theta)}$. A very similar expression may be derived for the boundary layer thickness, D_{BL} , using a friction velocity formulation [e.g., Cushman-Roisin, 1994]:

$$D_{BL} = \frac{0.4}{f} \sqrt{\frac{\rho_a C_d}{\rho_w}} W \sim 4W \quad (\text{in S.I. units}) \quad (5)$$

where f is the Coriolis parameter ($1.43 \times 10^{-4} \text{ s}^{-1}$ for 80°N).

Separating our data by basin, three levels of ice cover, (i.e., ice-free where ice concentration (ic) < 15%; ice-covered for 15% < ic < 80%; fully ice-covered for ic > 80%) and season (i.e., summer (June to September) and winter (November to May)), we seek (for each set) a best fit of MLD to wind speed, W , i.e., the value of m in

$$\text{MLD} = mW + \text{constant} \quad (6)$$

as illustrated for summer in Fig. 10, and computing statistics assuming all measurements are independent (see Section 'Monthly climatology of MLD properties (depth, temperature and salinity) in 6 regions of the Arctic' for discussion of independence). Since a ML may remain deep for some days after the wind event [e.g., Rainville et al., 2011; Jackson et al., 2012], for W we take the maximum wind speed in the 5 days preceding the cast, though results are not sensitive to different (2 or 10 day) time windows.

Remarkably for such a simple test, we find several relationships that are significant at the 95% confidence level or above. In summer open water times (ic < 15%), all regions show significant, if weak, relationships with MLD deepening with increasing wind speed – in the western Arctic regions (Chukchi, Southern Beaufort Seas and, less clearly, the Canada Basin), the constant of proportionality, m (Eq. 6), is ~0.2–0.4 s (± 0.1 s in the Chukchi and Southern Beaufort Seas; ± 0.3 s in the Canada Basin), while m is generally greater in the eastern Arctic, i.e., Makarov and Eurasian Basins ($m \sim 0.9 \pm 0.7$ s) and the Barents Sea ($m \sim 1.1 \pm 0.1$ s). It should be stressed, however, that the MLD variance explained by these relationships is generally very small, only 1–5% in the western Arctic, though higher (up to 20%) in the eastern Arctic (Fig. 10), similar to previously reported weak MLD–wind speed relationships in ice-free oceans at lower latitudes [e.g., Lukas and Lindstrom, 1991]. Results presented here are using the NCEP wind product, but very similar relationships are found using ERA interim, MERRA and JRA55 wind products.

During summer ice covered times (ic > 15%, Fig. 10), significant correlations are less frequent, especially so for high values of ice cover (ic > 80%). We will return to this in Section 'Controlling effects of stratification and influence of sea ice cover', but note here that, when the fits are significant, m is of similar magnitude to the

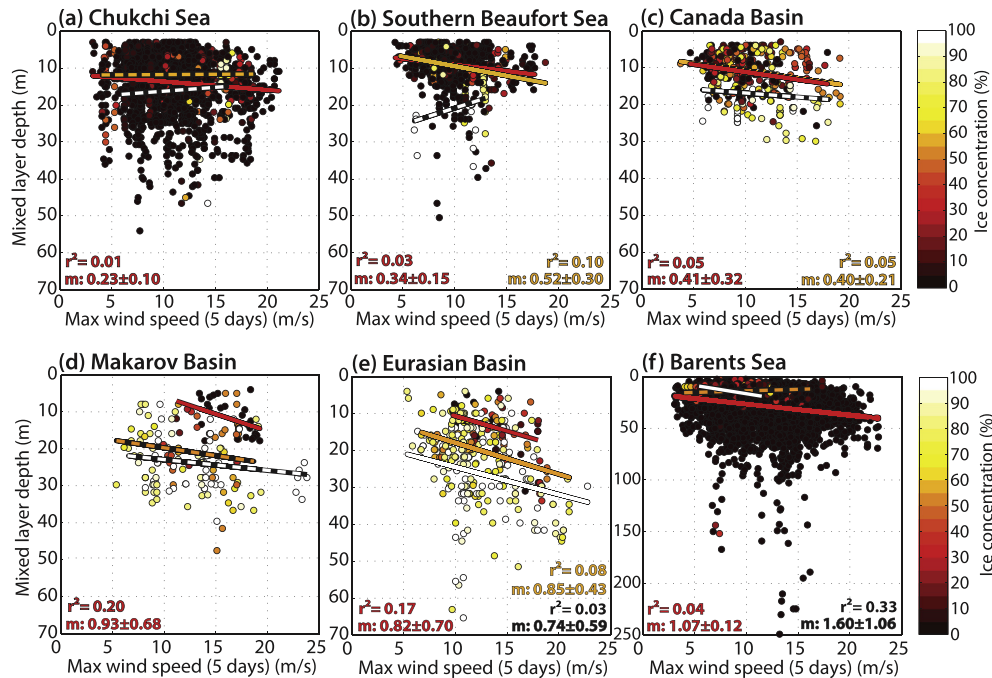


Fig. 10. Scatter plots of MLD versus maximum wind speed in the 5 days preceding the cast for the (a) Chukchi Sea, (b) Southern Beaufort Sea, (c) Canada Basin, (d) Makarov Basin, (e) Eurasian Basin, and (f) Barents Sea, for summer months (June to September). Data points are color-coded by ice concentration as per color scale. Also marked are linear fits (solid lines for significantly different from zero, and dashed lines for non-significant fits). Where fits are significant at the 95% level (assuming all points are independent), we also show m values (in seconds) (with 95% confidence intervals) from "MLD = $m \times$ Wind + constant", for different ranges of ice concentration, viz., red (<15%), orange (between 15% and 80%) and white lines/black numbers (>80%); and the fraction of variance explained, r^2 , for each significant fit. Note the different MLD scales in (d–f). (For interpretation of the references to color in this figure legend, the reader is referred to the web version of this article.)

ice-free values and the fit generally explains similarly small (3–33%) fractions of the variance.

During winter, we find no significant correlations between MLD and wind speed, in agreement with the hypothesis that convection effects in winter mix deeper than wind-driven effects.

All the m values obtained here are much less than predicted by the simple models above (Eqs. 4 and 5, $m \sim 4$ s), and including the suspected bias in NCEP wind (~20% weak, Section 'Supporting datasets: sea ice concentration and surface wind speed') further increases the discrepancy. This very likely reflects that these simple models assume no underlying stratification. Stratification will oppose ML deepening, and indeed, this is evident in our results – the value of m increases from ~0.2 to 0.4 s in the highly stratified western Arctic to ~1.0 s in the less stratified eastern Arctic. This change is dramatic, indicating that the same wind forcing is 2–3 times more effective at ML deepening in the eastern Arctic than the western Arctic, and by the Barents Sea, the MLD deepening per unit wind has increased 25–40% of that suggested by the no-stratification models. Thus, we next consider stratification effects.

Controlling effects of stratification and influence of sea ice cover

Yang et al. (2004), using data from ice-mounted buoys, found wind-driven mixing only in spring and winter, times when underlying stratification was weak. Rather than rely on a seasonal designation to describe stratification, we instead quantify the underlying stratification ($\Delta\rho$) for each cast as the potential density step across the ML base, calculating this as the average density of a 20 m thick layer below the ML minus the average ML density.

Separating our data by ice cover (Fig. 11), we then seek relationships between MLD and wind (as per Eq. 6) for different underlying stratifications.

Under ice cover, even when binning by underlying stratifications, there is no significant relationship between MLD and wind

(see also Fig. 10). This may be indicative of sea ice weakening the wind–water coupling, as found by Rainville and Woodgate (2009), and implies, as discussed by those authors, that future reductions in sea ice cover may have the potential to increase wind-driven mixing in the Arctic.

In ice-free times, however, the wind–MLD relationship is strongly influenced by stratification. Weak underlying stratification (taken as $\Delta\rho < 0.5 \text{ kg/m}^3$) yields m values of 4.6 ± 0.3 s, close to values from the simple models discussed above, and ~6 times greater than the relationship for strong ($\Delta\rho > 0.5 \text{ kg/m}^3$) underlying stratification, where m is 0.77 ± 0.06 s. Note however, that even though these fits of MLD to wind speed are significant, wind variability still explains only ~10% of the MLD variance (Fig. 11).

Pollard et al. (1973) using a simple, one-dimensional model, derive an expression for MLD as a function of wind speed (W) and buoyancy frequency ($N = \sqrt{-\frac{g}{\rho_w} \frac{\partial \rho}{\partial z}}$), viz.:

$$\text{MLD} = 1.7 \sqrt{\frac{\rho_a C_d}{\rho_w}} \frac{W}{\sqrt{Nf}} \sim 1.25 \frac{W}{\Delta\rho^{1/4}} \quad (\text{in S.I. units}) \quad (7)$$

evaluated as per Eq. 4, taking dz as 20 m.

A similar relationship, with a slightly different power relationship for $\Delta\rho$, was found in laboratory experiments by Manucharyan (2010), viz.:

$$\text{MLD} \propto \frac{1}{N^{2/3}} \propto \frac{1}{\Delta\rho^{1/3}} \quad (8)$$

To test these proposed relationships, using data only from ice-free times (to avoid complications from sea ice coupling), we use multiple regression between $\log(\text{MLD})$, and $\log(W)$ and $\log(\Delta\rho)$, to seek the exponents α and β and constant C in the hypothesized relationship

$$\text{MLD} = C \frac{W^\alpha}{\Delta\rho^\beta} \quad (9)$$

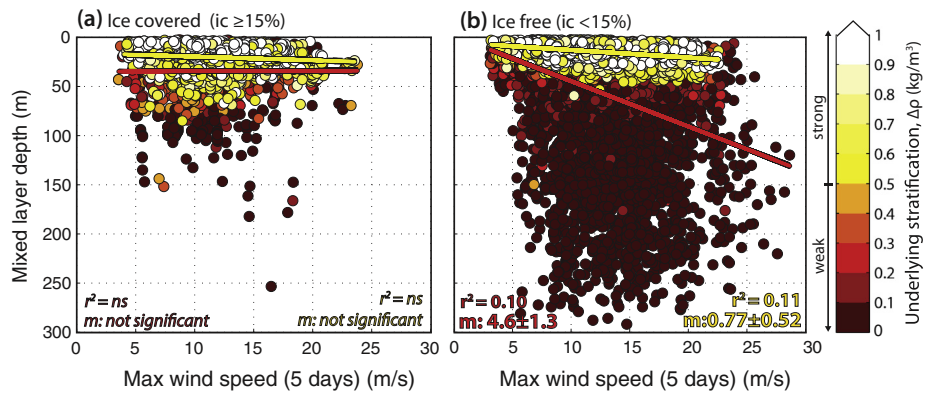


Fig. 11. Scatter plots of MLD versus maximum wind speed in the 5 days preceding the cast for all the Arctic regions during (a) ice-covered (ice concentration, $ic \geq 15\%$) and (b) ice-free times. Data points are color-coded according to underlying stratification (see color scale), defined as the potential density step across the ML base, see Section 'Controlling effects of stratification and influence of sea ice cover'. Also marked are linear fits (lines) and m values (in seconds) (with 95% confidence intervals) for fits significant at the 95% level of "MLD = $m \times$ Wind + constant" for data points with weak ($\Delta\rho < 0.5 \text{ kg/m}^3$) stratification (red) and strong ($\Delta\rho > 0.5 \text{ kg/m}^3$) stratification (yellow). Fraction of variance explained (r^2) is shown for weakly versus strongly stratified points in each panel. ns indicates correlation is not significant at the 95% confidence level. (For interpretation of the references to color in this figure legend, the reader is referred to the web version of this article.)

obtaining a fit (which explains 65% of the variance) of $\alpha = 0.55 \pm 0.03$; $\beta = 0.43 \pm 0.01$; and $C = 3.6 \pm 1.1$ (in S.I. units), viz.:

$$\text{MLD} = [3.6 \pm 1.1] \frac{W^{0.55 \pm 0.03}}{\Delta\rho^{0.43 \pm 0.01}} \quad (10)$$

However, the contribution of wind to this fit is only slight. Seeking a dependence only on stratification (i.e., assuming $\alpha = 0$), we find a fit of $\beta = 0.45 \pm 0.01$; and $C = 13 \pm 1$ (in S.I. units), viz.:

$$\text{MLD} = [13 \pm 1] \frac{1}{\Delta\rho^{0.45 \pm 0.01}} \quad (11)$$

This exercise yields several interesting results. We note, firstly, α is ~ 0.5 , much less than the linear exponent of Eqs. 4, 5 and 7, suggesting that MLD is less dependent on wind than simple theory suggests. Secondly, we see that expression 11 still explains 58% of the variance of MLD (compared to 65% of the variance, fitting also to wind). This also suggests that wind variability has only a weak influence on MLD change in our data. Tests show this result is not sensitive to using maximum wind speed within other time windows (including day of the cast). Neither are significantly better correlations obtained with tests using the other wind products of MERRA, JRA55 and ERA interim.

This lack of correlation between MLD and wind may reflect that the daily wind product may have erroneous energy in the ~ 12 h spectral band (which can force a resonance inertial wave response driving ML deepening, see e.g., Alford (2003)), or, more simply, that the reanalysis wind products may have insufficient skill over the data-poor Arctic Ocean (although see Lindsay et al. (2014) for an overview of reanalysis skill in the Arctic). Alternatively, it may just illustrate that such a simple ocean model is insufficient for describing these processes.

Thirdly, this exercise yields a value for β of ~ 0.5 , suggesting a stronger dependence on stratification than the theoretical and laboratory models of Pollard et al. (1973) ($\beta \sim 0.25$, Eq. 7) and Manucharyan (2010) ($\beta \sim 0.33$, Eq. 8), possibly due to density-driven restratification processes [e.g., mesoscale and submesoscale eddies, Mahadevan et al., 2010]. To investigate these issues requires a ML model, beyond the scope of this paper.

However, the strong correlation of MLD with underlying stratification is remarkable and suggests that in order to understand the long-term changes in Arctic MLD, we should focus on investigating processes affecting upper ocean stratification, rather than changes in wind speed, which in any case appear (so far) to be small [Spreen et al., 2011].

Interannual and decadal variability in Arctic mixed layer properties

Finally, we consider to what extent are interannual and decadal changes (the latter computed simplistically as a linear record-length trend) evident in the six regions in our ~ 30 year dataset (1979–2012) (Figs. 12 and 13 and complete statistics in Table 5 and Fig. 14). As discussed in Section 'Monthly climatology of MLD properties (depth, temperature and salinity) in 6 regions of the Arctic', we consider all points in our data collection to be independent.

The long-term loss of Arctic sea ice over this period [e.g., Stroeve et al., 2007] is clearly reflected in average ice concentration (ic) data in each region. Although winter (taken as November to May) changes are small other than in the Barents Sea (Table 5), in summer (taken as June–September) the ~ 30 -year trends of western Arctic sea ice retreat ($\sim 0.9\%/\text{yr}$) are almost twice those of eastern Arctic sea ice retreat ($\sim 0.4\%/\text{yr}$). However, these regional sea ice losses are generally not evident in ice concentrations at the cast locations – for example, despite overall ice loss in the regions, the summer casts in the Chukchi and the Southern Beaufort Sea show small ice concentration increases, indicating a bias to preferred sampling in ice-covered waters. To avoid aliasing such biases, we thus compute ice-free ($ic < 15\%$) and ice-covered ($ic \geq 15\%$) trends separately.

Interannual changes in ML depth, temperature and salinity

Where there is sufficient data coverage, the annual summer and winter means for each region (ice-covered or ice free) generally show significant interannual variability (e.g., Figs. 12 and 13).

The years of 2007 and 2008 show dramatic sea ice retreat in the Arctic, as is evident in our summer full-basin ice concentration averages in the Canada Basin (top row, Fig. 12c) and the Chukchi Sea and Makarov Basin (Fig. 12a and d, respectively), those being the regions of greatest ice loss. (Sea ice retreat was even greater in 2012. However, our data coverage is very low in 2012, and thus we focus on the earlier 2007 and 2008 sea ice minima.) As just discussed, even in these regions, however, sampling locations do not indicate particularly anomalous sea ice loss. Yet, consistent with reported sea surface temperature changes [Steele et al., 2010], our ML data show this sea ice retreat is reflected in warmer ML temperatures in the summer Canada and Eurasian basins, in the Chukchi Sea and perhaps the Makarov Basin (2nd and 3rd rows,

Fig. 12). Note our MLD data do not show 2007 being anomalously warm in the Southern Beaufort or the Barents seas (2nd and 3rd rows, **Fig. 12b** and f).

A coincident summer 2007 ML freshening is evident in the central Arctic (Canada, Makarov and Eurasian basins), with Eurasian Basin waters remaining fresh for a few years (4th row, **Fig. 12**). A winter ML freshening of the Eurasian and Makarov basins starts in 2008 and also remains for several years (4th row, **Fig. 13**). (We lack the data to comment on winter Canada Basin salinity change in this time period, see **Fig. 13c**.) Prior work indicates an increase in freshwater (FW) storage in the Beaufort Gyre since ~1990 [e.g., Proshutinsky et al., 2009] and an increase in Arctic FW storage between 1992–1999 and 2006–2008 [e.g., Rabe et al., 2011]. Those studies are somewhat biased towards summer (July–September) data in the western Arctic, although Rabe et al. (2014) extend the seasonal coverage of their work, confirming the freshening between 1992 and 2012 (the largest change being between 2002 and 2008). Generally, these studies consider only regions of the Arctic with water depths deeper than 500 m, and waters above the 34 psu isohaline (typically ~250 m deep in the western Arctic). However, it is interesting that to some extent our ML salinities reflect the changes found by those prior studies over a larger fraction of the water column, although our winter results suggest a more recent (2011 onwards) return to prior saltier conditions, in contrast to Rabe et al. (2014)'s results for the deeper water column.

While the year-to-year pattern of winter ML freshenings in the central Arctic (Canada Makarov and Eurasian basins) appear to be associated with winter MLD shoaling (4th and 5th rows, 13), summer ML freshenings (4th and 5th rows, **Fig. 12**), with the exception of those in the Canada Basin and the Chukchi Sea, show only modest shoaling of the already shallow summer MLD.

With the exception of these signals, and possibly warm summers in Southern Beaufort Sea in 1987 and 2011 (2nd column, 2nd and 3rd rows, **Fig. 12**), and a decade long cooling of the winter Barents Sea from 1996 to 2007 (6th column, 2nd and 3rd rows, **Fig. 13**), interannual coverage is generally too sparse to study interannual change in these regions in detail. Instead thus, we look for change spanning the entirety of our time period (1979–2012).

Multi-year (up to 30-year) trends and decadal change in Arctic ML properties

Though a linear trend is a crude method of describing a system with rich interannual variability, to allow some quantification of ML changes we compute linear trends in ML properties over the available data (**Figs. 12–14** and **Table 5**). This is typically over ~30 years (1979–2012), although the period is shorter in regions with less data coverage (e.g., **Figs. 12 and 13**). The details of the time periods for each region, season and ice cover are given in **Table 5**. Although annual means are marked on **Figs. 12 and 13**,

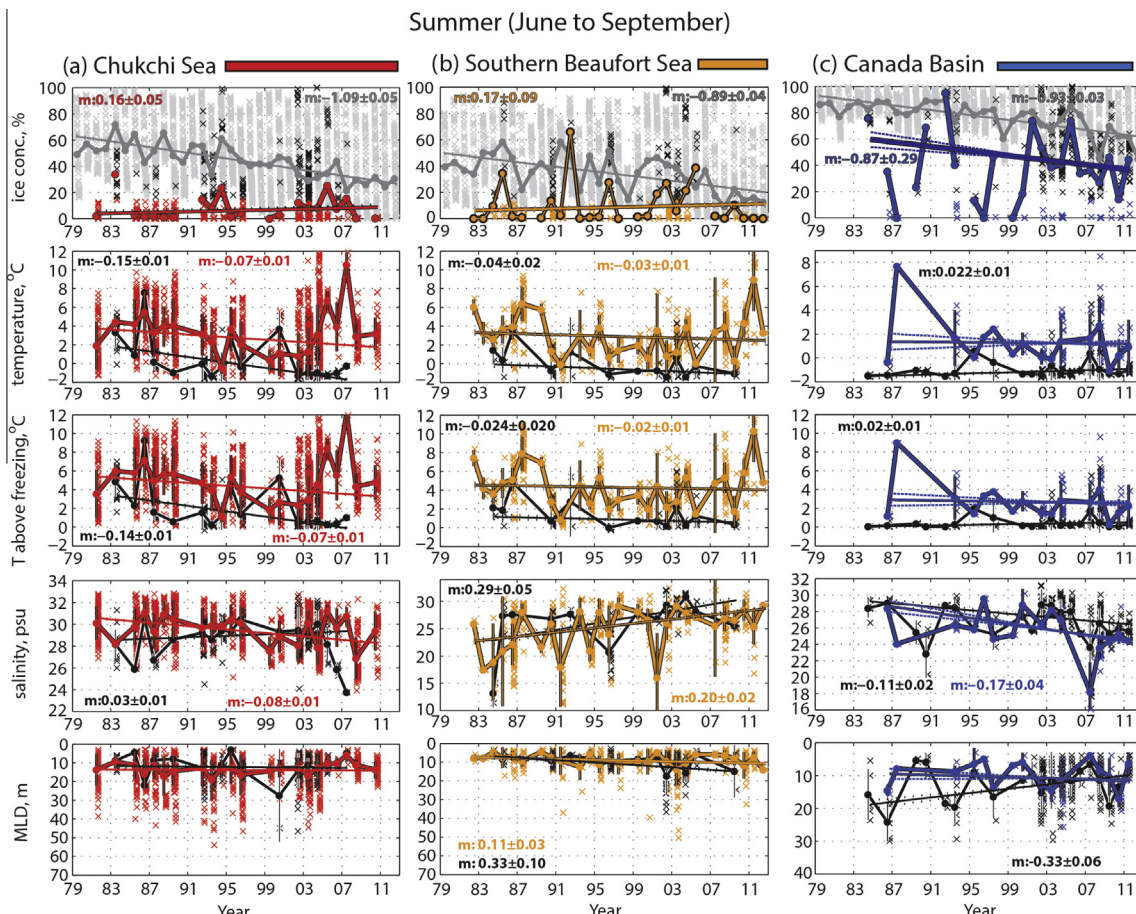


Fig. 12. For all regions (columns: (a) Chukchi Sea, (b) Southern Beaufort Sea, (c) Canada Basin, (d) Makarov Basin, (e) Eurasian Basin and (f) Barents Sea), Mixed Layer (ML) properties for each summer (June to September) from 1979 to 2012 showing individual measurements (black/color crosses) and annual average (black/color dots, joined by solid lines, with standard deviation as vertical bars), black indicating ice-covered and color (other than in row 1) indicating ice-free casts (ice-covered defined as $\text{ic} \geq 15\%$). From the top, rows show (i) ice concentration (with gray symbols indicating average over entire area, and black/colored symbols indicating average over all cast locations (combining ice-covered and ice-free)); (ii) temperature averaged over the MLD for ice-covered (black) and ice-free (colored); (iii) temperature above freezing averaged over the MLD; (iv) salinity averaged over the MLD; and (v) MLD. In each panel solid straight lines show the long-term trend, estimated as a best linear fit to all the data (not just the annual averages) with dashed lines showing the 95% C.I. and text giving slope ($m \pm \text{C.I.}$) when trend is significantly different from zero, black/color indicating ice-covered/ice-free casts. (For interpretation of the references to color in this figure legend, the reader is referred to the web version of this article.)

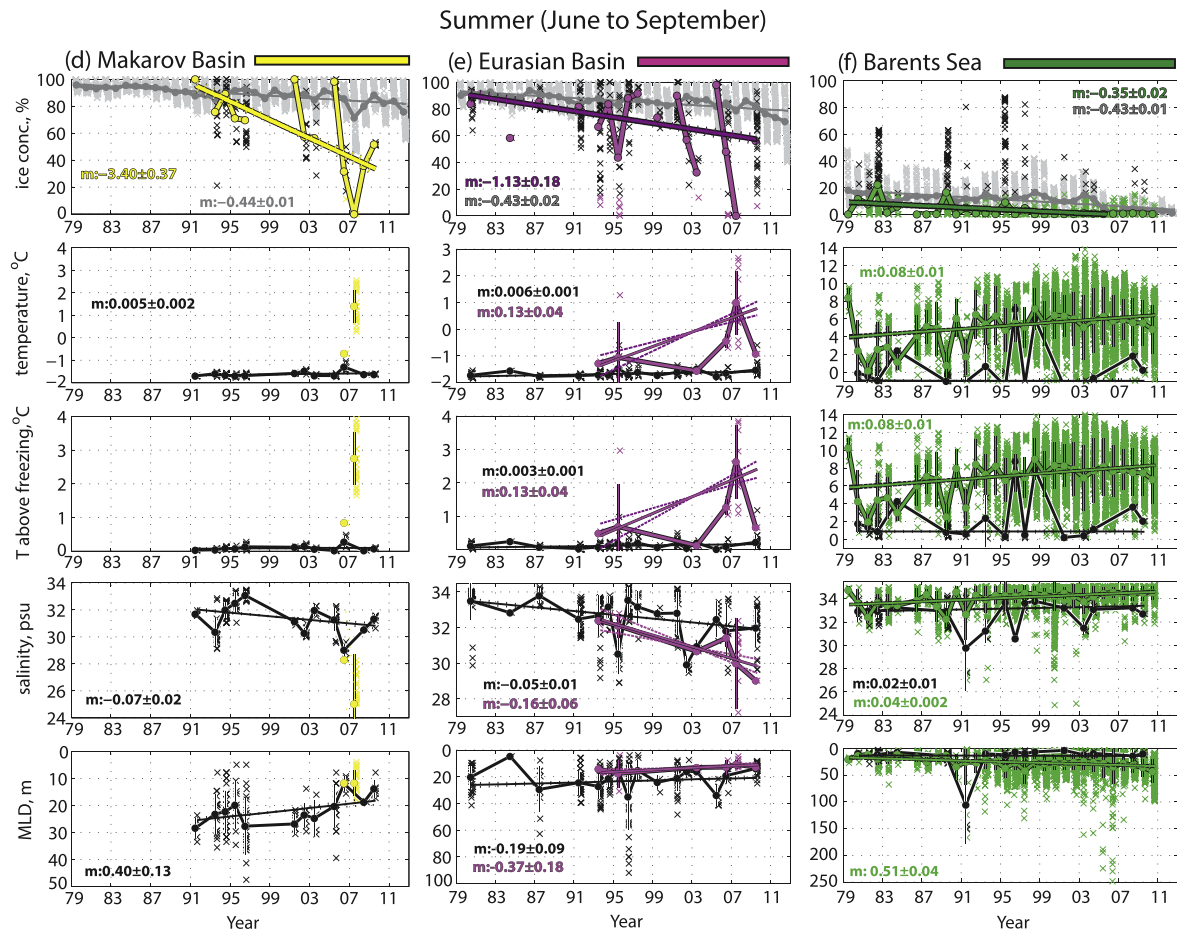


Fig. 12 (continued)

we compute the trends by applying a linear fit to all the data points available per ice coverage, per season, and per region. Thus, our trend weights all measurements from all years equally, to avoid biasing results to years with few data.

For completeness, all regions are included in Figs. 12 and 13, although we discuss below only trends that are statistically different from zero and are significantly large to be of interest (bold entries with asterisk in Table 5, color-coded in Fig. 14).

Trends in ML temperature

Ice cover generally constrains ML temperatures to be near freezing. Thus, under ice cover (both in winter and summer), temperature changes are generally very small (Fig. 14 and Table 5) or related to a warming due to freshening (e.g., compare 2nd and 3rd rows in Fig. 13). There are examples of apparent warming (Canada Basin summer and Barents Sea winter) and cooling (Chukchi and Southern Beaufort Seas winter and summer) under ice cover, although these trends are strongly influenced by measurements of temperatures several degrees C above freezing apparently below sea ice, suggesting the satellite ice concentrations at these points (often close to the coast or near the ice-edge) are misrepresenting the real world.

Even in ice-free regions, ML temperature trends are often small (<0.02 °C/yr) (Canada Basin), with the summer Southern Beaufort Sea showing a small (0.02 °C/yr) cooling. Although intuitively surprising, given recent sea ice retreat, in fact prior studies of Arctic Sea Surface Temperature (SST) [Steele et al., 2008] show significant SST warming only over the East Siberian Sea and the Barents Sea in the time-period of 1965–1995 they consider. The warming

reported in later papers [e.g., Steele et al., 2010] is a more recent phenomenon.

Our trends from the Chukchi Sea (summer and winter) suggest some cooling (~ 0.1 °C/yr) over the ~ 20 years of data, and this appears to be robust even when taking into consideration changes in the spatial sampling – early measurements (Fig. 16, and Section ‘Decadal change in temperature–salinity (T – S) space’) were constrained to the eastern Chukchi, which is warmer than the western Chukchi [e.g., Coachman et al., 1975; Woodgate et al., 2005]. Note that Bering Strait SST data show no significant trend from 1982 to 2011 [Woodgate et al., 2012].

The summer ice-free Eurasian Basin warming trend is larger (~ 0.1 °C/yr), but is strongly biased by warm values in 2007 and a short time series (Eurasian Basin, Fig. 12).

In the Barents Sea, ML temperatures (summer and winter) are sometimes some degrees above freezing and generally show a modest warming (~ 0.08 °C/yr) over ~ 30 years (Fig. 14, Table 5). This probably relates to the observed strengthening and warming of the Atlantic flow to the Barents Sea [e.g., Árthun et al., 2012], which also likely drives the salinity increase described below. In contrast, the summer ice-covered Barents shows no significant temperature trend, possibly because the waters maintaining an ice cover in summer are Arctic waters (entering the Barents from the north), rather than the warmer Atlantic waters from the south [e.g., Loeng and Drinkwater, 2007].

Trends in ML salinity

More dramatic, however, are the trends in salinity. Almost everywhere in the Arctic (except in the Barents and Southern Beau-

fort Seas), the observations show a significant ML freshening ($0.04\text{--}0.2 \text{ psu/yr}$) over the ~ 30 years of data (Fig. 14, Table 5). The ML freshening trend is largest in the Canada Basin (in winter ice-covered regions, $\sim 0.2 \text{ psu/yr}$). (Korhonen et al. (2013) also find a freshening in the winter ML salinity in their 1991–2011 dataset, although their trend is smaller ($\sim 0.1 \text{ psu/yr}$)). Although sparse winter Canada Basin data suggest this as a step change in the late 1990s (3rd column, Fig. 13), summer Canada Basin data suggest a more gradual freshening trend (3rd column, Fig. 12). The summer Eurasian Basin ML shows similar freshening (weaker in ice-covered waters). The validity of winter ML freshening in the Makarov and Eurasian basins (Fig. 13) is less clear, however, as the trends are dominated by sparse data from the 1980s with more recent years showing significant interannual variability, as discussed above.

To put these numbers in context, we estimate the quantity of freshwater needed to achieve these changes in ML depth and salinity in a manner analogous to the calculation of t_{melt} , using the end points of the trend as the starting and end points for the calculation, and normalizing with the number of years of the trend to give the change per year in Table 5. For the winter Canada Basin, a 0.2 psu/yr change requires actually remarkably little freshwater – a sea ice thickness change of 0.16 m/yr per unit area, or $\sim 115 \text{ km}^3/\text{yr}$ of FW input, which is even smaller than the uncertainties in the FW inflows into the Arctic [e.g., $\sim 200 \text{ km}^3/\text{yr}$, Woodgate et al., 2012]. Thus, Arctic MLDs may be very sensitive to small changes in freshwater.

In contrast to the wide-spread freshening of the Arctic ML, the MLs of the summer Southern Beaufort Sea, and to a lesser extent the Barents Sea and the ice-covered Chukchi Sea, show

salinization. The summer Barents Sea salinity increase, coincident with the Barents Sea warming described above, likely relates to increased Atlantic water inflow [Arthun et al., 2012], although could also relate to reduced freshwater sources to the Barents Sea. The summer Southern Beaufort Sea salinization trend, $\sim 0.2 \text{ psu/yr}$, is opposite but as large as the Canada Basin change. Given the much smaller area of the Southern Beaufort Sea, this is only equivalent to $\sim 10 \text{ km}^3/\text{yr}$ of FW, a small fraction ($\sim 10\%$) of the Canada Basin freshwater change estimated above. Note that the Mackenzie River, which strongly influences the Southern Beaufort Sea, discharges $\sim 310 \text{ km}^3/\text{yr}$ [Lammers et al., 2001], so the observed Southern Beaufort Sea salinization could easily arise from routing part of the river water into the deeper basin away from the Southern Beaufort Sea [e.g., Steele et al., 2006]. In addition, it could be that the spin-up of the Beaufort Gyre draws surface freshwater away from the coast via Ekman transport, resulting in the salinization of the Southern Beaufort Sea.

Decadal change in temperature–salinity (T–S) space

For further insight into physical processes and to check for sampling bias, we view these changes in temperature–salinity (T–S) space (Figs. 15 and 16), binned by region, decade and season, regardless of ice coverage, including maps of cast locations to assist identification of spatial bias. Since T–S diagrams visually overstress outliers, we include also frequency histograms of data points in T–S bins.

The summer Chukchi T–S results (Fig. 16a) are consistent with the trends identified above of freshening and cooling. Note that

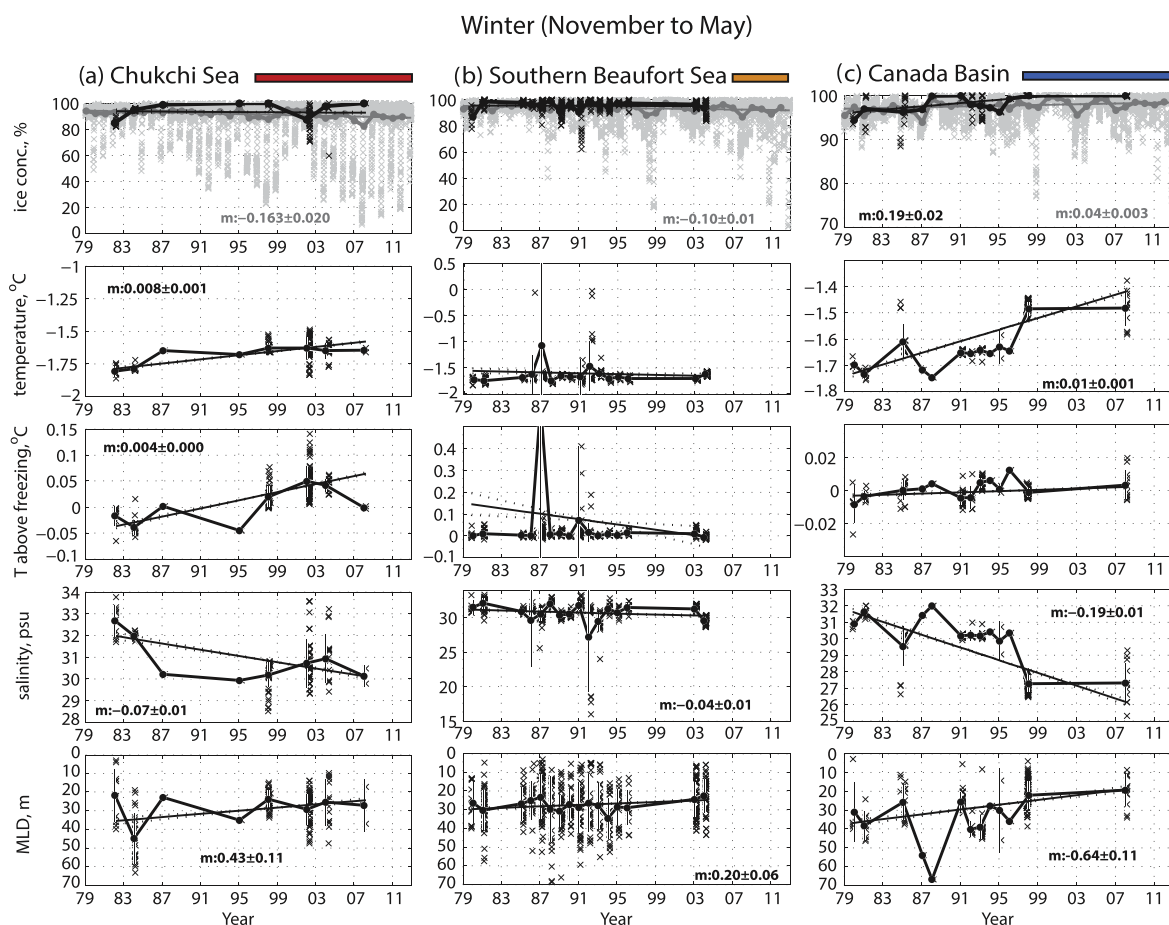


Fig. 13. As per Fig. 12, but for winter (winter being the preceding November to the May of the year in question) for all regions.

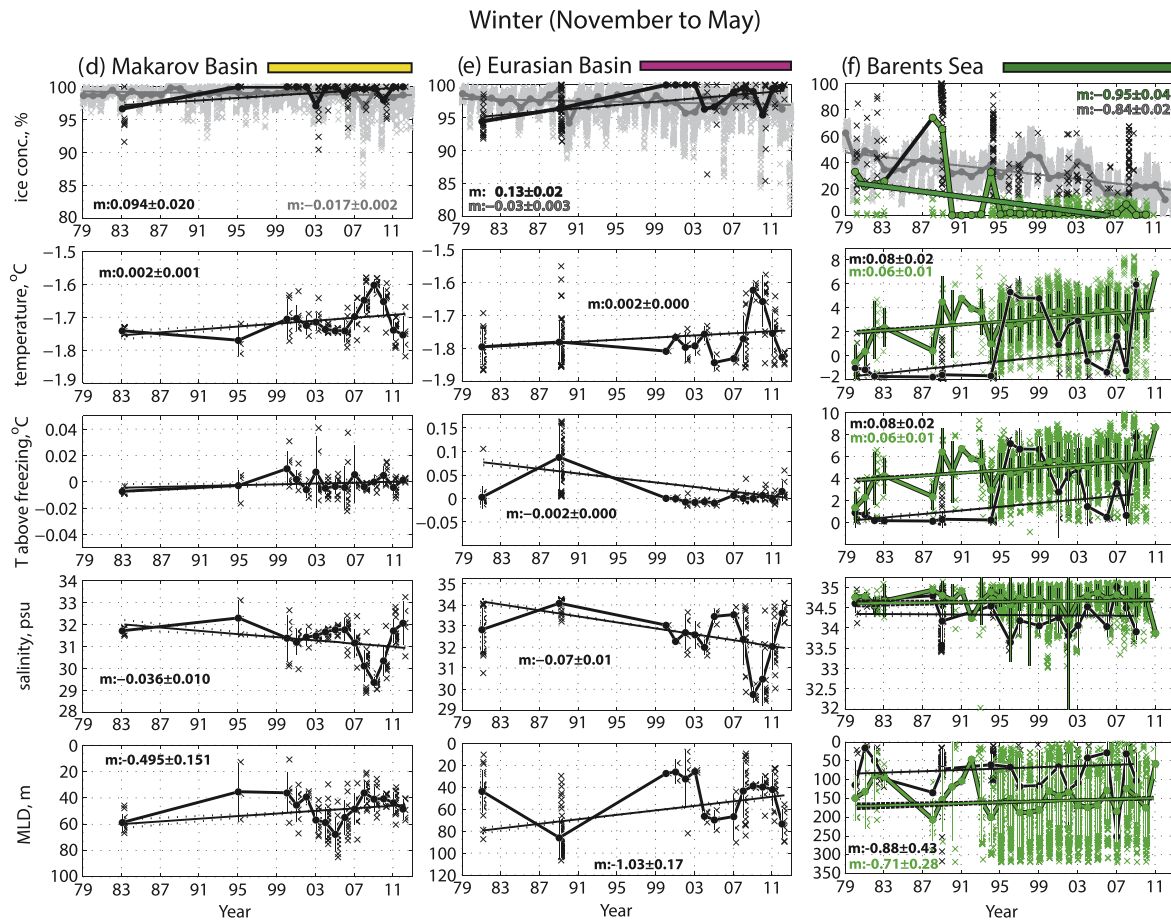


Fig. 13 (continued)

although the maps of Fig. 16 suggest some spatial bias of the data, with only the 1990s having access to the western Chukchi [Coachman et al., 1975], in fact comparable trends are found considering data only in US waters (e.g., excluding T - S plots in 2nd column of Fig. 16a). Similar issues are found with the winter Chukchi Sea coverage (Fig. 15a), with the 1990s being somewhat anomalous, but the 1980s and the 2000s more comparable.

The summer Southern Beaufort Sea coverage (Fig. 16b), reasonably consistent in each decade, suggests the most dramatic changes are in the freshest ($S < 22$ psu) components of the waters, likely strongly influenced by the Mackenzie River. These waters are warm in the 1980s, cool near freezing in the 1990s and absent in the 2000s. The absence of these low salinities in the 2000s may be due to waters being driven from the shelf, as speculated above. The winter Southern Beaufort Sea coverage (Fig. 15b) is generally good, other than in the 2000s when data are sparse.

In the winter Canada Basin (Fig. 15c), the T - S plots indicate primarily two classes of water – fresher (~27 psu) waters near the freezing point, and saltier (~30 psu) waters at or slightly warmer than the freezing point. There is no obvious decadal pattern to this distribution – in the 1990s, the saltier waters are found closest to the coast; however in the 1980s and the 2000s, it is the fresher water type which is nearer to the coast. Since spatial coverage is reasonably consistent between decades, we conclude our trends in Table 5 are representative. The summer Canada Basin coverage is poor in the 1980s, but comparable for the later time periods.

Spatial bias skews the trend results from the summer Makarov Basin (Fig. 16d) – the fresh, warm (~26–28 psu, 0–2.5 °C) data

points from the 2000s, are all from one section near the Laptev shelf-break (~78–82°N, ~160°E), taken only in the 2000s. Possibly these points are indicative of input from the Russian rivers, but the section is not occupied in other decades and this skews our summer decadal trends. While some of the same problems are also present in the winter Makarov Basin (Fig. 15d), there are fewer anomalous points, although the trends should still be treated with caution.

Coverage in the summer Eurasian Basin (Fig. 16e) is confined to near Spitsbergen in the 1980s, but is across the basin for the 1990s and 2000s, suggesting that the warming, freshening trends discussed above are representative, although note the time series is short and biased by the 2007 warming, as discussed in Section 'Trends in ML temperature'.

For the winter Eurasian Basin (Fig. 15e), in the 1990s there are almost no data and in the 2000s data points are concentrated in the Lincoln Sea (location marked in map of Fig. 15). Since the Lincoln Sea data are fresher than the rest of the basin, this suggests the freshening trend found above is an artifact of changes in spatial sampling. However, comparing the T - S from the 1980s and the 2000s (Fig. 15e) suggests interesting changes in T - S regime usually defined as Lower Halocline Water [e.g., Kikuchi et al., 2004]. The 1980s data show a sharp corner in T - S space (at ~34 psu) and warm (>−1.6 °C) waters at high salinities, suggestive of a strong well defined front between fresher waters at freezing and warmer, saltier waters. Recall these are ML properties, and thus the warm, saltier waters suggest that convection has reached and mixed waters from underlying Atlantic Waters (AW) into the ML. Data

Table 5

Interannual trends (best fit lines $\pm 95\%$ confidence interval) for the six regions, from all available data from 1979 to 2012 (see Figs. 12 and 13), separated by season (winter being the preceding November to the May of the year in question; summer = June–September) and ice concentration, ic (ice-covered = $ic \geq 15\%$), indicating (for each region, season and ice cover) the time period over which the trend is calculated. “Ice conc. avg” is ic averaged over the entire region; “Ice conc. casts” is ic averaged over the cast locations only. Temperature and salinities are averaged over the Mixed Layer Depth (MLD) at each cast. Temperatures (T) above freezing are relative to the freezing point of water at the MLD salinity and 1-dbar pressure. The freshening/salinification trend is converted to equivalent freshwater content trend (FW) and also converted to ice-growth as per Eq. 2 (Section ‘Quantifying influence of sea ice growth/melt’, with negative values indicating freshening/ice melt). The percentage of ice growth/melt trend relative to the seasonal ice change (as per Eq. 2) is also shown. Gray values are not significant at the 95% confidence level. Blue and red values are significant at the 95% confidence level, with blue showing negative trends and red showing positive trends. Bold font values and asterisk indicate the larger trends discussed in Section ‘Multi-year (up to 30-year) trends and decadal change in Arctic ML properties’. No entry signifies insufficient data (i.e., <6 years of measurements). Parentheses indicate possible bias as discussed in Section ‘Multi-year (up to 30-year) trends and decadal change in Arctic ML properties’.

Region	Parameter	Winter (Nov-May)		Summer (Jun-Sept)	
		Ice-covered	Ice-free	Ice-covered	Ice-free
Chukchi Sea	Ice conc. avg (%/yr)	-0.16 ± 0.02		-1.09 ± 0.05	
	Ice conc. casts (%/yr)	-0.05 ± 0.09		0.11 ± 0.05	
	Period (No. of years)	1981-2007 (8yr)	--	1983-2007 (17yr)	1981-2010 (22yr)
	Temperature (°C/yr)	0.008 ± 0.001	--	-0.14 ± 0.01	-0.07 ± 0.008
	T above freezing (°C/yr)	0.004 ± 0.00	--	* -0.14 ± 0.01	* -0.08 ± 0.01
	Salinity (psu/yr)	* -0.07 ± 0.01	--	0.02 ± 0.01	* -0.08 ± 0.01
	MLD (m/yr)	* -0.43 ± 0.11	--	-0.04 ± 0.06	-0.008 ± 0.02
	Freshwater (FW, km ³ /yr)	29.4 ± 7.8	--	-3.7 ± 4.2	18.4 ± 3.6
	Hypothetical ice growth % of seasonal ice change	-0.07 m/yr	--	0.01 m/yr	-0.05 m/yr
Southern Beaufort Sea	Ice conc. avg (%/yr)	-0.09 ± 0.01		-0.89 ± 0.04	
	Ice conc. cast (%/yr)	-0.02 ± 0.03		0.17 ± 0.09	
	Period (No. of years)	1980-2004 (16yr)	--	1984-2009 (13yr)	1982-2012 (27yr)
	Temp (°C/yr)	-0.004 ± 0.004	--	-0.04 ± 0.02	-0.03 ± 0.01
	T above freezing (°C/yr)	-0.006 ± 0.004	--	-0.024 ± 0.02	-0.017 ± 0.012
	Salinity (psu/yr)	-0.04 ± 0.01	--	* 0.29 ± 0.05	* 0.20 ± 0.02
	MLD (m/yr)	-0.20 ± 0.06	--	* 0.33 ± 0.10	0.11 ± 0.03
	Freshwater (FW, km ³ /yr)	6.04 ± 2.5	--	-14.4 ± 7.1	-9.4 ± 2.9
	Hypothetical ice growth % of seasonal ice change	-0.05 m/yr	--	0.11 m/yr	0.07 m/yr
Canada Basin	Ice conc. avg (%/yr)	0.04 ± 0.003		-0.93 ± 0.03	
	Ice conc. cast (%/yr)	0.19 ± 0.02		-0.87 ± 0.29	
	Period (No. of years)	1980-2008 (13yr)	--	1984-2011 (20yr)	1986-2011 (16yr)
	Temp (°C/yr)	0.01 ± 0.001	--	0.02 ± 0.01	-0.007 ± 0.04
	T above freezing (°C/yr)	0.00 ± 0.00	--	0.02 ± 0.01	-0.02 ± 0.04
	Salinity (psu/yr)	* -0.19 ± 0.01	--	* -0.11 ± 0.02	* -0.17 ± 0.04
	MLD (m/yr)	* -0.64 ± 0.11	--	* -0.33 ± 0.06	-0.08 ± 0.08
	Freshwater (FW, km ³ /yr)	114.4 ± 38.8	--	35.7 ± 12.3	60.00 ± 27.4
	Hypothetical ice growth % of seasonal ice change	-0.16 m/yr	--	-0.05 m/yr	-0.09 m/yr
Makarov Basin	Ice conc. avg (%/yr)	-0.017 ± 0.002		-0.44 ± 0.01	
	Ice conc. cast (%/yr)	0.09 ± 0.02		-3.40 ± 0.37	
	Period (No. of years)	1983-2012 (15yr)	--	1991-2009 (12yr)	--
	Temp (°C/yr)	0.002 ± 0.001	--	(0.005 ± 0.002)	--
	T above freezing (°C/yr)	0.00 ± 0.00	--	(0.001 ± 0.001)	--
	Salinity (psu/yr)	(-0.04 ± 0.01)	--	* (-0.07 ± 0.02)	--
	MLD (m/yr)	* (-0.50 ± 0.15)	--	* (-0.39 ± 0.13)	--
	Freshwater (FW, km ³ /yr)	39.6 ± 27.2	--	25.23 ± 5.2	--
	Hypothetical ice growth % of seasonal ice change	-0.07 m/yr	--	-0.04 m/yr	--
Eurasian Basin	Ice conc. avg (%/yr)	-0.03 ± 0.003		-0.43 ± 0.02	
	Ice conc. casts (%/yr)	0.13 ± 0.02		-1.13 ± 0.18	
	Period (No. of years)	1981-2012 (14yr)	--	1980-2009 (16yr)	1993-2009 (6yr)
	Temp (°C/yr)	(0.002 ± 0.00)	--	0.006 ± 0.001	(0.13 ± 0.04)
	T above freezing (°C/yr)	(-0.002 ± 0.00)	--	0.003 ± 0.001	* (0.13 ± 0.04)
	Salinity (psu/yr)	* (-0.07 ± 0.01)	--	-0.05 ± 0.01	* (-0.16 ± 0.06)
	MLD (m/yr)	* (-1.03 ± 0.17)	--	-0.19 ± 0.09	* (-0.37 ± 0.18)
	Freshwater (FW, km ³ /yr)	127 ± 36	--	42 ± 16	65.4 ± 34
	Hypothetical ice growth % of seasonal ice change	-0.12 m/yr	--	-0.04 m/yr	-0.06 m/yr
Barents Sea	Ice conc. avg (%/yr)	-0.84 ± 0.02		-0.43 ± 0.01	
	Ice conc. cast (%/yr)	-0.95 ± 0.04		-0.35 ± 0.02	
	Period (No. of years)	1980-2009 (18yr)	1980-2010(28yr)	1980-2009 (16yr)	1979-2010 (31yr)
	Temp (°C/yr)	0.08 ± 0.02	0.06 ± 0.01	-0.002 ± 0.012	0.08 ± 0.01
	T above freezing (°C/yr)	* 0.08 ± 0.02	* 0.06 ± 0.01	-0.001 ± 0.012	* 0.08 ± 0.01
	Salinity (psu/yr)	-0.002 ± 0.004	0.003 ± 0.003	0.02 ± 0.01	* 0.04 ± 0.002
	MLD (m/yr)	* -0.88 ± 0.43	* -0.71 ± 0.28	0.02 ± 0.17	* 0.51 ± 0.04
	Freshwater (FW, km ³ /yr)	--	--	-14.3 ± 9	-19.6 ± 8.6
	Hypothetical ice growth % of seasonal ice change	Not applicable: no freshening		0.01 m/yr	0.02 m/yr
				~ -6.3%	~ -6.3%

from the 2000s do not show these warmer waters, suggesting that in the regions sampled either convection is shallower (consistent with the MLD shoaling of Fig. 13e), or that the warm AWs are deeper (not evident in the data from the North Pole Environmental Observatory, <http://psc.apl.washington.edu/northpole/History.html>), or that there has been more spatial mixing. Indeed the 2000s do show a warmer lower halocline (compare temperatures at ~33.5 psu) indicative of mixing [e.g., Woodgate et al., 2005] or advective processes [see e.g., Kikuchi et al., 2004]. Note that these prior references refer to hydrographic profiles, while our data are illustrative of T - S change in the ML, i.e., in the horizontal, suggestive of surface fronts, and mixing across these fronts. These temperature changes are so small that they are not found to be significant in the linear trend, however, in T - S space they infer changes in physical processes.

The T - S clusters from the Barents Sea both in winter (Fig. 15f) and in summer (Fig. 16f) are highly indicative of the warm, salty (6°C , 35 psu) Atlantic inflow. Comparing plots from different decades shows the warming and salinization discussed above, consistent with a change in the inflow properties or a reduction in modification of the inflow.

Robust freshening and warming trends

Taking into consideration the spatial and temporal biases discussed above, the following trends appear to be robust:

Multi-year (up to 30 year) Arctic mixed layer Salinity Trends:

- Freshening in summer in the ice-free Chukchi Sea, and in all ice conditions in the Canada Basin and Eurasian Basin.
- Freshening in winter in most of the Arctic (Chukchi Sea, Southern Beaufort Sea, Canada Basin, and maybe the Makarov Basin and the Eurasian Basin).
- Salinization in summer in all ice conditions in the Southern Beaufort Sea and to a lesser extent in the ice-covered Chukchi, and the Barents Sea.
- No trends of salinization in winter.

Multi-year (up to 30-year) Arctic mixed layer Temperature Trends:

- Warming in summer in the ice-free Barents Sea and maybe the ice-free Eurasian Basin.
- Warming in winter in the Barents Sea under all ice conditions.

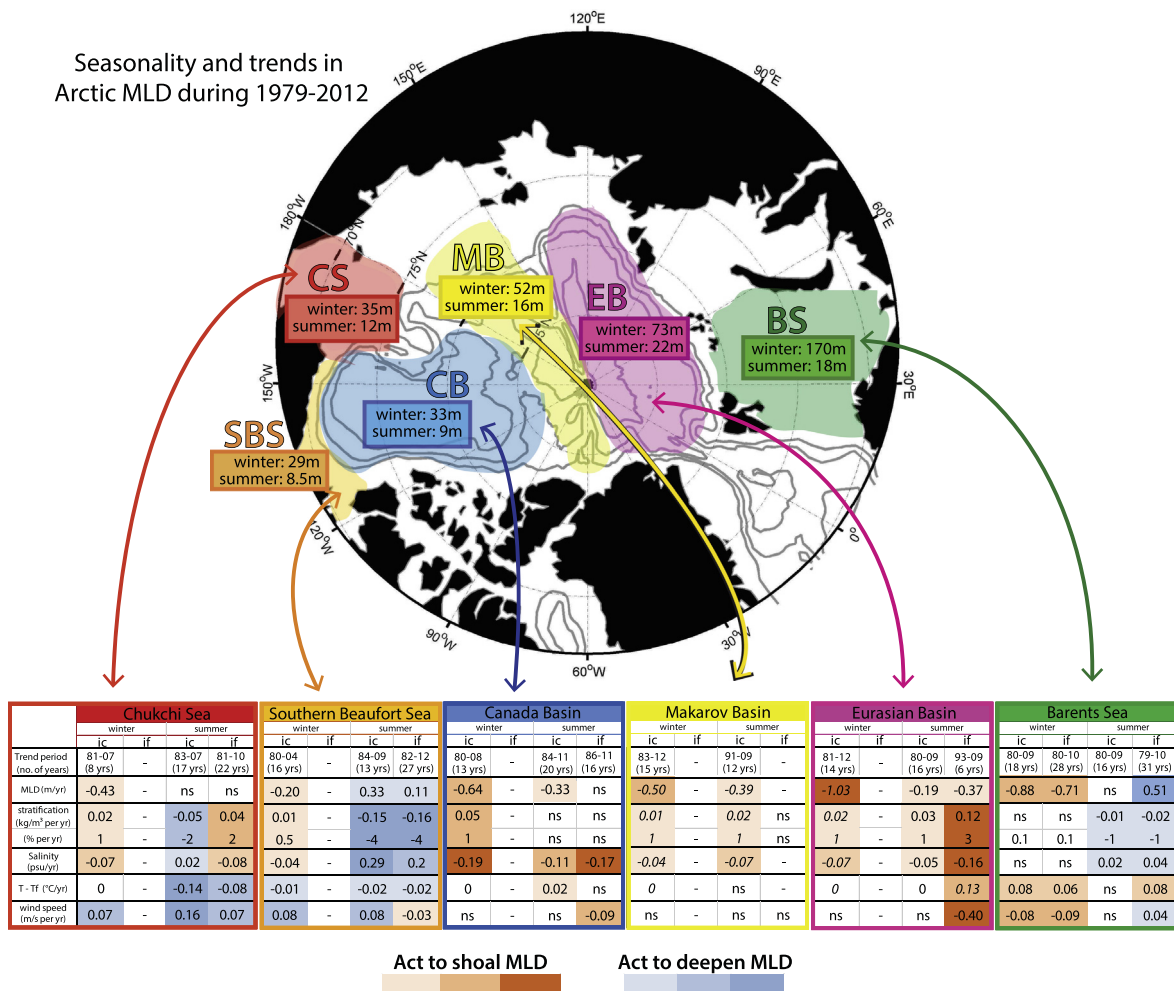


Fig. 14. Schematic with table showing the observed linear 30-year trends (units per year) in MLD, stratification ($\Delta\rho/\text{yr}$ as per Section 'Controlling effects of stratification and influence of sea ice cover' and in % of regional mean stratification), salinity, temperature above freezing (T-Tf), and wind speed (as per Table 5) from 1979 to 2012 for the six regions color-coded as in the map – Chukchi Sea (CS), Southern Beaufort Sea (SBS), Canada Basin (CB), Makarov Basin (MB), Eurasian Basin (EB), and Barents Sea (BS) – in ice-free (if) and ice-covered (ic) times (taken as ic $\geq 15\%$), for summer and winter. Table also gives period over which the trends were computed. Orange background indicates trends that would act to shoal the MLD, and blue background indicates trends that would act to deepen the MLD. Intensity of highlighted colors indicates the magnitude of the trend for each component, with darker colors indicating stronger trends. Trends are statistically significant at the 95% confidence level unless specified by ns. For errors, see Table 5. Dashes indicate insufficient data. Italics indicate possible bias on trends as discussed in Section 'Multi-year (up to 30-year) trends and decadal change in Arctic ML properties'. Winter maximum MLD and summer minimum MLD are given on the map for each region. Gray lines on the map are GSHHG bathymetry at 1000 m intervals. (For interpretation of the references to color in this figure legend, the reader is referred to the web version of this article.)

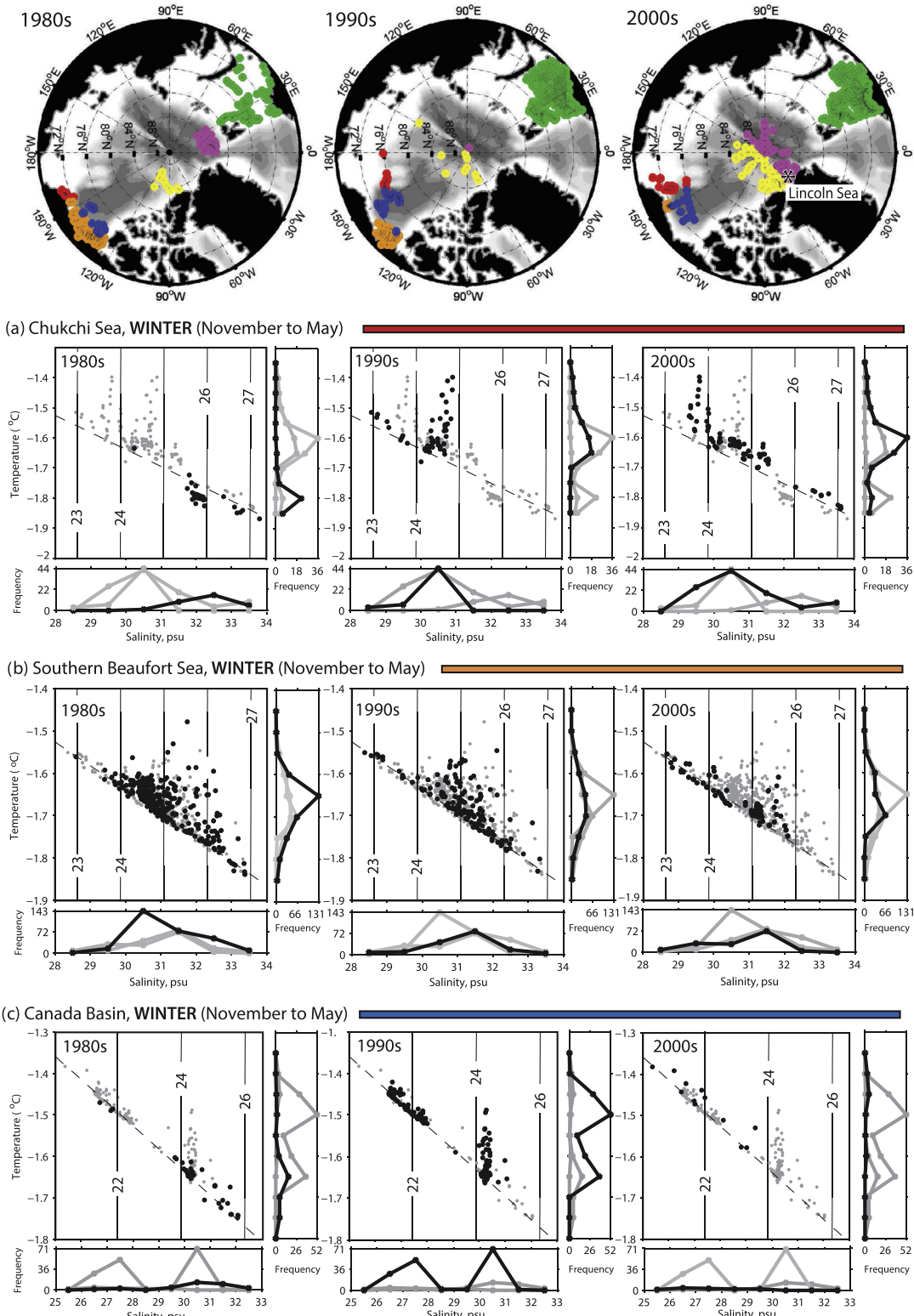


Fig. 15. Winter (preceding November to May) decadal temperature–salinity (T–S) diagrams. Columns indicate decade – (left) 1980s (1979–1989); (middle) 1990s (1990–1999); and (right) 2000s (2000–2012). Top row gives map of cast locations, color coded by region as in Fig. 1, with bathymetry from GSHHG. Subsequent rows show T–S diagrams for different regions, ((a) Chukchi Sea, (b) Southern Beaufort Sea, (c) Canada Basin, (d) Makarov Basin, (e) Eurasian Basin, and (f) Barents Sea), with panels to right of and below each T–S diagram indicating histogram of observations binned by temperature or salinity for each corresponding decade (black dots) and the data from the other two decades (gray dots). Solid contours show σ_0 (kg/m^3), and dashed lines mark the freezing point at 1-dbar. Note the different scales in all panels. Blue line in (b) highlights the Lincoln Sea data discussed in Section 'Decadal change in temperature–salinity (T–S) space'. (For interpretation of the references to color in this figure legend, the reader is referred to the web version of this article.)

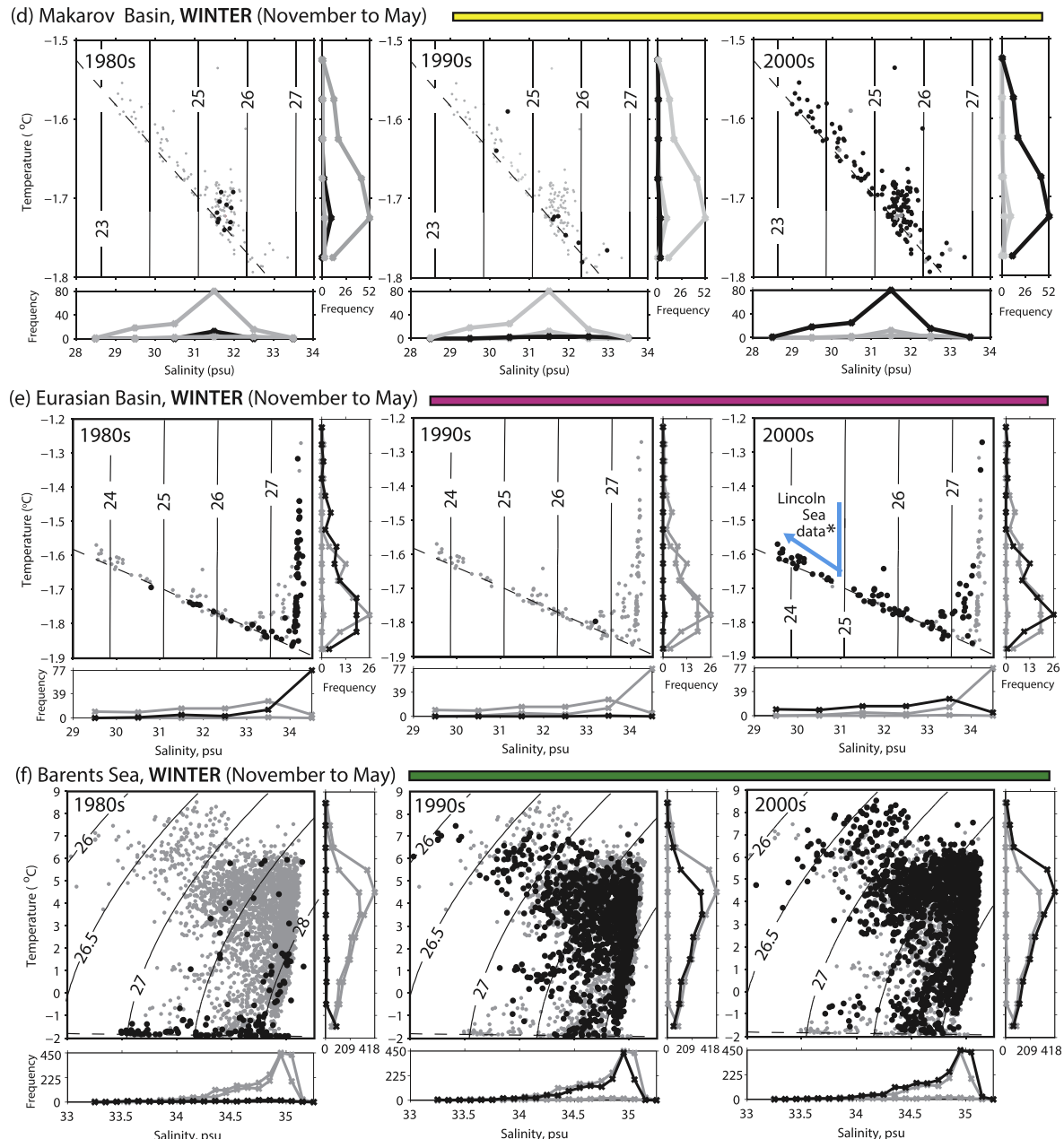


Fig. 15 (continued)

- Cooling in summer in all ice conditions in the Chukchi Sea and (marginally) in the Southern Beaufort Sea.

These are summarized in the schematic of Fig. 14, with blue/orange colors indicating trends that would deepen/shoal the MLD. Overall, there is a general pan-Arctic freshening trend, predominantly in the winter, the exceptions being the coastal areas – the Chukchi, the Southern Beaufort and the Barents seas, which show salinization. This freshening trend, albeit significant and of general basin-wide scale, represents a very small change in freshwater (Table 5), relative to both seasonal sea ice melt and the observed annual inputs of freshwater into the Arctic Basin. Warming trends are observed in the eastern Arctic (Barents Sea and maybe Eurasian Basin). In contrast, the coastal western Arctic (Southern Beaufort Sea and to a greater extent the Chukchi Sea) show ML cooling.

Trends in MLD and relationship to stratification and wind trends

Finally, we consider trends in MLD over the period of our dataset for each region, season, and ice cover conditions (Table 5, Figs. 12 and 13, with summary in Fig. 14), and compare to trends in stratification and local wind speed.

Arctic MLD shoaling is as equally ubiquitous and remarkable as the ML freshening. All regions in both winter and summer (except the summer Chukchi Sea – no trend, and the summer Southern Beaufort Sea and ice-free Barents Sea) show ML shoaling trends (typically 0.3–1 m/yr) (Figs. 12–14). While these trends are large (1 m/yr over 30 years is a 30 m total shoaling), it is important to remember this represents the shoaling of a mean, and there is still substantial spread about the mean. These shoalings are always related to freshening trends, although the largest shoalings do not coincide with the strongest freshenings (Table 5 and Fig. 14). (In their analysis of a shorter dataset (1991–2011), Korhonen

et al. (2013) find a significant trend in MLD only in the Nansen Basin, where their trend (shoaling ~ 0.2 m/yr) is in good agreement with our longer-term result.)

An interesting contradiction to the pan-Arctic shoaling of MLD is the Southern Beaufort Sea, where MLDs deepen ($\sim 0.3 \pm 0.1$ m/yr during ice-covered times, and $\sim 0.11 \pm 0.03$ m/yr during ice-free

times) over the period of our dataset, coincident with the sizeable salinization ($\sim 0.29 \pm 0.05$ psu/yr during summer ice-covered times, and $\sim 0.20 \pm 0.03$ psu/yr during summer ice-free times) previously mentioned. We argued above (Section 'Trends in ML salinity') that this salinization is likely due to export of river water from the Southern Beaufort Sea into the deeper Arctic.

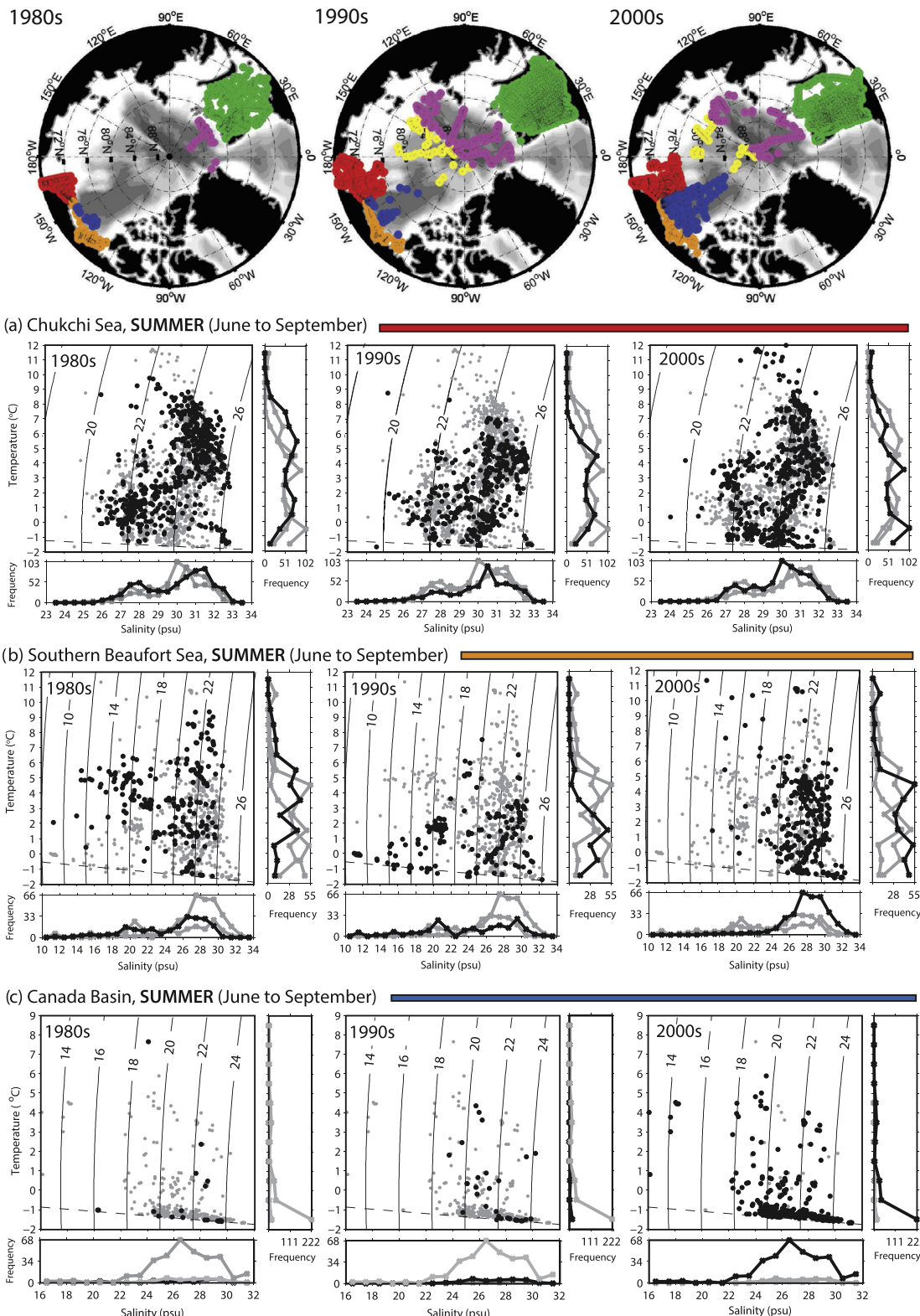


Fig. 16. As per Fig. 15 but for summer (June to September).

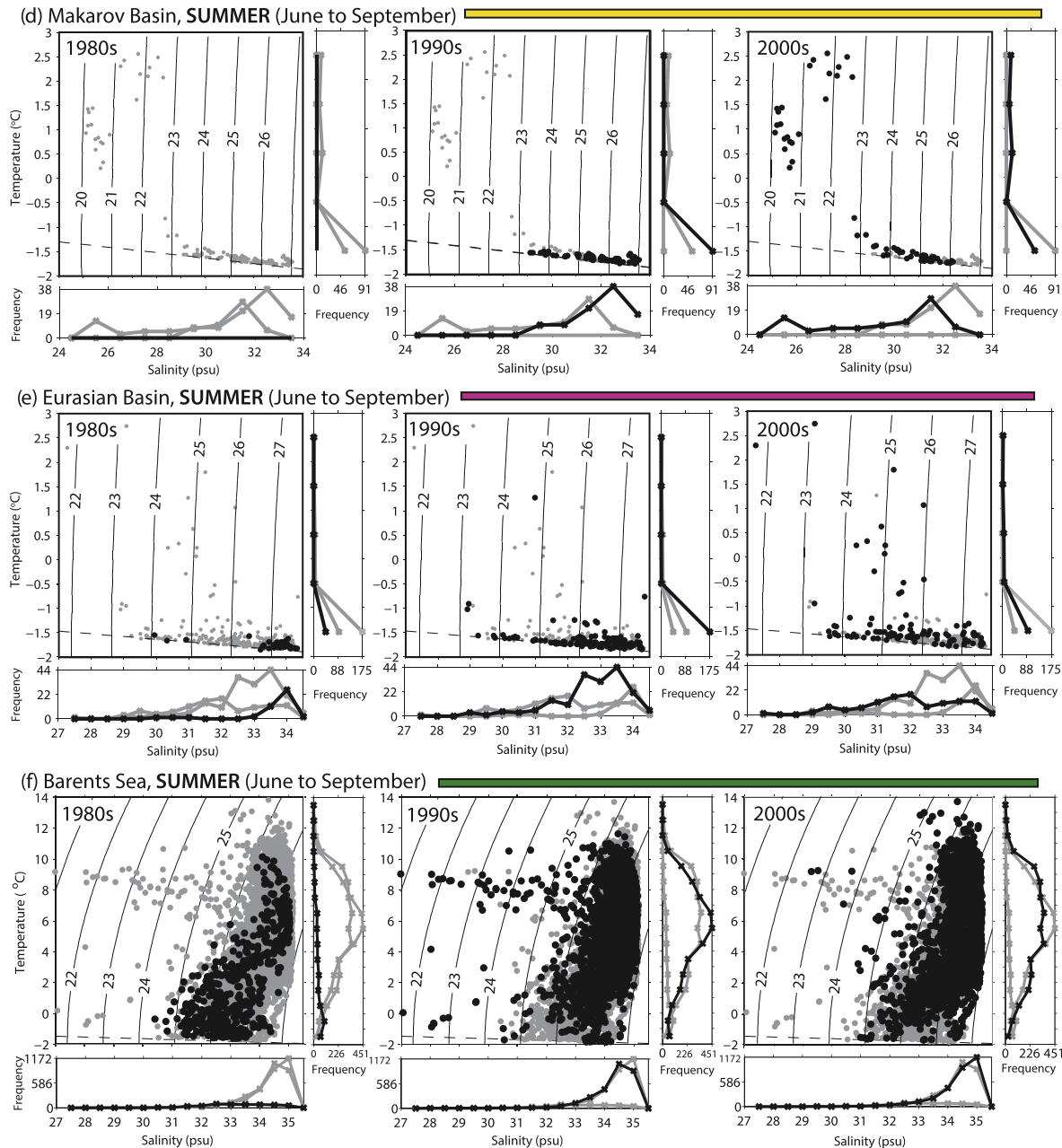


Fig. 16 (continued)

Fig. 14 also shows trends in stratification and in wind. Many of the stratification trends are significant (1–5% change per year of mean stratification for that region), and (unsurprisingly) increasing/decreasing stratification coincides with freshening/salinization changes in the ML. It is notable that the stratification trends always match in sign the MLD change – increased stratification is always coincident with ML shoaling, and vice versa.

The trends in wind speed are generally very modest (~ 0.1 m/s per year). These trends are different between the boundary regions (i.e., Chukchi, Southern Beaufort and Barents seas), which show modest increases in wind speed ($\sim +0.1$ m/s per year) and the higher central Arctic regions (i.e., Canada, Makarov and Eurasian basins), which generally have no significant trend or decreases in the wind (maximum in the Eurasian Basin, ~ -0.4 m/s per year). Changes in the MLD often, but not always match changes in the wind. For example, Southern Beaufort and Barents seas summer wind speed increase does match with ML deepening, and the Eur-

asian Basin shoaling is coincident with a reduction in wind. However, this relationship is not ubiquitous – and where wind and stratification effects have potentially opposite effects on ML, the ML change always matches the stratification change.

This suggests that MLDs are more strongly related to stratification, consistent with the strong links found between MLD and stratification in Section ‘Controlling effects of stratification and influence of sea ice cover’.

Summary and conclusions

The purpose of this work is to provide an observationally-based assessment of Arctic Ocean Mixed Layer (ML) properties in the last decades, to quantify seasonal and interannual change, and investigate driving mechanisms. To this end, using a threshold density-step criterion ($\Delta\sigma = 0.1 \text{ kg/m}^3$), we calculate ML depths and properties from 21,406 Arctic CTD and XCTD profiles

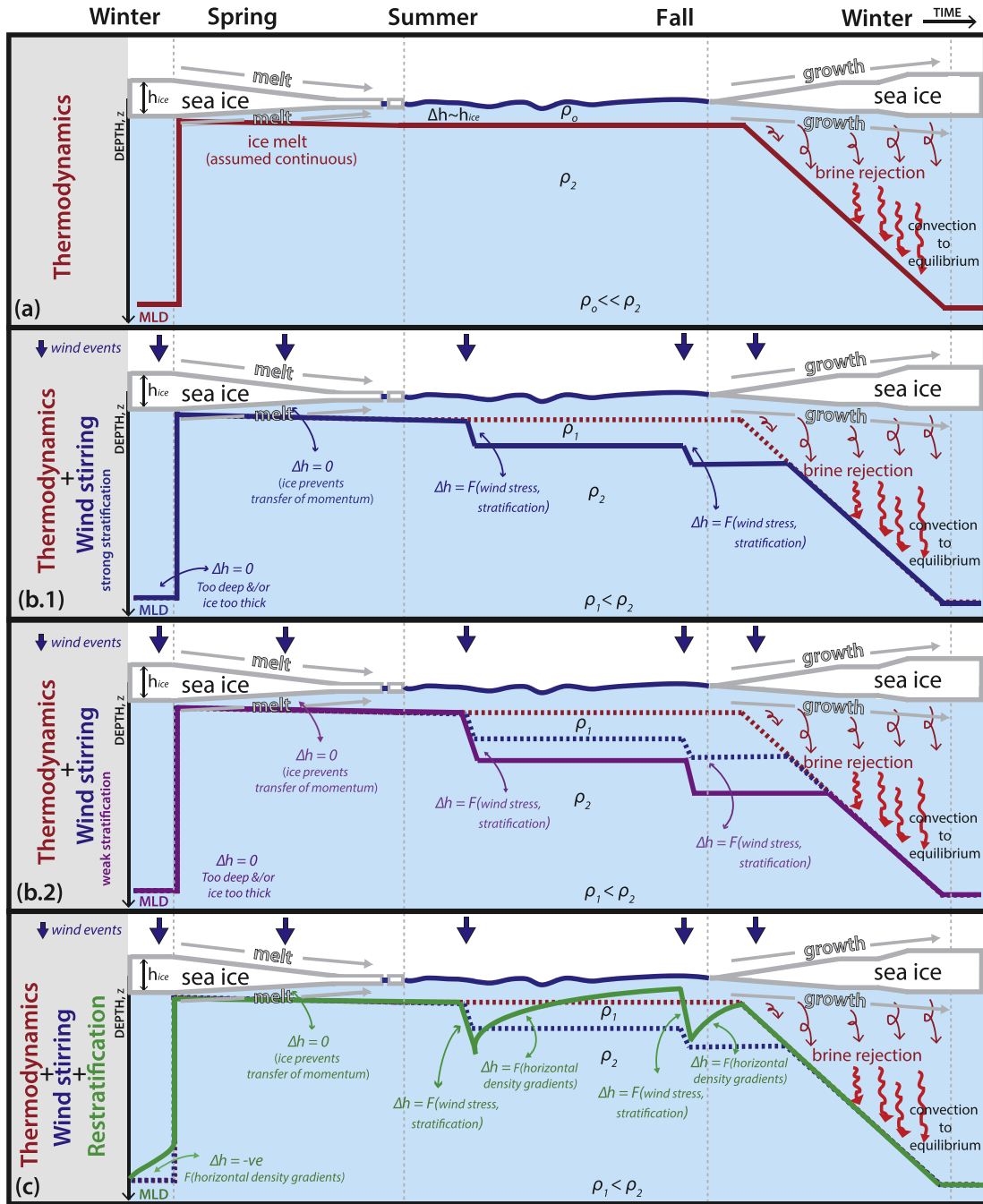


Fig. 17. Idealized schematic of the response of MLD to (a) thermodynamic forcing (i.e., ice melt and growth) only; (b) combined thermodynamics and wind-driven forcings with relatively strong (b.1) and relatively weak (b.2) underlying stratification; and (c) combined wind-driven and restratification processes. ρ_0 , ρ_1 , and ρ_2 denote different densities of sea water; Δh denotes change in MLD; h_{ice} is ice thickness; and z is depth. Vertical dashed gray lines separate the seasonal cycle of Arctic sea ice conditions (thick ice in winter, melting ice in spring, ice-free in summer, growing ice in fall). Thick blue arrows represent wind storms. See Section 'Driving mechanisms' for discussion. (For interpretation of the references to color in this figure legend, the reader is referred to the web version of this article.)

taken between 1979 and 2012 in a range of seasons and ice cover (Section 'Monthly seasonality of Arctic Mixed Layer Depths (MLDs)', Fig. 1). (ITP data are not used for this study as their minimum depth (~10 m) is greater than the shallowest Arctic ML we expect.)

Seasonality of Arctic MLD

A seasonal pan-Arctic analysis (Section 'Monthly seasonality of Arctic Mixed Layer Depths (MLDs)', Fig. 3) illustrates strong seasonality of the Mixed Layer Depth (MLD) throughout the Arctic

with MLDs being generally deeper (~25 to >50 m) in winter (i.e., November through May) than summer (~5–30 m) (e.g., June through September). MLDs vary consistently across the Arctic in all seasons, with MLDs being deeper in the eastern Arctic (regional mean ~20 m in summer, ~70 to 100+ m in winter) and shallower in the western Arctic (~8 m in summer, 30 m in winter) (Fig. 3, Table 3). These means hide sizeable variability on small space (and perhaps time) scales, standard deviations frequently being ~40% of the mean. This illustrates the patchiness of Arctic MLDs, possibly related to scales of variability of sea ice cover (Section 'Spatial variability of Arctic Mixed Layer Depths (MLDs)').

To compensate for sparse spatial and temporal coverage, we compute monthly climatologies of ML properties in 6 regions of the Arctic – the Chukchi Sea, the Southern Beaufort Sea, the Canada Basin, the Makarov Basin, the Eurasian Basin and the Barents Sea (Section ‘Defining Arctic regions for a regional monthly MLD climatology’, Figs. 6–8, and Table 3). The strong seasonality in ML properties is evident in all these regions, with MLDs being deeper and more variable in winter, and shallower and more homogeneous in summer (Fig. 6). In contrast, ML temperature and salinity properties are more homogeneous in winter, and more varied in summer (Figs. 7 and 8). Inherent to measurements taken primarily from ships, which likely mix the upper water column, our results possibly overestimate the ML depth of shallow layers (Section ‘Hydrographic data – inventory, quality control, and accuracy’).

Driving mechanisms

A 1-dimensional theoretical seasonal cycle in MLD is summarized schematically in Fig. 17, as a combination of ice-driven thermodynamics, wind-driven mixing and restratification (Section ‘Monthly seasonality of Arctic Mixed Layer Depths (MLDs)'). If driven only by the thermodynamics of sea ice growth and melt, the ML thins suddenly to ~zero at the onset of ice melt in spring, remains equal to the layer of melt water through the summer, and then deepens with brine rejection on sea ice formation in the fall/winter (Fig. 17a). Wind-driven mixing acts to deepen the ML. Our results (Section ‘Controlling effects of stratification and influence of sea ice cover’ and summarized below) indicating the depth of this mixing is strongly dependent on stratification below the ML (Fig. 17-b.1 and b.2), and that ice-cover severely inhibits ML deepening. In addition, restratification processes, initiated by horizontal inhomogeneities, act to shoal the ML (Fig. 17c).

With exceptions due to advection (see below), the observed ML seasonal cycle is mostly in good agreement with this theoretical picture, with the ML shoaling as sea ice retreats, then deepening slowly through the summer, with that deepening increasing at the onset of freeze (Fig. 6). We speculate that ML shoaling in late winter, before the onset of melt, may be indicative of restratification processes at depth (Section ‘Monthly climatology of MLD properties (depth, temperature and salinity) in 6 regions of the Arctic’).

Using simplistic scaling arguments, we ascertain that ML changes (depth and salinity) can be quantitatively related to the seasonal melt of the sea ice (~1–3 m) in most regions of the Arctic (Table 5, Section ‘Quantifying influence of sea ice growth/melt’). To drive the observed MLD change, ~1.5 times greater sea ice change is required in the western Arctic than in the eastern Arctic, a result consistent with spatial variation of seasonal sea ice melt. However, in the Southern Beaufort Sea and the Canada Basin, seasonal ice melt alone is insufficient to explain changes in ML properties, indicating the importance of advection of other freshwater sources (e.g., river water and Pacific water) into these regions.

Using various Arctic wind products (ERAinterim, MERRA and JRA55), we seek relationships between wind speed and MLD (Section ‘Relationship of MLD to wind forcing and sea ice cover’). During ice-covered (ice concentration > 15%) times, MLD is not significantly correlated with wind speed prior to the cast. In contrast, in ice-free periods, MLD to wind speed correlations are significant, and vary across the Arctic – the same wind is 2–3 times more effective at deepening the ML in the eastern Arctic than in the (more stratified) western Arctic (Fig. 10). We quantify the controlling role of stratification in this linkage – weak stratification permits a wind to MLD coupling comparable to a simple Ekman model, while the stronger stratifications of the western Arctic can reduce the effectiveness of the wind by a factor of 6 (Fig. 11,

Section ‘Controlling effects of stratification and influence of sea ice cover’). In all cases, although significant, these wind to MLD relationships explain only 1–20% of the MLD variance (Figs. 10 and 11).

Using all data from ice-free times, we seek a power law relationship between stratification, wind speed and MLD (Section ‘Controlling effects of stratification and influence of sea ice cover’), obtaining an empirical fit (Eq. 10) which explains 65% of the variance. Wind contributes only slightly to this fit – a fit to stratification only (Eq. 11) still explains 58% of the variance. These results show a slightly stronger dependency ($\Delta\rho^{-0.43}$) on stratification than expected from theory (Section ‘Controlling effects of stratification and influence of sea ice cover’).

Interannual and decadal change

Although sparse, our data do reflect oceanic effects of the anomalous 2007 sea ice retreat, indicating coincident ML warming in almost all of the Arctic (except the Southern Beaufort and Barents seas) and freshening (related to ice loss or to the spin-up of the Beaufort Gyre) in the high Arctic (Canada Basin, Makarov Basin and Eurasian Basin), with suggestions of a return to saltier conditions from 2011 (Figs. 12 and 13, Section ‘Interannual changes in ML depth, temperature and salinity’).

Between 1979 and 2012, summer Arctic sea ice loss is significant, being faster (~0.9%/yr) in the western Arctic than in the eastern Arctic (~0.4%/yr) (Table 5 and Figs. 12 and 13) [regionally-averaged from NSIDC data, Cavalieri et al., 1996]. However, ice concentrations at the sites of our data generally do not show this trend in sea ice loss, reflecting a measurement bias to ice-covered regions. Thus, our long-term results are restricted to treating ice-covered and ice-free regions separately.

Multi-year (up to 30-year) trends (though crude) are summarized in Table 5 and Fig. 14 (Section ‘Multi-year (up to 30-year) trends and decadal change in Arctic ML properties’). Most remarkably, our data indicate significant and ubiquitous ML shoaling in winter and summer over all the high Arctic (Canada Basin, Makarov Basin and Eurasian Basin) and in winter in the peripheral seas (Chukchi, Southern Beaufort and Barents seas). In the high Arctic, this shoaling is coincident with ML freshening and increased stratification, while wind speed trends are either not significant or decreasing (Fig. 14). The Barents Sea shoaling may be related to wind speed reduction or increased temperature and stratification, while in the Chukchi, stratification increases/ML shoaling are opposed by increasing wind. In stark contrast to this wide-spread shoaling, the summer Southern Beaufort Sea shows ML deepening, coincident with decreasing stratification, possibly related to diversion of river water into the deep basin and away from the coast.

In terms of temperature, again the high Arctic differs from the peripheral seas, with the high Arctic temperature trends being small or not significant, while the Barents Sea shows modest warming, likely related to increased Atlantic inflow. More informative are changes in T-S space (Figs. 15 and 16), which suggest decreased convection in the Eurasian Basin in the 2000s (Section ‘Decadal change in temperature–salinity (T-S) space’).

Discussion and implications for the future

Understanding and quantifying Arctic MLD are important for a range of physical and interdisciplinary studies. The properties of the ML affect ice–ocean–atmosphere exchanges, and surface layer mixing may affect fluxes of nutrients from lower layers into the photic zone, with implications for Arctic ecosystems. By quantifying variability (spatial, seasonal and interannual), this study provides a framework for various process and modeling studies.

The patchy nature of the Arctic ML (Section ‘Spatial variability of Arctic Mixed Layer Depths (MLDs)’, Figs. 4 and 5) has been so far unappreciated. This spatial and possibly temporal variability implies that, for example, nutrient fluxes into the photic zone (or subsurface heat to the base of the ice) is not only seasonal, but may also act intermittently and on small space scales, and this may help explain the observed patchiness in phytoplankton blooms [e.g., Gosselin et al., 1997; Arrigo et al., 2012].

A clear result of our work is the dominance of stratification in the relationship between MLD, wind speed and stratification, suggesting that, as we seek to understand and predict interannual and decadal change in the Arctic ML, changes in stratification rather than changes in wind will mediate the situation. However, do not forget that, at least in our results, it is the removal of ice-cover that allows the wind to act on the ocean (Fig. 11). Thus, the future of the Arctic ML in reduced sea ice conditions depends at least partly on a trade-off between ice-cover reduction increasing the area vulnerable to wind-driven mixing and changes in stratification increasing or decreasing the effectiveness of the wind.

Finally, we return to the observed ubiquitous shoaling and freshening of the Arctic ML over the ~30 years of our data. This implies in the present balance between increased wind-driven mixing and stratification change, freshening currently dominates. Important here also is that the volume of freshwater commensurate with these ML freshenings is only small compared to sources of Arctic freshwater, implying the stratification of the upper Arctic (and hence its vulnerability to wind-driven stirring) may be easily influenced by changes in the Arctic freshwater balance.

Acknowledgements

This work was supported by NSF Grants ARC-0901407, 0855748 and 0908124. We thank Bonnie Light, Torge Martin, Eleanor Frajka-Williams, Amala Mahadevan, Kathy Kelly, Cecilia Bitz and Edward Blanchard-Wrigglesworth for useful discussions and comments. We also thank Benjamin Rabe and an anonymous reviewer for their constructive suggestions.

Appendix A

These appendices detail the assumptions and derivations leading to the various estimates of sea ice growth and melt (t_{growth} , t_{melt} and $t_{profile}$) discussed in Section ‘Quantifying influence of sea ice growth/melt’, and utilized in the main text as Eqs. 1–3.

Estimate of sea ice growth, t_{growth} , associated with observed seasonal MLD change

For the results of Section ‘Quantifying influence of sea ice growth/melt’ and Table 4, we use a simplistic 1-dimensional idealized model to estimate the sea ice growth corresponding to MLD deepening due to brine rejection alone (i.e., no wind-driven stirring).

We start with an idealized summer profile (Fig. 9a, in the main text), with a summer MLD, H_s , of salinity S_s , and a salinity profile below this of S , where S is a function of depth z . We then assume that, during the transition from summer to winter, ice forms on this water, rejecting salt into the Mixed Layer (ML) below, which thus deepens by mixing with underlying water. We simplistically assume this mixing reaches an equilibrium depth, H_w , where the new density of the ML matches the density of the background stratification. Since density is primarily determined by salinity for temperatures less than 0 °C, this is equivalent to saying the ML deepens until the salinity of the ML matches the salinity of the background profile (Fig. 9b).

By conserving mass over the depth of the winter MLD, H_w , for both summer and winter conditions, we obtain:

$$\rho_w H_w = \rho_i t_{growth} + \rho_w d \quad (\text{A.1})$$

where ρ_w is the water density; ρ_i is the density of the sea ice; t_{growth} is the thickness of the sea ice formed; and d is the liquid water above the MLD, H_w .

Similarly, by conserving salt between summer and winter, we obtain:

$$\int_0^{H_w} \rho_w S(z) dz = \rho_i S_i t_{growth} + \rho_w S_w d \quad (\text{A.2})$$

where z is depth; S_i is the salinity of the sea ice; S_w is the salinity of the winter ML; and $S(z)$ is the depth-dependent summer salinity profile, assumed here for simplicity to be:

$$\begin{aligned} S(z) &= S_s && \dots \text{ for } 0 \leq z \leq H_s \\ S(z) &= S_s + \frac{(S_w - S_s)(z - H_s)}{(H_w - H_s)} && \dots \text{ for } H_s \leq z \leq H_w \end{aligned} \quad (\text{A.3})$$

where S_s is the summer ML salinity.

Substituting A.3 and A.1 in A.2, and solving for t_{growth} yields:

$$t_{growth} = \frac{\rho_w}{2\rho_i} \frac{(S_w - S_s)}{(S_w - S_i)} (H_w + H_s) \quad (\text{A.4})$$

which is Eq. 1 in Section ‘Quantifying influence of sea ice growth/melt’. This equation allow us to estimate the amount of ice growth required to transform a summer ML of thickness H_s and salinity S_s into a thicker, saltier winter ML (depth H_w , salinity S_w). Table 4 gives these estimates for the different regions of the Arctic using the MLD results of Section ‘Defining Arctic regions for a regional monthly MLD climatology’, assuming ρ_w of 1025 kg/m³, ρ_i of 920 kg/m³, and S_i of 6 psu.

Estimate of sea ice melt, t_{melt} , associated with observed seasonal MLD change

For the transition from winter to summer (Fig. 9b and c), we start with an idealized winter profile with an overlying sea ice of thickness, t_{melt} , (Fig. 9b), with a winter MLD, H_w , of salinity S_w . The salinity profile below the MLD, although shown in Fig. 9b as S , a function of depth, z , will prove to be irrelevant in this calculation. We assume the ice melts on this water, creating first a thin layer of freshwater that is then mixed by other surface processes to yield, in the simplest of the cases, the 2-step profile shown in Fig. 9c, with a ML thickness H_s and ML salinity S_{so} (Fig. 9c).

By conserving mass again to the depth of H_w , similarly to Eq. A.1, we obtain:

$$\rho_w H_w = \rho_i t_{melt} + \rho_w d \quad (\text{A.5})$$

where t_{melt} is now the thickness of the ice melted.

Again, by conserving salt between summer and winter, we obtain (similarly to Eq. A.2):

$$\int_0^{H_w} \rho_w S(z) dz = \rho_i S_i t_{melt} + \rho_w S_w d \quad (\text{A.6})$$

The derivation now diverges from the estimate of t_{growth} , due to differences in the summer salinity profile. In this melt case, we assume the depth-dependent summer salinity profile, $S(z)$, a 2-step salinity structure (Fig. 9c), is:

$$\begin{aligned} S(z) &= S_{so} && \dots \text{ for } 0 \leq z \leq H_s \\ S(z) &= S_w && \dots \text{ for } H_s < z \leq H_w \end{aligned} \quad (\text{A.7})$$

Substituting A.7 and A.5 in A.6, and solving for t_{melt} yields:

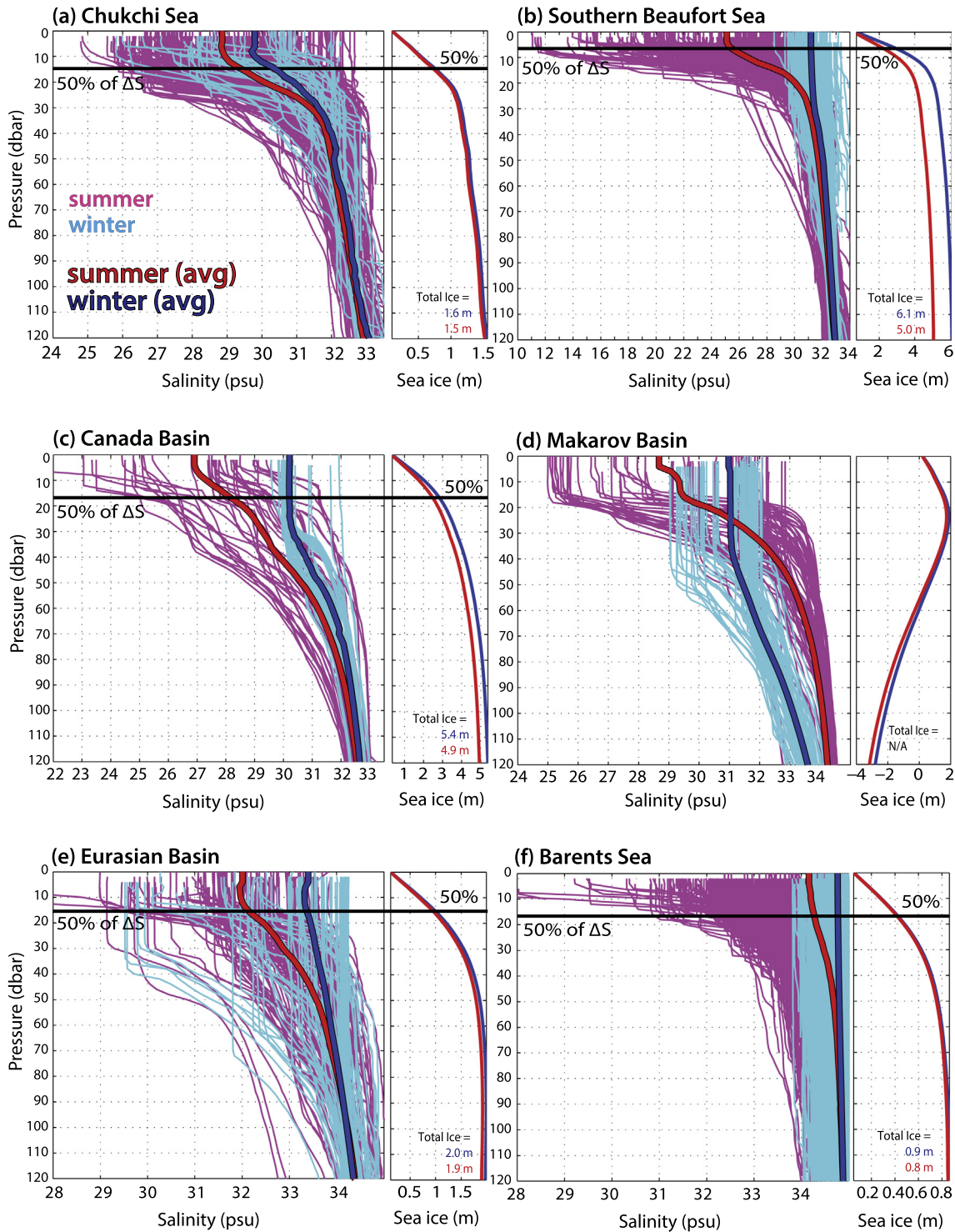


Fig. A1. Salinity profiles for the month of maximum winter (thin cyan lines) and minimum summer (thin magenta lines) MLD (as per Table 3), for (a) Chukchi Sea, (b) Southern Beaufort Sea, (c) Canada Basin, (d) Eurasian Basin, (e) Makarov Basin and (f) Barents Sea. For each region, thicker blue and red lines show the averaged salinity profiles for winter and summer, respectively. Note the profiles for the Makarov Basin suggest spatial bias in their measurements of winter and summer (see Table 4, and discussion in Section 'Quantifying influence of sea ice growth/melt'). Side panels for each sub-figure show the cumulative sum from the surface of Δd_i , per region, as per Eq. A.11 (blue solid line) and A.13 (red solid line). The $t_{profile}$ values from the two expressions A.12 and A.14 are indicated in blue and red respectively in each of these panels ($t_{profile}$ values from A.12 are also given in Table 4). Black horizontal lines mark the depth where the cumulative sum of A.11 reaches 50% of $t_{profile}$ (A.12) (values given in Table 4, penultimate column). (For interpretation of the references to color in this figure legend, the reader is referred to the web version of this article.)

$$t_{melt} = \frac{\rho_w}{\rho_i} \frac{(S_w - S_{so})}{(S_w - S_i)} (H_s) \quad (\text{A.8})$$

which is Eq. 2 in Section 'Quantifying influence of sea ice growth/melt'. This expression for t_{melt} is different from the expression for

t_{growth} because of the differing assumptions of the form of the summer salinity profile below the summer MLD.

Eq. A.8 allows us to estimate the amount of ice melt required to transform a winter ML of thickness H_w and salinity S_w into a thinner, fresher summer ML (depth H_s , salinity S_{so}). Table 4 includes

these estimates for the different regions of the Arctic using the MLD results of Section 'Defining Arctic regions for a regional monthly MLD climatology', assuming ρ_w of 1025 kg/m³, ρ_i of 920 kg/m³, and S_i of 6 psu.

Full water column winter-to-summer freshening, estimated as equivalent of sea ice melt, $t_{profile}$

The previous estimates (t_{growth} and t_{melt}) assume the impact of freshwater forcing is only within the mixed layer. To test if this is realistic, we consider a third calculation, which investigates changes in salinity over the whole water column from summer to winter.

Analogous to Appendix 'Estimate of sea ice growth, t_{growth} ', associated with observed seasonal MLD change, we consider a summer parcel of water at depth z , of area A and thickness, Δd_s , salinity, $S_s(z)$, and density, $\rho_{ws}(z)$ to be formed from the combination of a winter parcel of water, of area A , thickness, Δd_w , salinity, $S_w(z)$, and density, $\rho_{ww}(z)$, and melting of a volume of ice, of area A , thickness, $\Delta d_i(z)$, salinity, S_i , and density, ρ_i . Conserving mass and salinity, we obtain:

$$\rho_{ws}\Delta d_s A = \rho_{ww}\Delta d_w A + \rho_i\Delta d_i A \quad (\text{A.9})$$

and

$$S_s \rho_{ws} \Delta d_s A = S_w \rho_{ww} \Delta d_w A + S_i \rho_i \Delta d_i A \quad (\text{A.10})$$

Cancelling A , and combining these equations to remove Δd_s yields (as per Eq. A.2):

$$\Delta d_i = \frac{\rho_{ww}}{\rho_i} \frac{(S_w - S_s)}{(S_s - S_i)} \Delta d_w \quad (\text{A.11})$$

Using regional mean profiles of salinity for the month of maximum MLD in winter and the month of minimum summer MLD for each region (viz. $S_w(z)$ and $S_s(z)$, Fig. A1), we can then compute for each region, a corresponding profile of Δd_i , which indicates how much the water column has freshened at each depth. Summing this profile from the surface over the water column yields $t_{profile}$, viz. (Eq. 3, Section 'Quantifying influence of sea ice growth/melt'):

$$t_{profile} = \int_{bottom}^{surface} \frac{\rho_{ww}(z)}{\rho_i} \frac{(S_w(z) - S_s(z))}{(S_s(z) - S_i)} dz \quad (\text{A.12})$$

values of which are given in Table 4 and discussed in Section 'Quantifying influence of sea ice growth/melt'.

As well as showing salinity profiles, Fig. A1 gives the cumulative sum of Δd_i (from A.11) with depth for the 6 regions. $t_{profile}$ (A.12) is the limit of this cumulative sum at depth, the value being annotated on the figure. This cumulative sum profile indicates how the freshwater change is distributed in the water column, and we mark the depth above which 50% of the freshwater change is included.

Note that, alternatively, combining A.9 and A.10 to remove Δd_w yields:

$$\Delta d_i = \frac{\rho_{ws}}{\rho_i} \frac{(S_w - S_s)}{(S_w - S_i)} \Delta d_s \quad (\text{A.13})$$

and thus a very similar equation for $t_{profile}$, viz.:

$$t_{profile} = \int_{bottom}^{surface} \frac{\rho_{ws}(z)}{\rho_i} \frac{(S_w(z) - S_s(z))}{(S_w(z) - S_i)} dz \quad (\text{A.14})$$

Computing A.13 and A.14 over the summer profile yields slightly different values of Δd_i and $t_{profile}$. This reflects that Δd_s does not equal Δd_w , since adding ice melt changes the water column height, and that there is thus some ambiguity in the validity of matching salinity at a certain depth in summer profile with salinity at the same depth in the winter profile. Fig. A1 presents both results, suggesting the difference between them is a measure of the ambiguity in the calculation.

References

- Aagaard, K., Carmack, E.C., 1989. The role of sea ice and other fresh water in the Arctic circulation. *Journal of Geophysical Research* 94 (C10), 14485–14498.
- Alford, M.H., 2003. Improved global maps and 54-year history of wind-work on ocean inertial motions. *Geophysical Research Letters* 30 (8), 1424. <http://dx.doi.org/10.1029/2002GL016614>.
- Anderson, L.G., Bjork, G., Holby, O., Jones, E.P., Kattner, G., Koltermann, K.P., Liljeblad, B., Lindegren, R., Rudels, B., Swift, J., 1994. Water masses and circulation in the Eurasian basin: results from the Oden 91 expedition. *Journal of Geophysical Research* 99 (C2), 3273–3283.
- Arrigo, K.R. et al., 2012. Massive phytoplankton blooms under Arctic sea ice. *Science* 336 (6087), 1408. <http://dx.doi.org/10.1126/science.1215065>.
- Arthun, M., Eldevik, T., Smetsrud, L.H., Skagseth, Ø., Ingvaldsen, R.B., 2012. Quantifying the influence of Atlantic heat on Barents Sea ice variability and retreat. *Journal of Climate* 25 (13), 4736–4743. <http://dx.doi.org/10.1175/JCLI-D-11-00466.1>.
- Bauch, D., Dmitrenko, I., Kirillov, S., Wegner, C., Hölemann, J., Pivovarov, S., Timokhov, L., Kassens, H., 2009. Eurasian Arctic shelf hydrography: exchange and residence time of southern Laptev Sea waters. *Continental Shelf Research* 29 (15), 1815–1820.
- Bauch, D., Torres-Valdes, S., Polyakov, I., Novikhin, A., Dmitrenko, I., McKay, J., Mix, A., 2014. Halocline water modification and along-slope advection at the Laptev Sea continental margin. *Ocean Science* 10 (1), 141–154. <http://dx.doi.org/10.5194/os-10-141-2014>.
- Boccaletti, G., Ferrari, R., Fox-Kemper, B., 2007. Mixed layer instabilities and restratification. *Journal of Physical Oceanography* 37 (9), 2228–2250. <http://dx.doi.org/10.1175/JPO3101.1>.
- Cavalieri, D.J., Parkinson, C.L., Gloersen, P., Zwally, H., 1996. Sea Ice Concentrations from Nimbus-7 SMMR and DMSP SSM/I-SSMIS Passive Microwave Data [1979–2012], edited, Boulder, Colorado, USA: NASA DAAC at the National Snow and Ice Data Center.
- Coachman, L.K., Aagaard, K., 1974. Physical oceanography of arctic and subarctic seas. In: Herman, Y. (Ed.), *Marine Geology and Oceanography of the Arctic Seas*. Springer-Verlag, New York, pp. 1–72.
- Coachman, L.K., Aagaard, K., Tripp, R.B., 1975. *Bering Strait: The Regional Physical Oceanography*. University of Washington Press, Seattle.
- Coachman, L.K., Barnes, C.A., 1961. The contribution of Bering Sea water to the Arctic Ocean. *Arctic* 14 (3), 146–161.
- Coachman, L.K., Barnes, C.A., 1962. Surface water in the Eurasian Basin of the Arctic Ocean. *Arctic* 15, 251–277.
- Comiso, J.C., Kwok, R., 1996. Surface and radiative characteristics of the summer Arctic sea ice cover from multisensor satellite observations. *Journal of Geophysical Research: Oceans* 101 (C12), 28397–28416. <http://dx.doi.org/10.1029/96JC02816>.
- Cushman-Roisin, B., 1994. *Introduction to Geophysical Fluid Dynamics*. Prentice Hall Inc., Englewood Cliffs, NJ, 322 pp.
- de Boyer Montégut, C., Madec, G., Fischer, A.S., Lazar, A., Iudicone, D., 2004. Mixed layer depth over the global ocean: an examination of profile data and a profile-based climatology. *Journal of Geophysical Research: Oceans* 109 (C12), C12003. <http://dx.doi.org/10.1029/2004JC002378>.
- Ekwurzel, B., Schlosser, P., Mortlock, R.A., Fairbanks, R.G., Swift, J.H., 2001. River runoff, sea ice meltwater, and Pacific water distribution and mean residence times in the Arctic Ocean. *Journal of Geophysical Research* 106 (C5), 9075–9092. <http://dx.doi.org/10.1029/1999JC000024>.
- Fofonoff, N.P., 1985. Physical properties of seawater: a new salinity scale and equation of state for seawater. *Journal of Geophysical Research* 90 (C2), 3332–3342. <http://dx.doi.org/10.1029/JC090iC02p03332>.
- Giles, K.A., Laxon, S.W., Ridout, A.L., Wingham, D.J., Bacon, S., 2012. Western Arctic Ocean freshwater storage increased by wind-driven spin-up of the Beaufort Gyre. *Nature Geoscience* 5 (3), 194–197. <http://dx.doi.org/10.1038/ngeo1379>.
- Gimbert, F., Jourdain, N.C., Marsan, D., Weiss, J., Barnier, B., 2012. Recent mechanical weakening of the Arctic sea ice cover as revealed from larger inertial oscillations. *Journal of Geophysical Research* 117. <http://dx.doi.org/10.1029/2011jc007633>.
- Gosselin, M., Levasseur, M., Wheeler, P.A., Horner, R.A., Booth, B.C., 1997. New measurements of phytoplankton and ice algal production in the Arctic Ocean. *Deep Sea Research Part II: Topical Studies in Oceanography* 44 (8), 1623–1644.
- Harris, C.L., Plueddemann, A.J., Gawarkiewicz, G.G., 1998. Water mass distribution and polar front structure in the western Barents Sea. *Journal of Geophysical Research: Oceans* 103 (C2), 2905–2917. <http://dx.doi.org/10.1029/97JC02790>.
- Holte, J., Talley, L., 2009. A new algorithm for finding mixed layer depths with applications to argo data and subantarctic mode water formation*. *Journal of Atmospheric and Oceanic Technology* 26 (9), 1920–1939. <http://dx.doi.org/10.1175/2009JTECH0543.1>.
- Jackson, J.M., Allen, S.E., McLaughlin, F.A., Woodgate, R.A., Carmack, E.C., 2011. Changes to the near-surface waters in the Canada Basin, Arctic Ocean from 1993–2009: a basin in transition. *Journal of Geophysical Research* 116, C10008. <http://dx.doi.org/10.1029/2011jc007069>.
- Jackson, J.M., Carmack, E.C., McLaughlin, F.A., Allen, S.E., Ingram, R.G., 2010. Identification, characterization, and change of the near-surface temperature maximum in the Canada Basin, 1993–2008. *Journal of Geophysical Research* 115. <http://dx.doi.org/10.1029/2009JC005265>.

- Jackson, J.M., Williams, W.J., Carmack, E.C., 2012. Winter sea-ice melt in the Canada Basin, Arctic Ocean. *Geophysical Research Letters* 39, L03603. <http://dx.doi.org/10.1029/2011gl050219>.
- Japan Meteorological Agency, J., 2013. JRA-55: Japanese 55-year Reanalysis, Daily 3-Hourly and 6-Hourly Data, edited, Research Data Archive at the National Center for Atmospheric Research, Computational and Information Systems Laboratory, Boulder, CO.
- Jones, E.P., Anderson, L.G., Jutterstrom, S., Mintrop, L., Swift, J.H., 2008. Pacific freshwater, river water and sea ice meltwater across Arctic Ocean basins: results from the 2005 Beringia Expedition. *Journal of Geophysical Research* 113 (C8). <http://dx.doi.org/10.1029/2007jc004124>.
- Kalnay, E., Kanamitsu, R., Kistler, R., 1996. The NCEP/NCAR 40-year reanalysis project. *Bulletin of the American Meteorological Society* 77 (3), 437–471.
- Kara, A.B., Rochford, P.A., Hurlburt, H.E., 2000. An optimal definition for ocean mixed layer depth. *Journal of Geophysical Research: Oceans* 105 (C7), 16803–16821. <http://dx.doi.org/10.1029/2000JC000072>.
- Kara, A.B., Rochford, P.A., Hurlburt, H.E., 2003. Mixed layer depth variability over the global ocean. *Journal of Geophysical Research: Oceans* 108 (C3), 3079. <http://dx.doi.org/10.1029/2000JC000736>.
- Kikuchi, T., Hatakeyama, K., Morison, J.H., 2004. Distribution of convective Lower Halocline Water in the eastern Arctic Ocean. *Journal of Geophysical Research* 109 (C12), C12030. <http://dx.doi.org/10.1029/2003JC002223>.
- Korhonen, M., Rudels, B., Marnela, M., Wisotzki, A., Zhao, J., 2013. Time and space variability of freshwater content, heat content and seasonal ice melt in the Arctic Ocean from 1991 to 2011. *Ocean Science* 9 (6), 1015–1055. <http://dx.doi.org/10.5194/os-9-1015-2013>.
- Kwok, R., Cunningham, G.F., 2002. Seasonal ice area and volume production of the Arctic Ocean: November 1996 through April 1997. *Journal of Geophysical Research: Oceans* 107 (C10), 8038. <http://dx.doi.org/10.1029/2000JC000469>.
- Kwok, R., Rothrock, D.A., 2009. Decline in Arctic sea ice thickness from submarine and ICESat records: 1958–2008. *Geophysical Research Letters* 36 (15), L15501. <http://dx.doi.org/10.1029/2009GL039035>.
- Lammers, R.B., Shiklomanov, A.I., Vorosmarty, C.J., Fekete, B.M., Peterson, B.J., 2001. Assessment of contemporary Arctic river runoff based on observational discharge records. *Journal of Geophysical Research: Atmospheres* 106 (D4), 3321–3334.
- Large, W.G., McWilliams, J.C., Doney, S.C., 1994. Oceanic Vertical Mixing – a review and a model with a nonlocal boundary-layer parameterization. *Reviews of Geophysics* 32 (4), 363–403. <http://dx.doi.org/10.1029/94rg01872>.
- Lemke, P., Manley, T.O., 1984. The seasonal variation of the mixed layer and the pycnocline under polar sea ice. *Journal of Geophysical Research: Oceans* 89 (C4), 6494–6504. <http://dx.doi.org/10.1029/JC089iC04p06494>.
- Lentz, S.J., 1992. The surface boundary layer in coastal upwelling regions. *Journal of Physical Oceanography* 22 (12), 1517–1539. [http://dx.doi.org/10.1175/1520-0485\(1992\)022<1517:TSBLIC>2.0.CO;2](http://dx.doi.org/10.1175/1520-0485(1992)022<1517:TSBLIC>2.0.CO;2).
- Lewis, E.L., 1980. The practical salinity scale 1978 and its antecedents. *IEEE Journal of Oceanic Engineering* OE-5 (1), 3–8.
- Lindsay, R.W., 1998. Temporal variability of the energy balance of thick Arctic pack ice. *Journal of Climate* 11 (3), 313–333. [http://dx.doi.org/10.1175/1520-0442\(1998\)011<0313:TVOTEBC>2.0.CO;2](http://dx.doi.org/10.1175/1520-0442(1998)011<0313:TVOTEBC>2.0.CO;2).
- Lindsay, R.W., Wensnahan, M., Schweiger, A., Zhang, J., 2014. Evaluation of seven different atmospheric reanalysis products in the Arctic. *Journal of Climate* 27 (7), 2588–2606. <http://dx.doi.org/10.1175/JCLI-D-13-00014.1>.
- Loeng, H., Drinkwater, K., 2007. An overview of the ecosystems of the Barents and Norwegian Seas and their response to climate variability. *Deep Sea Research Part II: Topical Studies in Oceanography* 54 (23–26), 2478–2500. <http://dx.doi.org/10.1016/j.dsr.2007.08.013>.
- Lukas, R., Lindstrom, E., 1991. The mixed layer of the western equatorial Pacific Ocean. *Journal of Geophysical Research: Oceans* 96 (S01), 3343–3357. <http://dx.doi.org/10.1029/90JC01951>.
- Macdonald, R.W., Carmack, E.C., McLaughlin, F.A., Falkner, K.K., Swift, J.H., 1999. Connections among ice, runoff and atmospheric forcing in the Beaufort Gyre. *Geophysical Research Letters* 26 (15), 2223–2226.
- Macdonald, R.W., Paton, D.W., Carmack, E.C., Omstedt, A., 1995. The freshwater budget and under-ice spreading of Mackenzie River water in the Canadian Beaufort Sea based on salinity and ^{18}O , ^{16}O measurements in water and ice. *Journal of Geophysical Research* 100 (11), 895.
- Mahadevan, A., Tandon, A., Ferrari, R., 2010. Rapid changes in mixed layer stratification driven by submesoscale instabilities and winds. *Journal of Geophysical Research: Oceans* 115 (C3), C03017. <http://dx.doi.org/10.1029/2008JC005203>.
- Manucharyan, G.E., 2010. Dynamics of the mixed layers in stratified shear flows. Paper presented at WHOI GFD Summer School, Ann. Proc.
- Martin, T., Steele, M., Zhang, J., 2014. Seasonality and long-term trend of Arctic Ocean surface stress in a model. *Journal of Geophysical Research: Oceans*. <http://dx.doi.org/10.1002/2013JC009425>, n/a–n/a.
- Martini, K.I., Simmons, H.L., Stoudt, C.A., Hutchings, J.K., 2014. Near-inertial internal waves and sea ice in the Beaufort Sea. *Journal of Physical Oceanography*. <http://dx.doi.org/10.1175/JPO-D-13-0160.1>.
- McLaughlin, F.A., Carmack, E.C., 2010. Deepening of the nutricline and chlorophyll maximum in the Canada Basin interior, 2003–2009. *Geophysical Research Letters* 37 (24), L24602. <http://dx.doi.org/10.1029/2010GL045459>.
- McLaughlin, F.A., Carmack, E.C., Macdonald, R.W., Bishop, J.K.B., 1996. Physical and geochemical properties across the Atlantic/Pacific water mass front in the southern Canadian basin. *Journal of Geophysical Research* 101 (C1), 1183–1197.
- McLaughlin, F.A., Carmack, E.C., Macdonald, R.W., Melling, H., Swift, J.H., Wheeler, P.A., Sherr, B.F., Sherr, E.B., 2004. The joint roles of Pacific and Atlantic-origin waters in the Canada Basin, 1997–1998. *Deep Sea Research Part I: Oceanographic Research Papers* 51 (1), 107–128.
- Mizobata, K., Shimada, K., 2012. East–west asymmetry in surface mixed layer and ocean heat content in the Pacific sector of the Arctic Ocean derived from AMSR-E sea surface temperature. *Deep Sea Research Part II: Topical Studies in Oceanography* 77–80, 62–69. <http://dx.doi.org/10.1016/j.dsr2.2012.04.005>.
- Morison, J., Smith, J.D., 1981. Seasonal-variations in the upper Arctic Ocean as observed at T-3. *Geophysical Research Letters* 8 (7), 753–756.
- Overeem, I., Syvitski, J.P.M., 2010. Shifting discharge peaks in Arctic Rivers, 1977–2007. *Geografiska Annaler: Series A, Physical Geography* 92 (2), 285–296. <http://dx.doi.org/10.1111/j.1468-0459.2010.00395.x>.
- Perovich, D.K., Grenfell, T.C., Richter-Menge, J.A., Light, B., Tucker III, W.B., Eicken, H., 2003. Thin and thinner: sea ice mass balance measurements during SHEBA. *Journal of Geophysical Research* 108 (C3), 26–21.
- Perovich, D.K., Richter-Menge, J.A., Jones, K.F., Light, B., 2008. Sunlight, water, and ice: extreme Arctic sea ice melt during the summer of 2007. *Geophysical Research Letters* 35 (11), L11501. <http://dx.doi.org/10.1029/2008GL034007>.
- Pollard, R.T., Rhines, P.B., Thompson, R.O.R.Y., 1973. The deepening of the wind-mixed layer. *Geophysical Fluid Dynamics* 4 (1), 381–404. <http://dx.doi.org/10.1080/03091927208236105>.
- Polyakov, I.V., Pnyushkov, A.V., Rembert, R., Padman, L., Carmack, E.C., Jackson, J.M., 2013. Winter convection transports Atlantic water heat to the surface layer in the Eastern Arctic Ocean. *Journal of Physical Oceanography* 43 (10), 2142–2155. <http://dx.doi.org/10.1175/JPO-D-12-0169.1>.
- Pond, S., Pickard, G.L., 1983. *Introductory Dynamical Oceanography*, second ed. Pergamon Press.
- Popova, E.E., Yool, A., Coward, A.C., Aksenov, Y.K., Alderson, S.G., de Cuevas, B.A., Anderson, T.R., 2010. Control of primary production in the Arctic by nutrients and light: insights from a high resolution ocean general circulation model. *Biogeosciences* 7 (11), 3569–3591. <http://dx.doi.org/10.5194/bg-7-3569-2010>.
- Price, J.F., Weller, R.A., Pinkel, R., 1986. Diurnal cycling: observations and models of the upper ocean response to diurnal heating, cooling, and wind mixing. *Journal of Geophysical Research: Oceans* 91 (C7), 8411–8427. <http://dx.doi.org/10.1029/JC091iC07p08411>.
- Proshutinsky, A., Bourke, R.H., McLaughlin, F.A., 2002. The role of the Beaufort Gyre in Arctic climate variability: seasonal to decadal climate scales. *Geophysical Research Letters* 29 (23), 2100. <http://dx.doi.org/10.1029/2002GL015847>.
- Proshutinsky, A., Krishfield, R., Timmermans, M.-L., Toole, J., Carmack, E., McLaughlin, F., Williams, W.J., Zimmerman, S., Itoh, M., Shimada, K., 2009. Beaufort Gyre freshwater reservoir: State and variability from observations. *Journal of Geophysical Research: Oceans* 114 (C1), C00A10. <http://dx.doi.org/10.1029/2008JC005104>.
- Rabe, B., Karcher, M., Kauker, F., Schauer, U., Toole, J.M., Krishfield, R.A., Pisarev, S., Kikuchi, T., Su, J., 2014. Arctic Ocean basin liquid freshwater storage trend 1992–2012. *Geophysical Research Letters* 41 (3), 961–968. <http://dx.doi.org/10.1002/2013GL058121>.
- Rabe, B., Karcher, M., Schauer, U., Toole, J.M., Krishfield, R.A., Pisarev, S., Kauker, F., Gerdes, R., Kikuchi, T., 2011. An assessment of Arctic Ocean freshwater content changes from the 1990s to the 2006–2008 period. *Deep Sea Research Part I* 58 (2), 173–185. <http://dx.doi.org/10.1016/j.dsr.2010.12.002>.
- Rainville, L., Lee, C.M., Woodgate, R.A., 2011. Impact of wind-driven mixing in the Arctic Ocean. *Oceanography* 24 (3), 136–145. <http://dx.doi.org/10.5670/oceanog.2011.65>.
- Rainville, L., Woodgate, R.A., 2009. Observations of internal wave generation in the seasonally ice-free Arctic. *Geophysical Research Letters* 36, L23604. <http://dx.doi.org/10.1029/2009GL041291>.
- Rampal, P., Weiss, J., Marsan, D., 2009. Positive trend in the mean speed and deformation rate of Arctic sea ice, 1979–2007. *Journal of Geophysical Research: Oceans* 114 (C5), C05013. <http://dx.doi.org/10.1029/2008JC005066>.
- Rothrock, D.A., Yu, Y., Maykut, G.A., 1999. Thinning of the Arctic sea-ice cover. *Geophysical Research Letters* 26 (23), 3469–3472. <http://dx.doi.org/10.1029/1999GL010863>.
- Rudels, B., Anderson, L.G., Jones, E.P., 1996. Formation and evolution of the surface mixed layer and halocline of the Arctic Ocean. *Journal of Geophysical Research* 101 (C4), 8807–8821.
- Rudels, B., Jones, E.P., Schauer, U., Eriksson, P., 2004. Atlantic sources of the Arctic Ocean surface and halocline waters. *Polar Research* 23 (2), 181–208.
- Sallée, J.B., Shuckburgh, E., Bruneau, N., Meijers, A.J.S., Bracegirdle, T.J., Wang, Z., 2013. Assessment of Southern Ocean mixed-layer depths in CMIP5 models: historical bias and forcing response. *Journal of Geophysical Research: Oceans* 118 (4), 1845–1862. <http://dx.doi.org/10.1002/jgrc.20157>.
- Schauer, U., Loeng, H., Rudels, B., Ozhigin, V.K., Dieck, W., 2002. Atlantic water flow through the Barents and Kara Seas. *Deep Sea Research Part I* 49 (12), 2281–2298.
- Serreze, M.C., Barrett, A.P., Slater, A.G., Woodgate, R.A., Aagaard, K., Lammers, R.B., Steele, M., Moritz, R., Meredith, M., Lee, C.M., 2006. The large-scale freshwater cycle of the Arctic. *Journal of Geophysical Research* 111, C11010. <http://dx.doi.org/10.1029/2005JC003424>.
- Shaw, W.J., Stanton, T.P., McPhee, M.G., Morison, J.H., Martinson, D.G., 2009. Role of the upper ocean in the energy budget of Arctic sea ice during SHEBA. *Journal of Geophysical Research: Oceans* 114 (C6), C06012. <http://dx.doi.org/10.1029/2008JC004991>.
- Shimada, K., Kamoshida, T., Itoh, M., Nishino, S., Carmack, E., McLaughlin, F., Zimmerman, S., Proshutinsky, A., 2006. Pacific Ocean inflow: influence on

- catastrophic reduction of sea ice cover in the Arctic Ocean. *Geophysical Research Letters* 33, L08605. <http://dx.doi.org/10.1029/2005GL025624>.
- Sirevaag, A., de la Rosa, S., Fer, I., Nicolaus, M., Tjernström, M., McPhee, M.G., 2011. Mixing, heat fluxes and heat content evolution of the Arctic Ocean mixed layer. *Ocean Science* 7, 335–349. <http://dx.doi.org/10.5194/os-7-335-2011>.
- Skagseth, Ø., Drinkwater, K.F., Terrie, E., 2011. Wind- and buoyancy-induced transport of the Norwegian Coastal Current in the Barents Sea. *Journal of Geophysical Research: Oceans* 116 (C8), C08007. <http://dx.doi.org/10.1029/2011JC006996>.
- Smith, W.O., Niebauer, H.J., 1993. Interactions between biological and physical processes in Arctic Seas: investigations using numerical models. *Reviews of Geophysics* 31 (2), 189–209. <http://dx.doi.org/10.1029/93RG00318>.
- Spreen, G., Kwok, R., Menemenlis, D., 2011. Trends in Arctic sea ice drift and role of wind forcing: 1992–2009. *Geophysical Research Letters* 38 (19), L19501. <http://dx.doi.org/10.1029/2011GL048970>.
- Steele, M., Ermold, W., Zhang, J., 2008. Arctic Ocean surface warming trends over the past 100 years. *Geophysical Research Letters* 35 (2), L02614. <http://dx.doi.org/10.1029/2007GL031651>.
- Steele, M., Ermold, W., Zhang, J., 2011. Modeling the formation and fate of the near-surface temperature maximum in the Canadian Basin of the Arctic Ocean. *Journal of Geophysical Research: Oceans* 116 (C11), C11015. <http://dx.doi.org/10.1029/2010JC006803>.
- Steele, M., Morison, J.H., 1993. Hydrography and vertical fluxes of heat and salt northeast of Svalbard in autumn. *Journal of Geophysical Research: Oceans* 98 (C6), 10013–10024. <http://dx.doi.org/10.1029/93JC00937>.
- Steele, M., Porcelli, A., Zhang, J., 2006. Origins of the SHEBA freshwater anomaly in the Mackenzie River delta. *Geophysical Research Letters* 33 (9), L09601. <http://dx.doi.org/10.1029/2005GL024813>.
- Steele, M., Zhang, J., Ermold, W., 2010. Mechanisms of summertime upper Arctic Ocean warming and the effect on sea ice melt. *Journal of Geophysical Research: Oceans* 115 (C11), C11004. <http://dx.doi.org/10.1029/2009JC005849>.
- Stroeve, J., Holland, M.M., Meier, W., Scambos, T., Serreze, M., 2007. Arctic sea ice decline: faster than forecast. *Geophysical Research Letters* 34 (9). <http://dx.doi.org/10.1029/2007GL029703>.
- Stroeve, J., Serreze, M., Drobot, S., Gearhead, S., Holland, M., Maslanik, J., Meier, W., Scambos, T., 2008. Arctic Sea ice extent plummets in 2007. *Eos Transactions* 89 (2), 13–14.
- Swift, J.H., Jones, E.P., Aagaard, K., Carmack, E.C., Hingston, M., MacDonald, R.W., McLaughlin, F.A., Perkin, R.G., 1997. Waters of the Makarov and Canada basins. *Deep Sea Research Part II: Topical Studies in Oceanography* 44 (8), 1503–1529.
- Thomson, R.E., Fine, I.V., 2003. Estimating mixed layer depth from oceanic profile data. *Journal of Atmospheric and Oceanic Technology* 20 (2), 319–329. [http://dx.doi.org/10.1175/1520-0426\(2003\)020<0319:EMLFO>2.0.CO;2](http://dx.doi.org/10.1175/1520-0426(2003)020<0319:EMLFO>2.0.CO;2).
- Timmermans, M.-L., Cole, S., Toole, J., 2012. Horizontal density structure and restratification of the Arctic Ocean surface layer. *Journal of Physical Oceanography* 42 (4), 659–668. <http://dx.doi.org/10.1175/JPO-D-11-0125.1>.
- Toole, J.M., Krishfield, R.A., Timmermans, M.L., Proshutinski, A., 2011. The ice-tethered profiler: Argo of the Arctic. *Oceanography* 24 (3), 126–135.
- Toole, J.M., Timmermans, M.L., Perovich, D.K., Krishfield, R.A., Proshutinsky, A., Richter-Menge, J.A., 2010. Influences of the ocean surface mixed layer and thermohaline stratification on Arctic Sea ice in the central Canada Basin. *Journal of Geophysical Research* 115. <http://dx.doi.org/10.1029/2009JC005660>.
- Travers, C.S., 2012. Quantifying Sea-Ice Volume Flux using Moored Instrumentation in the Bering Strait. University of Washington, 85 pp. <psc.apl.washington.edu/HLD>.
- Treshnikov, A., and G. I. Baranov (1973). Water circulation in the Arctic basin, 145 pp., Israel Program for Scientific Translations (Jerusalem).
- Understeiner, N., 1964. Calculations of temperature regime and heat budget of sea ice in the central Arctic. *Journal of Geophysical Research* 69 (22), 4755–4766. <http://dx.doi.org/10.1029/JZ069i022p04755>.
- Woodgate, R.A., Aagaard, K., 2005. Revising the Bering Strait freshwater flux into the Arctic Ocean. *Geophysical Research Letters* 32 (2), L02602. <http://dx.doi.org/10.1029/2004GL021747>.
- Woodgate, R.A., Aagaard, K., Swift, J.H., Smethie, W.M., Falkner, K.K., 2007. Atlantic water circulation over the Mendelev ridge and Chukchi borderland from thermohaline intrusions and water mass properties. *Journal of Geophysical Research* 112 (C02005), C02005. <http://dx.doi.org/10.1029/2005JC003416>.
- Woodgate, R.A., Aagaard, K., Weingartner, T.J., 2005. A year in the physical oceanography of the Chukchi Sea: moored measurements from autumn 1990–1991. *Deep Sea Research Part II: Topical Studies in Oceanography* 52 (24–26), 3116–3149. <http://dx.doi.org/10.1016/j.dsrrb.2005.10.016>.
- Woodgate, R.A., Weingartner, T.J., Lindsay, R., 2012. Observed increases in Bering Strait oceanic fluxes from the Pacific to the Arctic from 2001 to 2011 and their impacts on the Arctic Ocean water column. *Geophysical Research Letters* 39 (24), 6. <http://dx.doi.org/10.1029/2012gl054092>.
- Yang, J., Comiso, J., Krishfield, R., Honjo, S., 2001. Synoptic storms and the development of the 1997 warming and freshening event in the Beaufort Sea. *Geophysical Research Letters* 28 (5), 799–802. <http://dx.doi.org/10.1029/2000GL011896>.
- Yang, J., Comiso, J., Walsh, D., Krishfield, R., Honjo, S., 2004. Storm-driven mixing and potential impact on the Arctic Ocean. *Journal of Geophysical Research: Oceans* 109 (C4), C04008. <http://dx.doi.org/10.1029/2001JC001248>.